2012

Xeno Property

Fugro Airborne Surveys

Geophysical Survey Report

Airborne Magnetic, Radiometric and DIGHEM Survey

RARA TERRA MINERALS CORP.
(Formerly known as Rara Terra Capital Corp.)
Suite 830 -1100 Melville St.
Vancouver, BC V6E 4A6

Tenures:
848815, 848819, 865260, 865262, 976912, 976952, 976992,
977512, 978032, 981662, 1012337, 1012338, 1012339,
1012340, 1012342, 1012343, 1012344, 1012345, 1012346

Liard Mineral Division, Northern B.C.
Latitude: 58° 46' North Longitude: 127° 38' West

UTM Zone 9N (WGS84) 578349E, 6515408N
BCGS Mapsheets 094L.081, 082, 083, 072, 073, 063, 064

Claim Owners: Rara Terra Minerals Corp.

Author: Bob Friesen, B.Sc., P. Geo.

Date Submitted: May 27, 2013

Table of Contents

List of Figures 2
List of Tables 2
List of Appendixes 2
1.0 Summary 3
2.0 Introduction 4
3.0 Location, Access, and Topography 5
4.0 Claims 7
5.0 Exploration History 11
1986 Exploration Program (Assessment Reports 15220 and 16420) 11
1988 Exploration Program (Assessment Report 18538) 11
1989 Exploration Program (Assessment Reports 20229 and 20895) 11
1992 Exploration Program (Assessment Report 22746) 11
2000 Exploration Program 11
2001 Exploration Program (Assessment Report 26853) 11
6.0 Geologic Setting 12
6.1 Regional Geology (Figure 3) 12
6.2 Project Geology (Figure 3) 12
Rare Earth Potential 13
Diamond Potential 15
7.0 Objective and Scope of Airborne Geophysical Survey 15
8.0 Results and Conclusions 16
9.0 Recommendations 17
10.0 Statement of Costs 18
11.0 References 18
12.0 Statement of Qualifications 19

List of Figures

Figure 1 - Location MAP 6
Figure 2 - Xeno Property Claim Map 10
Figure 3 - Geology of the Xeno Property 13

List of Tables

TABLE 1 - CLAIMS INFORMATION 7

List of Appendixes

APPENDIX 1 - XENO GEOLOGY MAP LEGEND 20
APPENDIX 2 - XENO TOPOGRAPHIC FEATURES MAP 21
APPENDIX 3 - FUGRO AIRBORNE SURVEY REPORT 22

1.0 Summary

In order for Rara Terra Minerals Corp to initiate their search primarily for rare earth elements on the Xeno rare earth element (REE) property, they contracted Fugro Airborne Surveys to perform a DIGHEM EM/Mag/Radiometric survey over their Xeno Property, near Terminus Mountain in the Rocky Mountain trench of British Columbia and approximately 175 kilometers south by air from Watson Lake, Yukon Territory. The survey was completed between July 8 and July 14, 2012 and totaled 696.4-line km. at a cost of $236,000.

At the time of the survey, the Xeno property consisted of 57 claims covering 14,904.4 hectares. Since then, the company has added and amalgamated the claims to 27 claims totaling 15,861.25 hectares.

The Xeno property is located within the Kechika Ranges subdivision of the Cassiar Mountains physiographic province. The claims are situated within a 35-40 kilometer tectonically complex belt of metamorphosed Precambrian and unmetamorphosed to weakly metamorphosed Lower Paleozoic to Middle Paleozoic platformal facies sedimentary rocks. They are situated within a crustal block that is bounded to the north and east by the Rocky Mountain Trench and Burnt Rose fault systems, and to the south and west by the Kechika fault.

Geological, geochemical, and geophysical features make the XENO property of interest as a potential source of rare earth elements (REEs). For example, the local presence of syenite-hosted fluorite veins, mottled phyllites containing monazite and xenotime, a *diatreme breccia, tuff breccia, and related dykes hosting a stockwork of fluorite-carbonate veins,* fine-grained, igneous carbonate rocks hosting rare earth minerals occurring as relatively thin dykes and cross cutting both alkaline intrusive rocks and carbonate host rocks. Elevated rare earth concentrations have been found in numerous historical geochemical stream and rock sample analyses in the property area. These results indicate the presence of both light and heavy REE's, as well as yttrium and thorium. Radiometric surveys completed in 1988 and 1992 indicated areas of elevated radiation levels, which can coincide with rare earth mineral zones. The surveys found radiation anomalies occurring throughout the syenite and carbonatite complexes. In addition, magnetic data also suggests the presence of a nearby large, magnetic anomaly.

Detailed rock sampling on several internal claims in 2001, *not all currently owned by Rara Terra* confirmed the presence of several REE occurring zones. The average of 34 samples taken from the RAR 5 Zone was 3747 g/t total Rare Earth Oxides (REO's); Eleven samples taken from RAR 3 Zone averaged 2116g/t REO's; Rar 4 Zone averaged 1214 g/t REO's; and RAR 7 Zone, the largest RE zone on the property, had an average of 321123 g/t REO's from grab samples.

The Fugro airborne survey conducted for Rara Terra over the property provided a more technologically updated property scale tool for confirming and characterizing existing area showings, with the potential for enhancing their sizes and trends; plus offering up new exploration targets on Rara Terra's property. Fugro considers the radiometrics to be the best component for locating REE occurrences, due to their known association with potassium, uranium and thorium. Magnetics can also be useful if the REE-occurring host rocks contain magnetite. Regardless both it and EM conductiveness are often very useful in making lithological and structural interpretations.

Five of seven radiometric anomalies with identifiable thorium and/or uranium anomalies were selected by Fugro as being of interest. All five lie in the southern half of the property and some are located on Rara Terra's claims.

It is recommended that a comprehensive study be made of the survey results that would also incorporate all known geological, geophysical and geochemical data as it pertains primarily to the location of rare earth elements that would eventually justify and enable future follow-up work in the field and hopefully lead to the location of diamond drill targets.

2.0 Introduction

This report describes the Xeno rare earth element property with respect to mineral tenure, history of exploration, regional and local geology. It also describes the logistics, data acquisition, processing and presentation of results of a DIGHEM electromagnetic / magnetic / radiometric airborne geophysical survey carried out by Fugro Airborne Surveys for Rara Terra Minerals Corp. over the Xeno property in Northern British Columbia. Total coverage of the survey block amounted to 696.4 line km. The survey was flown between July 8th and July 14th, 2012.

The purpose of the survey was to map the geology and structure of the area and to locate and characterize existing and possibly new REE showings. Data were acquired using a DIGHEM electromagnetic system, supplemented by a high-sensitivity cesium magnetometer and a spectrometer. The information from these sensors was processed to produce maps and images that display the magnetic, radiometric and conductive properties of the survey area. A GPS electronic navigation system ensured accurate positioning of the geophysical data with respect to the base map coordinates.

The survey data were processed and compiled in the Fugro Airborne Surveys Toronto office. Maps and data in digital format are provided with this report.

Finally, this report includes a summary and conclusion with recommendations for follow-up exploration based primarily on the results of this airborne survey.

3.0 Location, Access, and Topography

The following description has been summarized from a Geological Survey Branch Assessment Report entitled "Geological and Rock Sampling Evaluation of the Rare Earth and Diamond Potential of the Xeno Property" dated May 1, 2002 prepared for Pacific Ridge Explorations Ltd. by Brian G. Thurston, BSc. and Wayne J. Roberts, P.Geo.

The Xeno Project is located in the Kechika River-Terminus Mountain area, Liard Mining Division, Northern British Columbia. The Claims are located approximately 20km west-southwest from the 'Skook Davidson Ranch' airstrip, near Terminus Mountain in the Rocky Mountain Trench, and approximately 175 km by air from Watson Lake, Yukon Territory. The geographic center of the Project is located at approximately 58° 46' N. Lat. and 127° 30' W. Long (Figure 1).

The Claims are accessible by helicopter from Watson Lake, YT or Dease Lake, BC. The Claims can also be accessed by helicopter or small fixed wing aircraft via the Terminus Mountain airstrip and then by overland means (by crossing the Kechika River), or by small float equipped aircraft to Colt Lake and then by overland means.

The Property is located within the Kechika Ranges subdivision of the Cassiar Mountains physiographic province. The region is characterized by well developed rectangular to angulate drainage patterns with northwesterly trending master valleys (Kechika River, Dall River) connected by shorter northeasterly trending valleys (Moodie Creek, Denetiah Creek, Frog River). Tributary streams of the northwesterly trending valleys drain areas of higher elevations and trend west northwesterly, parallel and sub parallel to the regional strike.

Within the claim block, elevation ranges from 1180 to 2237 meters A.S.L. Topographic relieve is extreme with steep slopes at lower elevations and sheer cliff faces at higher elevations.

Evidence of glaciation is widespread and includes cirques, horns, occasional razorback ridges or arêtes, and tarns. Glacially cut valleys have been modified by down cutting in post-glacial time. Rare glacial erratics (granitic boulders) indicate that ice cover was extensive.

There is a fairly heavy snow pack in this area of the Rocky Mountain Trench during the winter months. The snow pack is likely present from late October through to late June. Most rain during the field season occurs from June to mid-July, with a relatively dry period from then to late September.

RARA TERRA
MINERALS CORP

XENO PROJECT
LOCATION MAP

FIGURE 1

Figure 1 - Location Map

4.0 Claims

At the time of the Fugro airborne survey was carried out in July 2012, the Xeno property consisted of 57 mineral tenures totaling 14,904.4 hectares (Figure 2, Table 1). However, between then and the writing of this report, Rara Terra Minerals Corp. has added and amalgamated tenures to the property, which results in a total of 27 mineral tenures totaling 15861.25 hectares. (Figure 2, Table 1, [in grey]).

Mineral tenures in British Columbia are acquired through an internet-based mineral titles administration system. It is assumed, therefore, that the Xeno property is precisely as shown on the province's mineral tenure map and as displayed in Figure 2. The tenures are for mineral rights only and do not include surface rights.

Original Tenures as of Fugro Survey Date

	TENURE NUMBER	TENURE NAME	OWNER NAME	OWNER MTO CODE	NTS MAP NUMBER	GOOD TO DATE	Hectares
1	631184	ODS	RARA TERRA CAPITAL	251749 (100%)	094L	2012/dec/13	402.96
2	631223	ODS 3	RARA TERRA CAPITAL CORP.	251749 (100%)	094L	2012/dec/13	167.96
3	631225	BOREAL 4	RARA TERRA CAPITAL CORP.	251749 (100%)	094L	2012/dec/13	419.95
4	676383	RAR 5	RARA TERRA CAPITAL CORP.	251749 (100%)	094L	2012/dec/13	168.12
5	676385	RAR 4 - S	RARA TERRA CAPITAL CORP.	251749 (100%)	094L	2012/dec/13	100.96
6	676404	XENO E	RARA TERRA CAPITAL CORP.	251749 (100%)	094L	2012/dec/13	134.63
7	676483	XENO E- 2	RARA TERRA CAPITAL CORP.	251749 (100%)	094L	2012/dec/13	67.32
8	676503	RAR 7 - E	RARA TERRA CAPITAL CORP.	251749 (100%)	094L	2012/dec/13	117.65
9	678923	RAR 7 - W	RARA TERRA CAPITAL CORP.	251749 (100%)	094L	2012/dec/13	117.64
10	678943	RAR 3 - W	RARA TERRA CAPITAL CORP.	251749 (100%)	094L	2012/dec/13	33.65
11	698543	RADAR LOVE	RARA TERRA CAPITAL CORP.	251749 (100%)	094L	2012/dec/13	403.2
12	698563	MOODIE	RARA TERRA CAPITAL CORP.	251749 (100%)	094L	2012/dec/13	285.48
13	698623	INAGODADIVIDA	RARA TERRA CAPITAL CORP.	251749 (100%)	094L	2012/dec/13	285.78
14	698643	TWILIGHT ZONE	RARA TERRA CAPITAL CORP.	251749 (100%)	094L	2012/dec/13	420.1
15	834720	ODS 2	RARA TERRA CAPITAL CORP.	251749 (100%)	094L	2012/dec/13	302.35
16	836389	RAR DIATREME	RARA TERRA CAPITAL CORP.	251749 (100%)	094L	2012/dec/13	336.35
17	837896	XENOSIX	RARA TERRA CAPITAL CORP.	251749 (100%)	094L	2012/dec/13	100.99
18	837897	XENOFOUR	RARA TERRA CAPITAL CORP.	251749 (100%)	094L	2012/dec/13	67.31
19	837902	XENOTHREE	RARA TERRA CAPITAL CORP.	251749 (100%)	094L	2012/dec/13	50.44
20	838588	XENO WEST	RARA TERRA CAPITAL CORP.	251749 (100%)	094L	2012/dec/13	184.99
21	845191		RARA TERRA CAPITAL CORP.	251749 (100%)	094L	2012/dec/13	100.93
22	845194		RARA TERRA CAPITAL CORP.	251749 (100%)	094L	2012/dec/13	134.54
23	847284	XENO NORTH	RARA TERRA CAPITAL CORP.	251749 (100%)	094L	2012/dec/13	268.95
24	847286	XENO NORTH 2	RARA TERRA CAPITAL CORP.	251749 (100%)	094L	2012/dec/13	403.65
25	848815	XENO WEST	RARA TERRA CAPITAL CORP.	251749 (100%)	094L	2015/may/06	402.8
26	848816	NEXO WEST II	RARA TERRA CAPITAL CORP.	251749 (100%)	094L	2012/dec/13	419.75
27	848817	XENO WEST III	RARA TERRA CAPITAL CORP.	251749 (100%)	094L	2012/dec/13	134.38
28	848819	XENO WEST IV	RARA TERRA CAPITAL CORP.	251749 (100%)	094L	2015/may/06	318.7
29	865260	LIARD 1	RARA TERRA CAPITAL CORP.	251749 (100%)	094L	2015/may/06	286.08
30	865262	LIARD 2	RARA TERRA CAPITAL CORP.	251749 (100%)	094L	2015/may/06	420.61
31	976912	XENO45	RARA TERRA CAPITAL CORP.	251749 (100%)	094L	2015/may/06	67.23
32	976952	XENO46	RARA TERRA CAPITAL CORP.	251749 (100%)	094L	2015/may/06	369.65

33	976992	XENO SOUTH88	RARA TERRA CAPITAL CORP.	251749 (100%)	094L	2015/may/06	420.51
34	977512	XENO 50	RARA TERRA CAPITAL CORP.	251749 (100%)	094L	2015/may/06	402.96
35	977513	XENOHIGH2	RARA TERRA CAPITAL CORP.	251749 (100%)	094L	2013/apr/03	402.77
36	977514	XENOHIGH	RARA TERRA CAPITAL CORP.	251749 (100%)	094L	2013/apr/03	302.15
37	977518	XENOHIGH3	RARA TERRA CAPITAL CORP.	251749 (100%)	094L	2013/apr/03	100.66
38	978032	XENO NORTH15	RARA TERRA CAPITAL CORP.	251749 (100%)	094L	2015/may/06	134.15
39	978284	XENO 55	RARA TERRA CAPITAL CORP.	251749 (100%)	094L	2013/apr/05	201.33
40	978285		RARA TERRA CAPITAL CORP.	251749 (100%)	094L	2013/apr/05	251.66
41	978292	XENOHIGH5	RARA TERRA CAPITAL CORP.	251749 (100%)	094L	2013/apr/05	184.44
42	978295	XENO 56	RARA TERRA CAPITAL CORP.	251749 (100%)	094L	2013/apr/05	100.63
43	978298	XENOHIGHSIX	RARA TERRA CAPITAL CORP.	251749 (100%)	094L	2013/apr/05	117.4
44	981642	WESTERN WALL	RARA TERRA CAPITAL CORP.	251749 (100%)	094L	2013/apr/21	150.95
45	981643	NEW XENO NORTHWEST 1	RARA TERRA CAPITAL CORP.	251749 (100%)	094L	2013/apr/21	419.14
46	981644	NEW XENO NORTHWEST 2	RARA TERRA CAPITAL CORP.	251749 (100%)	094L	2013/apr/21	419.01
47	981645	NEW XENO NORTHWEST 3	RARA TERRA CAPITAL CORP.	251749 (100%)	094L	2013/apr/21	418.89
48	981646	NEW XENO NORTHWEST 4	RARA TERRA CAPITAL CORP.	251749 (100%)	094L	2013/apr/21	401.96
49	981647	NEW XENO NORTHWEST 5	RARA TERRA CAPITAL CORP.	251749 (100%)	094L	2013/apr/21	418.35
50	981648	NEW XENO NORTHWEST 6	RARA TERRA CAPITAL CORP.	251749 (100%)	094L	2013/apr/21	401.46
51	981649	NEW XENO NORTHWEST 7	RARA TERRA CAPITAL CORP.	251749 (100%)	094L	2013/apr/21	384.99
52	981650	NEW XENO NORTHWEST 8	RARA TERRA CAPITAL CORP.	251749 (100%)	094L	2013/apr/21	402.02
53	981651	NEW XENO NORTHWEST 9	RARA TERRA CAPITAL CORP.	251749 (100%)	094L	2013/apr/21	402.24
54	981662	NEW XENO NORTHWEST 10	RARA TERRA CAPITAL CORP.	251749 (100%)	094L	2015/may/06	368.98
55	981664	XENOHIGH7	RARA TERRA CAPITAL CORP.	251749 (100%)	094L	2013/apr/22	284.47
56	981668	NEW XENO NORTHWEST 11	RARA TERRA CAPITAL CORP.	251749 (100%)	094L	2013/apr/22	133.95
57	981673	NEW XENO NORTHWEST 12	RARA TERRA CAPITAL CORP.	251749 (100%)	094L	2013/apr/22	184.24
							14,904.4

Up to Date Tenures

1	848815	XENO WEST	RARA TERRA CAPITAL CORP.	251749 (100%)	094L	2015/may/06	402.8
2	848819	XENO WEST IV	RARA TERRA CAPITAL CORP.	251749 (100%)	094L	2015/may/06	318.7
3	865260	LIARD 1	RARA TERRA CAPITAL CORP.	251749 (100%)	094L	2015/may/06	286.08
4	865262	LIARD 2	RARA TERRA CAPITAL CORP.	251749 (100%)	094L	2015/may/06	420.61
5	976912	XENO45	RARA TERRA CAPITAL CORP.	251749 (100%)	094L	2015/may/06	67.23
6	976952	XENO46	RARA TERRA CAPITAL CORP.	251749 (100%)	094L	2015/may/06	369.65
7	976992	XENO SOUTH88	RARA TERRA CAPITAL CORP.	251749 (100%)	094L	2015/may/06	420.51
8	977512	XENO 50	RARA TERRA CAPITAL CORP.	251749 (100%)	094L	2015/may/06	402.96
9	978032	XENO NORTH15	RARA TERRA CAPITAL CORP.	251749 (100%)	094L	2015/may/06	134.15
10	981662	NEW XENO NORTHWEST 10	RARA TERRA CAPITAL CORP.	251749 (100%)	094L	2015/may/06	368.98
11	1012337	XENO SUBSET 2	RARA TERRA CAPITAL CORP.	251749 (100%)	094L	2015/may/06	622.25
12	1012338	XENO 100	RARA TERRA CAPITAL CORP.	251749 (100%)	094L	2015/may/06	1189.25
13	1012339	XENO 200	RARA TERRA CAPITAL CORP.	251749 (100%)	094L	2015/may/06	2629.77
14	1012340	XENO 300	RARA TERRA CAPITAL CORP.	251749 (100%)	094L	2015/may/06	602.66

15	1012342	XENO 400	RARA TERRA CAPITAL CORP.	251749 (100%)	094L	2015/may/06	855.46
16	1012343	XENO 500	RARA TERRA CAPITAL CORP.	251749 (100%)	094L	2015/may/06	805.58
17	1012344	XENO 600	RARA TERRA CAPITAL CORP.	251749 (100%)	094L	2015/may/06	2452.9
18	1012345	XENO 700	RARA TERRA CAPITAL CORP.	251749 (100%)	094L	2015/may/06	1377.4
19	1012346	XENO 800	RARA TERRA CAPITAL CORP.	251749 (100%)	094L	2015/may/06	1177.46
20	1016160	XENO INTRUSION	RARA TERRA CAPITAL CORP.	251749 (100%)	094L	2014/jan/20	335.5231
21	1018254	XENO 1500	RARA TERRA CAPITAL CORP.	251749 (100%)	094L	2014/apr/04	268.6416
22	1018261	XENO 1501	RARA TERRA CAPITAL CORP.	251749 (100%)	094L	2014/apr/04	134.2259
23	1019621	XENO 2013	RARA TERRA CAPITAL CORP.	251749 (100%)	094L	2014/may/19	100.8252
24	1019625	XENO 2013 - 2	RARA TERRA CAPITAL CORP.	251749 (100%)	094L	2014/may/19	50.4037
25	1019626	XENO 2013 - 3	RARA TERRA CAPITAL CORP.	251749 (100%)	094L	2014/may/19	33.6144
26	1019630	XENO 2013 - 4	RARA TERRA CAPITAL CORP.	251749 (100%)	094L	2014/may/19	16.8092
27	1019632	XENO 2013 - 5	RARA TERRA CAPITAL CORP.	251749 (100%)	094L	2014/may/19	16.8032
							15,861.25

Table 1 - Claim Information

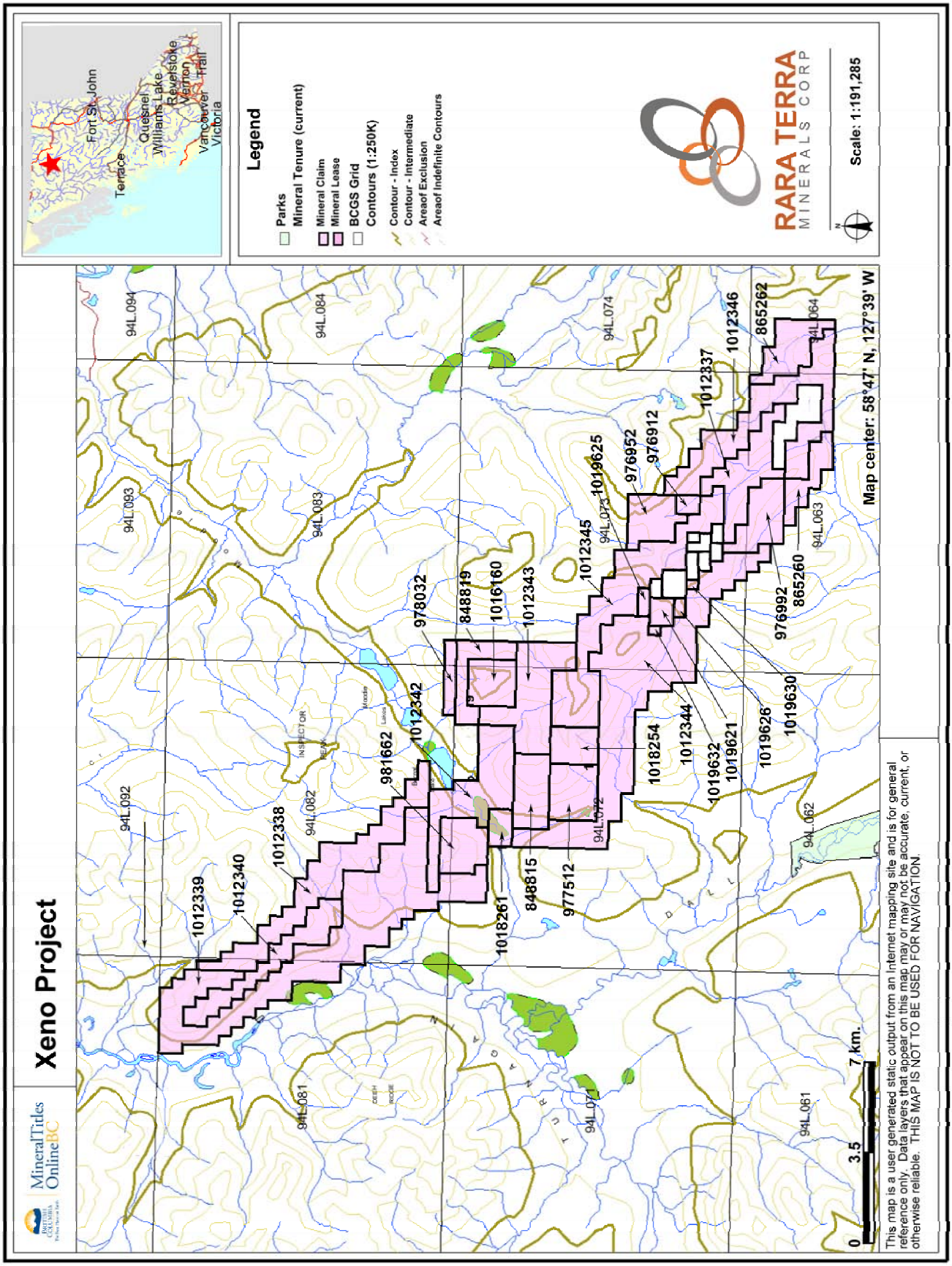

Figure 2 – Xeno Property Claim Map

5.0 Exploration History

The Xeno project area has been explored since the 1980's by various groups as summarized below. *Please note that some of the showings described here may still be covered by internal claims not owned by Rara Terra:*

1986 Exploration Program (Assessment Reports 15220 and 16420)

During the period of July to October 1986, helicopter supported reconnaissance and detailed geological mapping, prospecting, stream silt sampling, and rock geochemical sampling were carried out on the property to evaluate the potential for REEs. Detailed mapping was done in selected areas of the RAR 4, 5, 6 and 7 claims, A total of 125 rock samples and 122 stream silt samples were collected and analyzed for Ce, La, and Y by X-ray fluorescence. All of the rock samples were also analyzed for Nb and Ta by X-ray fluorescence and 60 rock samples were selected for 17-element neutron activation analysis (Ce, Dy, Er, Eu, Gd, Ho, La, Lu, Nd, Pr, Sc, Sm, Tb, Th, Tm, U, Yb). The results indicated significant enrichments in light rare earth elements (LREE) and heavy rare earth elements (HREE) as well as Y and Th.

1988 Exploration Program (Assessment Report 18538)

During the period August 16 to September 15, 1988, helicopter supported reconnaissance and detailed geological mapping, and rock sampling was carried out over areas of interest identified in 1986. This work included some continuous chip sampling of previously identified zones enriched in REEs and Yttrium for the purpose of metallurgical testing. Geochemical analyses of 223 rock samples were included in an assessment report describing 1988 fieldwork. Samples were analyzed for Au, Ba, Ce, Cr, Eu, Hf, Rb, Sc, Sm, Ta, Tb, Th, U, Yb, Zr and Y. The analytical results indicated that a zone of potentially economic mineralization was present within an area referred to as the '2237 Ridge' zone on the RAR 7 claim.

1989 Exploration Program (Assessment Reports 20229 and 20895)

In 1989 a program was carried out to define the distribution, grade and continuity or Yttrium mineralization on the RAR 7 claim. Four short trenches, with a combined linear distance of 35.5 metres, were chip sampled from outcrop in the '2237 Ridge' zone area. Due to the early onset of winter conditions the program was cut short. A detailed radiometric survey, measuring total count gamma radiated was carried out over the immediate area of the '2237 Ridge' zone. Little work was done on the other targets in the area.

1992 Exploration Program (Assessment Report 22746)

A grid controlled radiometric survey (17.1 line km) was carried out over portions of the RAR 1 and RAR 4 claims utilizing a Series 2 Saphmo-Stel SPP2NF scintillometer. This work outlined a zone of above background response corresponding to an area underlain by mafic syenites.

2000 Exploration Program

After the 1992 program was completed, no further work was conducted in the area and the RAR claims were allowed to lapse. In 2000, Andrew Harman staked the XENO 1-10 claims over the RAR 5 and RAR 7 occurrences and optioned the claims to Pacific Ridge Exploration Ltd. These were then forfeited in 2005-2006 and re-staked and optioned thereafter.

2001 Exploration Program (Assessment Report 26853)

A detailed prospecting and rock-sampling program was carried out in August 2001. A total of 152 samples were collected from REE enriched zones along an 11-kilometre length. The samples were analyzed for rare earth elements. Very little prospecting or mapping of new zones was done during this program. The program confirmed and outlined rare earth occurrences and one microdiamond was found.

6.0 Geologic Setting

6.1 Regional Geology (Figure 3)

The following description has been excerpted from a Geological Survey Branch Assessment Report entitled "Geological and Rock Sampling Evaluation of the Rare Earth and Diamond Potential of the Xeno Property" dated May 1, 2002 prepared for Pacific Ridge Explorations Ltd. by Brian G. Thurston, BSc. and Wayne J. Roberts, P.Geo.

The area has been mapped at a scale of 1:253,440 (G.S.C. Map 42-1962, "Kechika", H. Gabrielse). Reports written by Michael Fox (1987, 1993) describe in detail the geology, stratigraphy, structure and igneous rocks of the property area. Information from these reports is summarized below.

The claims are situated within a 35-40 kilometer tectonically complex belt of metamorphosed Precambrian and unmetamorphosed to weakly metamorphosed Lower Paleozoic to Middle Paleozoic platformal facies sedimentary rocks. The claims are situated within a crustal block that is bounded to the north and east by the Rocky Mountain Trench and Burnt Rose fault systems, and to the south and west by the Kechika fault. These faults are major structural features in the northern Cordillera along which dextral, transcurrent movements of hundreds of kilometers are believed to have taken place (Templemann-Kluitt, 1976, Gabrielse, 1985). Estimated transcurent displacements may have moved the Kechika crustal block as much as 450km northwestwards in late Cretaceous time, after the rocks and been deformed by late Jurassic-Cretaceous thrusting during the Laramide orogeny.

Metamorphic grade in the Precambrian rocks is lower greenschist facies. Northeastwards directed compression has produced broad, open, to tight isoclinal or overturned folds within a series of thrust panels, which juxtapose lithologies of markedly different age and metamorphic grade.

6.2 Project Geology (Figure 3)

The following description of the property geology has been partially excerpted from a Geological Survey Branch Assessment Report entitled "Geological and Rock Sampling Evaluation of the Rare Earth and Diamond Potential of the Xeno Property" dated May 1, 2002 prepared for Pacific Ridge Explorations Ltd. by Brian G. Thurston, BSc. and Wayne J. Roberts, P.Geo. and by a compilation of other available reports by in-house geologists.

The Xeno Property is located in a 35-40 km tectonically complex belt of metamorphosed sedimentary rocks of varying grade. The area is characterized by numerous faults, including several thrust faults, which have a general northwestern trend.

A thick-bedded competent series of Lower Cambrian quartzites, correlatable with the Atan Group, is exposed in a broad, open, northwesterly striking anticline to the northeast of the claim group. In fault contact to the southwest with the quartzites, is a thick section of southwest dipping Middle to Upper Cambrian and Ordovician chlorite-sericite-quartz phyllites, marbles, and dolostones of the Kechika Group. To the southwest, the Kechika Group rocks are in turn overthrust on the southwest by graphite-sericite phyllites and graphite-chlorite-sericite phyllites of the Kechika Group, which contain occasional orange weathering sandy dolomite interbeds, up to 30 or 40 centimeters in thickness.

Alkaline intrusive rocks exposed within the Xeno claim block occur within the fault-bounded panel of Sandpile Group rocks bounded on the northeast and southwest by Kechika Group Rocks.

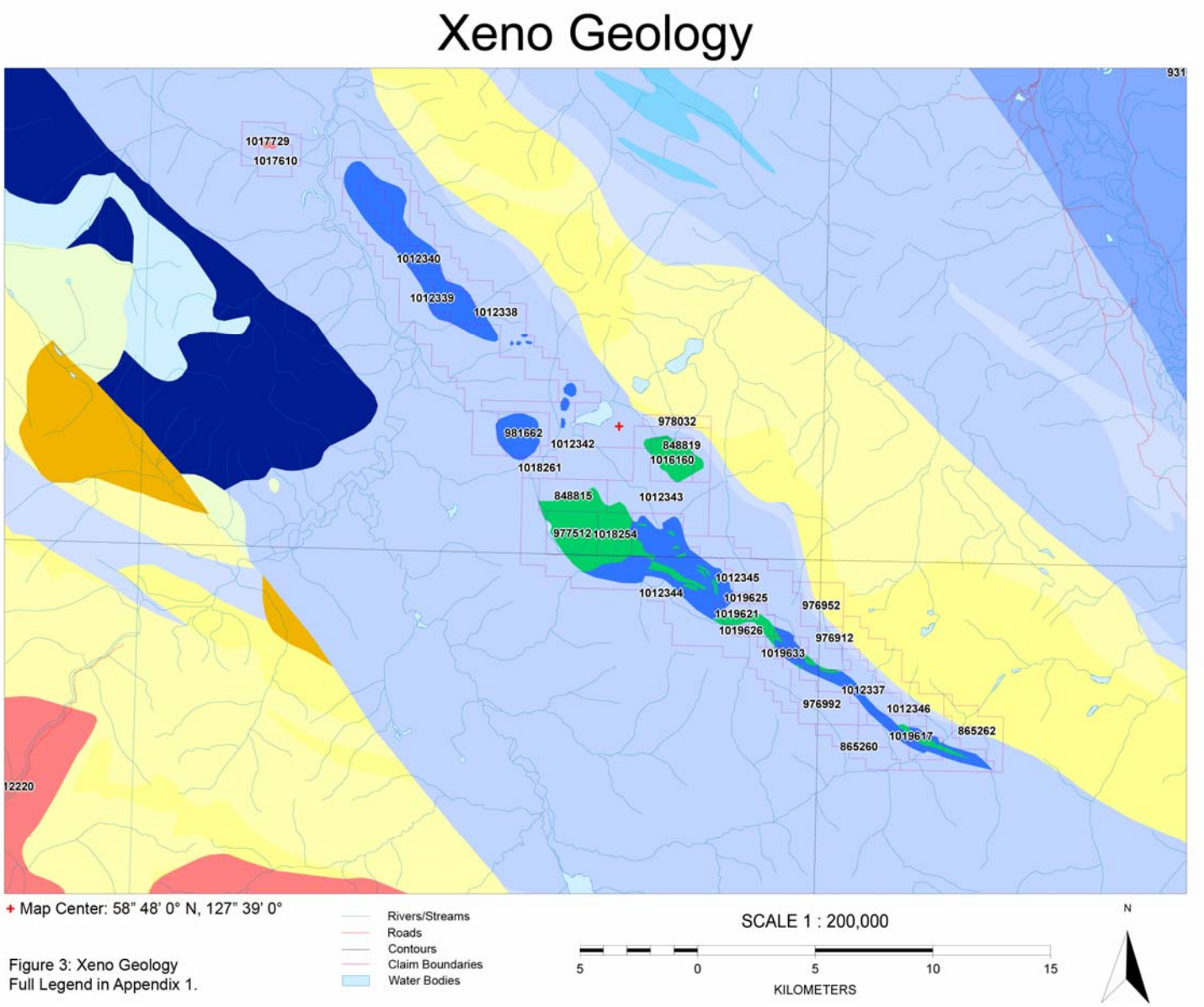

Figure 3: Geology of Xeno Property

Rare Earth Potential

The Xeno property is primarily of interest as a potential source of rare earth elements (REEs). Several factors make this particular area promising including the geology of the property, and related geochemical and geophysical data.

Geology

The presence of several distinct geological features supports potential rare earth mineralization in the area. These features include:

Syenites, including melanocratic titan-augite syenites and leucocratic syenites, are present at the south end of the property and are distributed towards the centre of the property along the general trend. These syenites are

intrusive bodies and are usually elongate stocks or dykes. Fluorite veins and shear zones within the syenites could contain REEs.

Mottled phyllites—fine-grained, extremely fissile and micaceous, and are often associated with other alkaline rocks in the area. Certain minerals in these rocks, notably monazite and xenotime, have been found in these rocks and are known sources of REEs.

A complex diatreme, containing a number of breccia phases, related pyroclastic tuffs and breccia dykes, crops out across the property. This complex diatreme crosscuts many of the various rock types in the area and hosts a stockwork of fluorite-carbonate veins in some areas. These veins, and the fenitized host rock, could be potential sources of REEs.

Fine-grained carbonatites, which occur as relatively thin dykes (less than 1 metre wide) and cross cut both alkaline intrusive rocks and carbonate host rocks. While relatively small in terms of volume, these dykes do have some RE mineral content.

Geochemistry

Throughout the past twenty-five years there have been numerous geochemical analyses covering the property and the surrounding area. These analyses include both stream sampling as well as rock sampling. Overall, the geochemical studies indicate elevated rare earth concentrations. This elevation includes both light and heavy rare earth elements, as well as yttrium and thorium. Surveys in the surrounding area also indicate elevated levels of barium.

Geophysics

Radiometric surveys completed in 1988 and 1992 indicated areas of elevated radioactivity. Anomalous levels of radiation can coincide with rare earth mineral zones. The surveys found radiation anomalies occurring throughout the syenite and carbonatite complexes. These results support potential rare earth mineralization. The radiometric surveys can be found in the appendix of this report.

Assay Highlights

In 2001, a detailed rock-sampling program was carried out on the Xeno Property as it existed then.152 samples were collected from REE enriched zones. The highlights are summarized below (note that some of these sample sites may occur on internal claims not owned by Rara Terra):

RAR 5 Zone

The RAR 5 zone is located in the center of The Company's Xeno Property. It has been identified as containing a carbonatite diatreme breccia complex exposed over a length of 350m with an average exposed width of 25m. The zone remains open in all directions. The samples averaged 3,747 g/t total REOs, and assay highlights included an average grade of 386 g/t Neodymium oxide (Nd_2O_3), 1,689 g/t Cerium oxide (CeO_2), and 1,295 g/t Lanthanum oxide (La_2O_3). Three of 34 samples were assayed for Scandium and averaged 15g/t.

RAR 3 Zone

The RAR 3 zone is located 3km southeast of RAR 5. Sampling in 2001 was done along a 300m long portion of the zone averaging 12m in width. The zone is comprised of sheared carbonatite schist with semi-continuous carbonate-quartz-pyrite boudins, which occur in areas of strong shearing and increased schistosity. These particular zones appear to be most enriched in REEs. The samples averaged 2,116 g/t total REOs, and assay highlights included an average grade of 185 g/t Neodymium oxide (Nd_2O_3), 968 g/t Cerium oxide (CeO_2), and 744 g/t Lanthanum oxide (La_2O_3). Two of 11 samples were assayed for Scandium and averaged 12g/t.

RAR 4/RAR 6 Zones

The RAR 4 zone is located approximately 1 km east-southeast of the RAR 3 zone. Previous mapping and petrographical work concluded that the zone consists of a syenite intrusive complex. The syenite complex is exposed over a length of 300m with an average width of 40-50m and appears to cut a silicified to carbonatized, mafic, laminated tuff. The zone remains open along its length although it disappears under a thrust of Precambrian schist to the northwest. The southeastern extension of the zone, approximately 1km from the main RAR 4 zone, is known as the RAR 6 zone. The width of the syenite complex in the RAR 6 zone is up to 200m. Sampling of the RAR 4 zone was concentrated along outcrop exposures on the west cliff face within the central portion of the zone. The samples averaged 1,214 g/t total REOs, and assay highlights included an average grade of 167 g/t Neodymium oxide (Nd_2O_3), 538 g/t Cerium oxide (CeO_2), and 329 g/t Lanthanum oxide (La_2O_3).

RAR 7 Zone

The RAR 7 zone has the largest known exposure of RE mineralization in the Xeno Property area. It is located approximately 2 km northwest of the RAR 5 zone and measures over 1,000m in length and 300m wide. It consists of a syenite-carbonatite complex within sedimentary rocks. The main rock type observed in this area is an assemblage of quartz-feldspar-carbonate-sericite. Grab samples yielded an average grade of 3,113 g/t REOs, and assay highlights included 1,497 g/t Yttrium oxide (Y_2O_3), 255 g/t Dysprosium oxide (Dy_2O_3), and 55 g/t Europium oxide (Eu_2O_3).

Diamond Potential

A sample, taken from 500 metres northwest of the main carbonatite-diatreme breccia complex, is believed to be kimberlite. The sample was medium to dark green multilithic breccia with possible altered olivine crystals. The 32-kilogram sample was analyzed for diamonds. One transparent, green, cuboid, diamond fragment was recovered measuring 0.38 by 0.30 by 0.25 millimetres. As a result, the diatreme-breccia complex has potential to be diamondiferous.

7.0 Objective and Scope of Airborne Geophysical Survey

This report describes the logistics, data acquisition, processing and presentation of results of a DIGHEM electromagnetic / magnetic / radiometric airborne geophysical survey carried out by Fugro Airborne Surveys for Rara Terra Minerals Corp. over the Xeno in Northern British Columbia. Total coverage of the survey block amounted to 696.4 line km. The survey was flown between July 8th and July 14th, 2012.

The purpose of the survey was to map the geology and structure of the area and to characterize existing showings and to locate new ones. Data were acquired using a DIGHEM electromagnetic system, supplemented by a high-sensitivity cesium magnetometer and a spectrometer. The information from these sensors was processed to produce maps and images that display the magnetic, radiometric and conductive properties of the survey area. A GPS electronic navigation system ensured accurate positioning of the geophysical data with respect to the base map coordinates.

The survey data were processed and compiled in the Fugro Airborne Surveys Toronto office. Maps and data in digital format are provided with this report.

8.0 Results and Conclusions

Note: the following is excerpted from the aforementioned Fugro report; an entire copy of which is included as an Appendix to this report.

According to Fugro, the magnetic data from the airborne survey may be used as a direct identification for follow-up targets if the deposits within the survey area contain sufficient quantities of magnetite or other magnetic minerals. Anomalous radiometric highs can also be used as an exploration guide in particular high thorium and uranium concentrations. Radiometrics is considered the best choice of the three to characterize REE occurrences. Carbonatite and REE's generally do not yield a distinctive EM anomaly, but the resistivity data, along with the magnetic and radiometric datasets can be useful in highlighting changes in lithologies, alteration zones and mapping structural features within the survey area.

Fugro determined that the northern portion of the survey block generally yields lower radiometric concentrations than those in the southern portion of the block. There also appears to be relatively higher potassium and uranium concentrations in the north while the southern area contains relatively higher thorium and uranium than potassium.

The magnetic patterns generally exhibit a NW/SE trend direction across the block. Most linear magnetic anomalies appear quite narrow with strike lengths ranging from a few hundred metres to over a few kilometres in length. They are well-defined, discrete anomaly shapes, which indicate they are near-surface features.

Within the northern limb of the survey area, a large conductive unit dominates the region, which consists of numerous interpreted bedrock conductors. This conductive zone is truncated in the south by a weakly conductive NE/SW trending river valley. Along an inferred break in close proximity to the north side of the valley, the data suggest a slight increase in relative uranium concentrations.

Two large, radiometric anomalous zones are located in the northern half of the property (R1 & R2). R1 is a large zone displaying low K, Th, and U counts. Within it, there is a slight relative increase in Th and U. Along the eastern boundary of this zone, is a relative increase of K counts. Fugro interprets this feature to be near surface. There is no obvious corresponding anomalous magnetic unit associated with R1.

Zone R2 is a large, circular feature displaying relatively high potassium. It appears as a low within the Th/K ration data. Within the center of R2, there is a small anomalous area of higher Th counts and a slight corresponding increase in conductivity. There is little evidence of this small feature within the magnetic data.

Along the southern and eastern boundary of R2, there is a slight relative increase in Th and U. The eastern area corresponds to a conductive unit. Both of these features extend further south and may be related to additional zones noted below.

The southern half of the survey block shows an overall increase in background resistivity values. There are some discrete EM conductors, but not as prominent as in the northern half. As well there are higher Th and U concentrations and an increase in the magnetic amplitudes towards the south.

In total, there were nine responses of > 100 Siemens (mhos), equivalent to the highest conductor grade of 7. This is followed by another fourteen responses of 50 – 1000 Siemens (mhos) equivalent to the next highest conductor grade of 6. See the attached Fugro report for the full list of EM anomaly statistics.

Fugro identified 5 main potential zones of interest—all in the southern half of the survey/claim block. They were selected primarily on the basis of identifiable thorium an/or uranium anomalies on their ternary and ratio images.

The five zones (R3, R4, R5, R6, and R7) are clearly outlined within the Th/K ratio image and the ternary image and the reader is again referred to the appended Fugro report (pp34-37).

9.0 Recommendations

As the purpose of the survey was to determine the magnetic, radiometric and conductive signatures over the favorable REE-hosting rock units/structures (syenites, phyllites, carbonatites, diatremes, etc.) and to aid in our understanding of the geology and structure of the survey block, it is recommended that as per the Fugro report that "the survey results be assessed and fully evaluated in conjunction with all other available geophysical, geological and geochemical information. In particular, structural analysis of the data should be undertaken and areas of interest should be selected. It is important that careful examination of these areas be carried out on the ground in order to eliminate possible man-made sources of the EM anomalies. An attempt should be made to determine the geophysical signatures over any known zones of mineralization in the survey areas or their vicinity.

The anomalous zones defined by the survey should be subjected to further investigation using appropriate surface exploration techniques. Aomalous zones that are currently considered to be of moderately low priority may require upgrading if follow-up results are favorable, or if they occur in areas of favorable geology."

Fugro further recommends that we consider image processing of existing geophysical data in order to extract the maximum amount of information from the survey results, as current software can provide enhancement images of older data."

a complete assessment and detailed evaluation of the survey results be carried out utilizing all available geological, geophysical, and geochemical data available as it pertains primarily to the location of rare earth elements. This work would initially be carried out in office-oriented studies to composite all data and prioritize areas of interest. This work would then be followed by further ground proofing that hopefully, would lead to the location of future drill targets.

Bob Friesen, B.Sc., P.Geo
27th May, 2013

10.0 Statement of Costs

Fugro Survey Charges (CAD):

696.4 line km @ fixed charges	$215,000
Standby charges	$21,000
Total Contract Value:	$236,000

11.0 References

Thurston, Brian G, Roberts, Wayne J. (2002) Geological and Rock Sampling Evaluation of the Rare Earth and Diamond Potential of the Xeno Property, British Columbia Ministry of Energy, Mines and Petroleum Resources, Assessment report 26,853.

Leighton, D.G.F. (1992) Geophysical Report on the Kechika Property, British Columbia Ministry of Energy, Mines and Petroleum Resources, Assessment report 22,746.

Pell, J (1990) Geological and Trenching Report on the Kechika Property RAR Group (RAR 1,4,6,7,8 claims) REE Group (REE 1,2,7,8 claims), British Columbia Ministry of Energy, Mines and Petroleum Resources, Assessment report 20,895.

Pell, J, Leighton, D.G., Culbert, R.R. (1990) Geological, Geophysical and Trenching Report on the Kechika North/Kechika South Groups and RAR 2,3, REE 3 to 6 and REO 1,2, Claims, , British Columbia Ministry of Energy, Mines and Petroleum Resources, Assessment report 20,229.

Leighton, D.G., Culbert, R.R. (1989) Geological Report on the Kechika Property Including RAR 1-9, REE 1-8, and REO 1-2 claims, British Columbia Ministry of Energy, Mines and Petroleum Resources, Assessment report 18,538.

Fox, Michael (1987) Geological and Geochemical Report RAR 1-9 REE 1-8 and REO 1 and 2 Mineral Claims, British Columbia Ministry of Energy, Mines and Petroleum Resources, Assessment report 16,420.

Fox, Michael (1986) Geological and Geochemical Report RAR 1-5 Mineral Claims, British Columbia Ministry of Energy, Mines and Petroleum Resources, Assessment report 15,220.

Galbrielse, H. (1985) Major Dextral Transcurrent Displacements along the Northern Rocky Mountain Trench and Related Lineaments in north-central British Columbia; Geological Society of America Bulletin Vol. 96, pp. 1-14

Pell, J., Cullbert, R.R. and Fox M. (1989) The Kechika Yttrium and Rare Earth Prospect; in Geological Fieldwork, 1988, BCMEMPR Paper 89-1, pp. 417-421

Templemann-Kluitt, D.J. (1976) The Yukon Crystalline Terrane: Enigma in the Canadian Cordillera; in Geological Society of America Bulletin, vol. 87, pp. 1343-1357

12.0 Statement of Qualifications

Statement of Qualifications — Robert Friesen

I, Robert G. Friesen of #23 – 758 Riverside Drive, Port Coquitlam BC, V3B 7V8, do hereby certify that:

1) I am a consulting geologist, owner of Friesen Geological Services Inc. I am contracted to Rara Terra Minerals Corp. who has an office at #830 – 1100 Melville St., Vancouver, BC.

2) I am a graduate of the University of British Columbia in 1967 with a B.Sc. (Geology major).

3) I have practiced my profession continuously since 1967; and have extensive experience in mining and exploration geology, both nationally and internationally.

4) I am a member in good standing of the Association of Professional Engineers and Geoscientists of the Province of British Columbia.

5) This report is based on my consulting experience to Rara Terra Minerals Corp.. re: the Xeno property that began in May of 2011 and that is the subject of this report.

Dated this 27th day of May, 2013

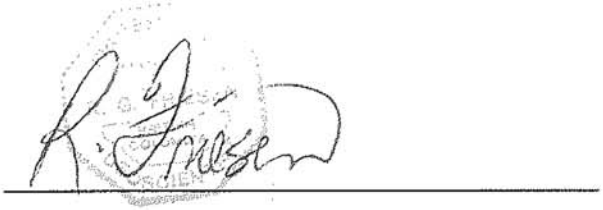

Robert G. Friesen, P. Geo. B.Sc.
Friesen Geological Services Inc.

Appendix 1: Xeno Project Geology Map Legend

Appendix 2: Xeno Topographic Features

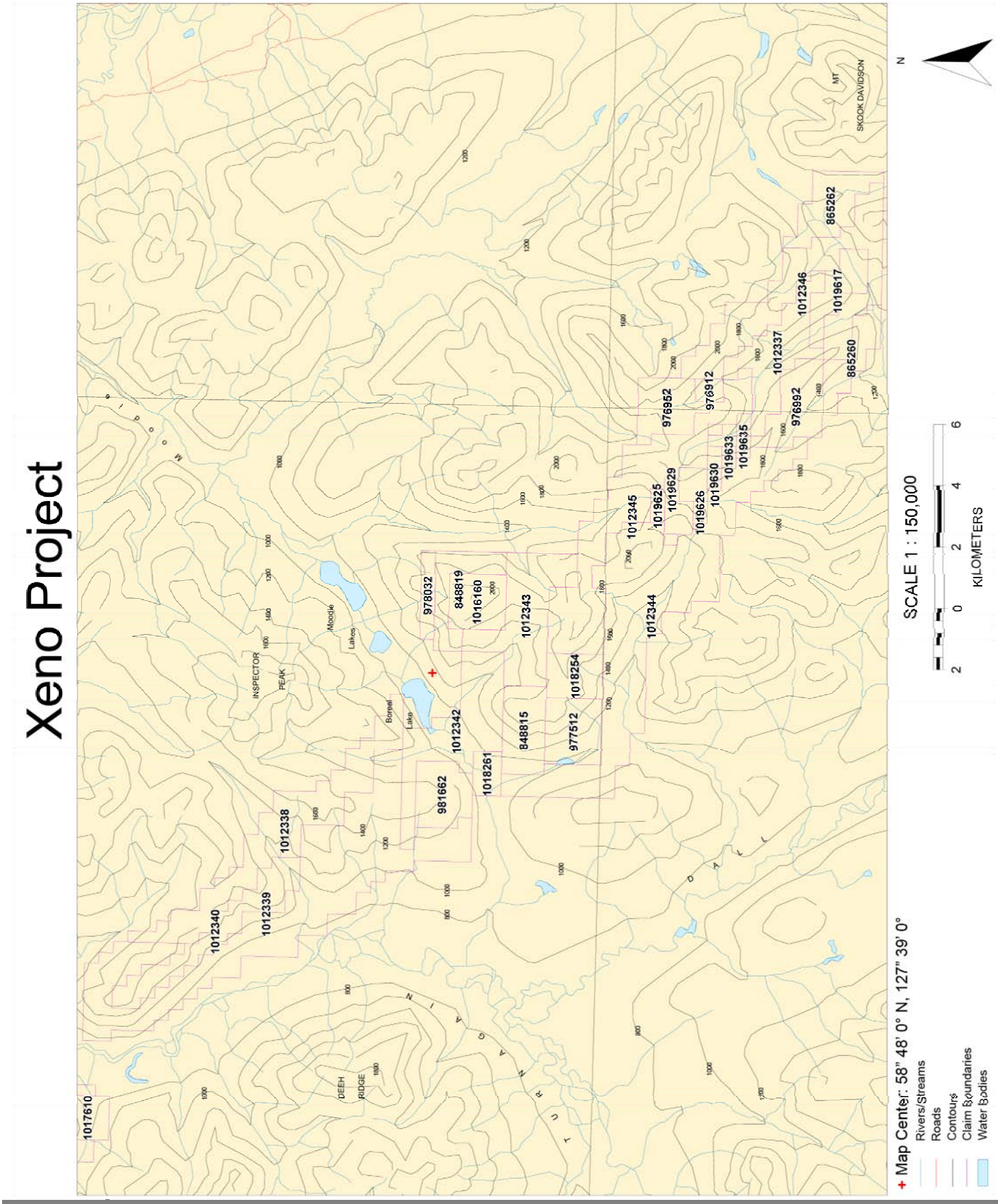

Appendix 3: Fugro Airborne Survey Report

Fugro Airborne Surveys

GEOPHYSICAL SURVEY REPORT
AIRBORNE MAGNETIC, RADIOMETRIC AND DIGHEM SURVEY
XENO PROJECT, DEASE LAKE AREA, BC
PROJECT 11075
RARA TERRA MINERALS CORP.

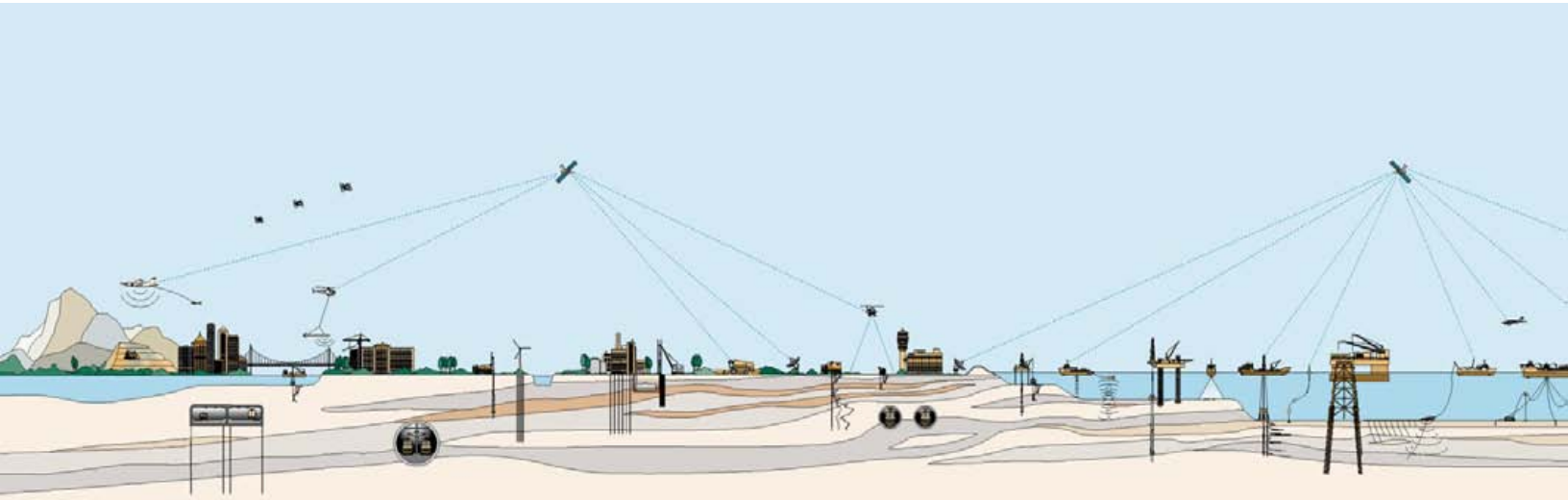

October 31, 2012

2505 Meadowvale Boulevard, Mississauga, Ontario Canada L5N 5S2 (905) 812-0212 www.fugroairborne.com.

FUGRO AIRBORNE SURVEYS

Fugro Airborne Surveys was formed in early 2000 through the global merger of leading airborne geophysical survey companies: Geoterrex-Dighem, High-Sense Geophysics, and Questor of Canada; World Geoscience of Australia; and Geodass and AOC of South Africa. Sial Geosciences of Canada joined the Fugro Airborne group in early 2001, and Spectra Exploration Geosciences followed thereafter. In mid 2001, Fugro acquired Tesla 10 and Kevron in Australia, and certain activities of Scintrex. Fugro also works with Lasa-Geomag located in Brazil for surveys in South America. With a staff of over 400, Fugro Airborne Surveys now operates from 12 offices worldwide.

Fugro Airborne Surveys is a professional services company specializing in low level remote sensing technologies that collects, processes, and interprets airborne geophysical data related to the subsurface of the earth and the sea bed. The data and map products produced have been an essential element of exploration programs for the mining and petroleum industries for over 50 years. Engineers, scientists and others with a need to map the earth's subsurface geology use Fugro Airborne Surveys for environmental and engineering solutions. From mapping kimberlite pipes and oil and gas deposits to detecting water tables and unexploded ordnance, Fugro Airborne Surveys designs systems dedicated to specific targets and survey needs. State of the art geophysical systems and techniques ensure that clients receive the highest quality survey data and images.

Fugro Airborne Surveys acquires both time domain and frequency domain electromagnetic data as well as magnetic, radiometric and gravity data from a wide range of fixed wing (airplane) and helicopter platforms. Depending on the geophysical mapping needs of the client, Fugro Airborne Surveys can field airborne systems capable of collecting one or more of these types of data concurrently. The company offers all data acquisition, processing, interpretation and final reporting services for each survey.

Fugro Airborne Surveys is a founding member of IAGSA, the International Airborne Geophysics Safety Association. Our health, safety and environment management system has successfully achieved certification to the international standard *OHSAS 18001* and our quality management system has also successfully achieved certification to the international standard *ISO 9001:2000 Quality Management Systems – Requirement*s.

Disclaimer

1. The Survey that is described in this report was undertaken in accordance with current internationally accepted practices of the geophysical survey industry, and the terms and specifications of a Survey Agreement signed between the CLIENT and FUGRO. Under no circumstances does FUGRO make any warranties either expressed or implied relating to the accuracy or fitness for purpose or otherwise in relation to information and data provided in this report. The CLIENT is solely responsible for the use, interpretation, and application of all such data and information in this report and for any costs incurred and expenditures made in relation thereto. The CLIENT agrees that any use, reuse, modification, or extension of FUGRO's data or information in this report by the CLIENT is at the CLIENT's sole risk and without liability to FUGRO. Should the data and report be made available in whole or part to any third party, and such party relies thereon, that party does so wholly at its own and sole risk and FUGRO disclaims any liability to such party.

2. Furthermore, the Survey was performed by FUGRO after considering the limits of the scope of work and the time scale for the Survey.

3. The results that are presented and the interpretation of these results by FUGRO represent only the distribution of ground conditions and geology that are measurable with the airborne geophysical instrumentation and survey design that was used. FUGRO endeavours to ensure that the results and interpretation are as accurate as can be reasonably achieved through a geophysical survey and interpretation by a qualified geophysical interpreter. FUGRO did not perform any observations, investigations, studies or testing not specifically defined in the Agreement between the CLIENT and FUGRO. The CLIENT accepts that there are limitations to the accuracy of information that can be derived from a geophysical survey, including, but not limited to, similar geophysical responses from different geological conditions, variable responses from apparently similar geology, and limitations on the signal which can be detected in a background of natural and electronic noise, and geological variation. The data presented relates only to the conditions as revealed by the measurements at the sampling points, and conditions between such locations and survey lines may differ considerably. FUGRO is not liable for the existence of any condition, the discovery of which would require the performance of services that are not otherwise defined in the Agreement.

4. The passage of time may result in changes (whether man-made or natural) in site conditions. The results provided in this report only represent the site conditions and geology for the period that the survey was flown.

5. Where the processing and interpretation have involved FUGRO's interpretation or other use of any information (including, but not limited to, topographic maps, geological maps, and drill information; analysis, recommendations and conclusions) provided by the CLIENT or by third parties on behalf of the CLIENT and upon which FUGRO was reasonably entitled or expected to rely upon, then the Survey is limited by the accuracy of such information. Unless otherwise stated, FUGRO was not authorized and did not attempt to independently verify the accuracy or completeness of such information that was received from the CLIENT or third parties during the performance of the Survey. FUGRO is not liable for any inaccuracies (including any incompleteness) in the said information.

Introduction

This report describes the logistics, data acquisition, processing and presentation of results of a DIGHEM electromagnetic, radiometric and magnetic airborne geophysical survey carried out for Rara Terra Minerals Corp over one property near Dease Lake, British Columbia. Total coverage of the survey block amounted to 696.4 km. The survey was flown between July 8 and July 14, 2012.

The purpose of the survey was to map the geology and structure of the area. Data were acquired using a DIGHEM electromagnetic system, supplemented by a high-sensitivity cesium magnetometer and a spectrometer. The information from these sensors was processed to produce maps and images that display the magnetic, radiometric and conductive properties of the survey area. A GPS electronic navigation system ensured accurate positioning of the geophysical data with respect to the base map coordinates.

The survey data were processed and compiled in the Fugro Airborne Surveys Toronto office. Maps and data in digital format are provided with this report.

TABLE OF CONTENTS

SURVEY AREA DESCRIPTION **8**
Location of the Survey Area 8
SYSTEM INFORMATION **11**
Aircraft and Geophysical On-Board Equipment 12
Base Station Equipment 14
QUALITY CONTROL AND IN-FIELD PROCESSING **15**
Navigation 15
Flight Path 15
Clearance 15
Flying Speed 16
Airborne High Sensitivity Magnetometer 16
Magnetic Base Station 16
Electromagnetic Data 16
In-Flight EM System Calibration 17
DATA PROCESSING **18**
Flight Path Recovery 18
Altitude Data 18
Magnetic Base Station Diurnal 19
Residual Magnetic Intensity 19
Magnetic First Vertical Derivative 20
Electromagnetic Data 20
Apparent Resistivity 20
Electromagnetic Anomalies 21
Radiometrics 23
Pre-filtering *23*
Live Time Correction *23*
Aircraft and Cosmic Background *23*
Compton Stripping *24*
Attenuation Corrections *25*
Conversion to Concentration and Ratios *26*
Digital Elevation 26
Contour, Colour and Shadow Map Displays 26
FINAL PRODUCTS **27**
Maps 27
Digital Archives 28
Report 28
Flight Path Videos 28

SURVEY RESULTS **29**
General Overview 29
Potential Zones of Interest 34
CONCLUSIONS AND RECOMMENDATIONS **39**

APPENDICES

APPENDIX A **40**
LIST OF PERSONNEL **40**
APPENDIX B **42**
DATA ARCHIVE DESCRIPTION **42**
APPENDIX C **47**
MAP PRODUCT GRIDS **47**
APPENDIX D **59**
CALIBRATION AND TESTS **59**
APPENDIX E **71**
BACKGROUND INFORMATION **71**
APPENDIX F **86**
DATA PROCESSING FLOWCHARTS **86**
APPENDIX G **90**
GLOSSARY **90**

TABLE OF TABLES

TABLE 1 AREA CORNERS NAD83 UTM ZONE 9N 9
TABLE 2 LINE KILOMETRE SUMMARY 9
TABLE 3 GPS BASE STATION LOCATION 9
TABLE 4 MAGNETIC BASE STATION LOCATION 10
TABLE 5 DIGHEM CONFIGURATION 12
TABLE 6 EM SYSTEM NOISE SPECIFICATIONS 17
TABLE 7 EM ANOMALY INTERPRETATION 21
TABLE 8 RADIOMETRIC PARAMETERS 25
TABLE 9: CONVERSION FACTORS FOR CPS TO EQUIVALENCE 26
TABLE 10 FINAL MAP PRODUCTS 27
TABLE 11 EM ANOMALY STATISTICS 33
TABLE 12: GEOPHYSICAL SIGNATURE FOR TARGETS R3 AND R5 36
TABLE 13: GEOPHYSICAL SIGNATURE OF TARGETS R5, R6 AND R7 37
TABLE 14 EM ANOMALY GRADES 74

TABLE 15 EFFECTS OF PERMITTIVITY ON IN-PHASE/QUADRATURE/RESISTIVITY 82

TABLE OF FIGURES

FIGURE 1 XENO PROJECT, DEASE LAKE AREA, BC - LOCATION MAP 8
FIGURE 2 DIGHEM SYSTEM 11
FIGURE 3 FLIGHT PATH VIDEO 19
FIGURE 4: RADIOMETRIC, CONDUCTIVE AND MAGNETIC PROPERTIES 29
FIGURE 5: 900 HZ RESISTIVITY DATA WITH OUTLINES OF MAGNETIC UNITS AND BREAKS. 30
FIGURE 6 TERNARY IMAGE WITH MAGNETIC ANOMALIES AND BREAKS 31
FIGURE 7: CALCULATED VERTICAL MAGNETIC GRADIENT 31
FIGURE 8: 56KHZ RESISTIVITY DATA 32
FIGURE 9: TH/K RATIO DATA 34
FIGURE 10 U/K RATIO 35
FIGURE 11: POTENTIAL TARGETS R3 AND R4 36
FIGURE 12: POTENTIAL TARGETS R 5, R6 & R7 37
FIGURE 13 RESIDUAL MAGNETIC FIELD 48
FIGURE 14 CALCULATED VERTICAL MAGNETIC GRADIENT 49
FIGURE 15 APPARENT RESISTIVITY 900 HZ 50
FIGURE 16: APPARENT RESISTIVITY 7200 HZ 51
FIGURE 17: RADIOMETRIC POTASSIUM COUNT 52
FIGURE 18: RADIOMETRIC THORIUM COUNT 53
FIGURE 19: RADIOMETRIC URANIUM COUNT 54
FIGURE 20: RADIOMETRIC TOTAL COUNT 55
FIGURE 21: RADIOMETRIC EQUIVALENT THORIUM/POTASSIUM RATIO 56
FIGURE 22: RADIOMETRIC EQUIVALENT URANIUM/POTASSIUM RATIO 57
FIGURE 23: RADIOMETRIC EQUIVALENT URANIUM/THORIUM RATIO 58
FIGURE 24 EM ANOMALY SHAPES 73

Survey Area Description

Location of the Survey Area

One block near Dease Lake, British Columbia (Figure 1) was flown between July 8 and July 14, 2012, with Terminus Mountain Lodge, BC as the base of operations. Survey coverage consisted of 578.2 km of traverse lines flown with a spacing of 200 m and 118.2 km of tie lines with a spacing of 1000 m for a total of 696.4 km.

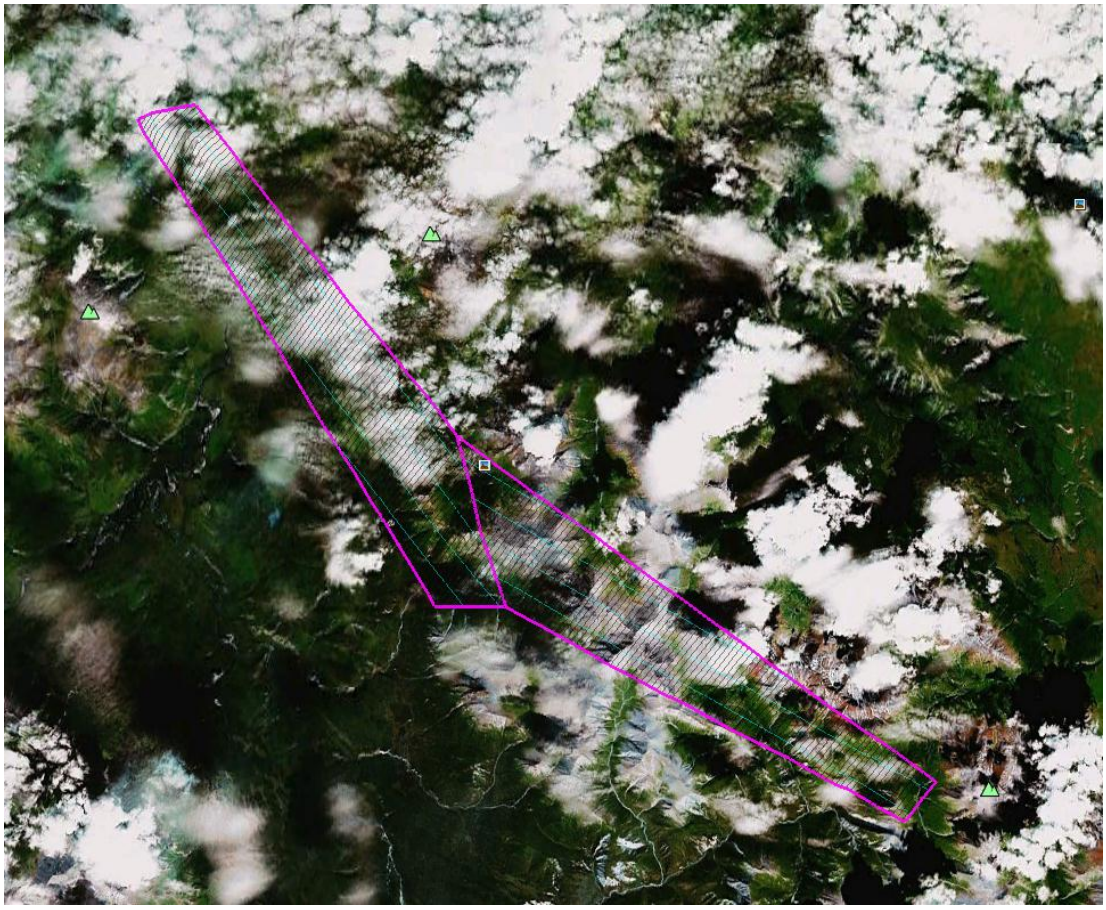

Figure 1 Xeno Project, Dease lake Area, BC - Location Map

Table 1 contains the coordinates of the corner points of the survey blocks.

Block	Corners	X-UTM (E)	Y-UTM (N)
11075-1	1	565821	6528528
Xeno Project, Dease lake Area, BC	2	567974	6529030
	3	577571	6517609
	4	594842	6505926
	5	593789	6504508
	6	579501	6511615
	7	576969	6511564

Table 1 Area Corners NAD83 UTM Zone 9N

Block	Line Numbers	Line direction	Line Spacing	Line km
1	10010 - 11840	37°/217°	200 m	578.2 km
Xeno Project, Dease lake Area, BC	19010 – 19040	140°/320°	1000 m	118.2 km
	29010 - 29040	118°/298°	1000 m	

Table 2 Line kilometre summary

During the survey GPS base stations were set up to collect data to allow post processing of the positional data for increased accuracy. The location of the GPS base stations are shown in Table 3.

Status	Location Name	WGS84 Longitude (deg-min-sec)	WGS84 Latitude (deg-min-sec)	Orthometric Height (m)
Primary (07-07-12)	Terminus Mountain Lodge, BC	127° 07’ 22.3235” W	58° 43’ 34.99964” N	681.100
Secondary 1 (07-07-12)	Terminus Mountain Lodge, BC	127° 07’ 25.98983” W	58° 43’ 35.48191” N	677.895
Secondary 2 (07-07-12)	Terminus Mountain Lodge, BC	127° 07’ 25.66963” W	58° 43’ 35.57227” N	670.120
Secondary 1 (07-12-12)	Terminus Mountain Lodge, BC	127° 07’ 23.64700” W	58° 43’ 31.29943” N	679.580
Secondary 2 (07-12-12)	Terminus Mountain Lodge, BC	127° 07’ 23.63668” W	58° 43’ 31.19769” N	670.120

Table 3 GPS Base Station Location

The location of the Magnetic base stations are shown in Table 4.

Status	Location Name	WGS84 Longitude (deg-min-sec)	WGS84 Latitude (deg-min-sec)
Primary (07-07-12)	Terminus Mountain Lodge, BC	127° 07’ 25.98983” W	58° 43’ 35.48191” N
Secondary (07-07-12)	Terminus Mountain Lodge, BC	127° 07’ 25.66963” W	58° 43’ 35.57227” N
Primary (07-12-12)	Terminus Mountain Lodge, BC	127° 07’ 23.64700” W	58° 43’ 31.29943” N
Secondary (07-12-12)	Terminus Mountain Lodge, BC	127° 07’ 23.63668” W	58° 43’ 31.19769” N

Table 4 Magnetic Base Station Location

System Information

Figure 2 DIGHEM System

The DIGHEM system comprises a 30 m cable which tows a 9 m bird containing the EM transmitter and receiver coil pairs (three coplanar and two coaxial), a magnetometer, a laser altimeter and a GPS antenna for flight path recovery. The helicopter has a tail boom mounted GPS antenna for in-flight navigation, radar and barometric altimeters, a 256-channel spectrometer, a video camera and a data acquisition system.

Aircraft and Geophysical On-Board Equipment

Helicopter: AS350 B3

Operator: Questral Helicopters

Registration: C-FHKM

Average Survey Speed: 68 km/h (19m/s)

EM System: DIGHEM, symmetric dipole configuration.

Dipole Moment (Atm^2)	Orientation	Nominal Frequency	Actual Frequency	Coil Separation (m)	Sensitivity
211	Coaxial	1,000 Hz	1,121 Hz	7.98	0.12 ppm
211	Coplanar	900 Hz	926 Hz	7.98	0.12 ppm
67	Coaxial	5,500 Hz	5,504Hz	7.98	0.24 ppm
56	Coplanar	7,200 Hz	7,308 Hz	7.98	0.24 ppm
15	Coplanar	56,000 Hz	55,470 Hz	6.33	0.44 ppm

Table 5 DIGHEM Configuration

Digital Acquisition: Fugro Airborne Surveys HeliDAS.

Video: Panasonic WVCD/32 Camera with Axis 241S Video Server. Camera is mounted to the exterior bottom of the helicopter between the forward skid tubes

Magnetometer: Scintrex Cesium Vapour (CS-2 or CS-3), mounted in the EM bird;

Operating Range: 15,000 to 100,000 nT
Operating Limit: -40°C to 50°C
Accuracy: ±0.002 nT
Measurement Precision: 0.001 nT
Sampling rate: 10.0 Hz

Spectrometer:	Radiation Solutions RS-500 with 16.8 L downward-looking crystals and 4.2 L upward-looking crystal Operating Range: 0 to 100,000 counts/sec Operating Limit: -20°C to 50°C Average Dead-Time: 5 µsec/pulse Sampling rate = 1.0 Hz
Radar Altimeter:	Honeywell Sperry Altimeter System. Radar antennas are mounted to the exterior bottom of the helicopter between the forward skid tubes Operating Range: 0 – 2500ft Operating Limit: -55°C to 70°C 0 to 55,000 ft Accuracy: ± 3% (100 – 500ft above obstacle) ± 4% (500 – 2500ft above obstacle) Measurement Precision: 1 ft Sample Rate: 10.0 Hz
Laser Altimeter:	Optech G-150 mounted in the EM bird; Operating Range: 0.2 to 250 m Operating Limit: -10°C to 45°C Accuracy: ±5 cm (10°C to 30°C) ±10 cm (-10°C to 45°C) Measurement Precision: 1 cm Sample Rate: 10.0 Hz
Aircraft Navigation:	NovAtel OEM4 Card with an Aero antenna mounted on the tail of the helicopter; Operating Limit: -40°C to 85°C Real-Time Accuracy: 1.2m CEP (L1 WAAS) Real-Time Measurement Precision: 6 cm RMS Sample Rate: 2.0 Hz
EM Bird Positional Data:	NovAtel OEM4 with Aero Antenna mounted on the EM bird. Operating Limit: -40°C to 85°C Real-Time Accuracy: 1.8m CEP (L1) Real-Time Measurement Precision: 6 cm RMS Sample Rate: 2.0 Hz
Barometric Altimeter:	Motorola MPX4115AP analog pressure sensor mounted in the

helicopter

Operating Range: 55 kPa to 108 kPa
Operating Limit: -40°C to 125°C
Accuracy:
± 1.5 kPa (0°C to 85°C)
± 3.0 kPa (-20°C to 0°C, 85°C to 105°C)
± 4.5 kPa (-40°C to -20°C, 105°C to 125°C)
Measurement Precision: 0.01 kPa
Sampling Rate = 10.0 Hz

Temperature: Analog Devices 592 sensor mounted on the camera box

Operating Range: -40°C to + 75°C
Operating Limit: -40°C to + 75°C
Accuracy: ± 1.5°C
Measurement Precision: 0.03°C
Sampling Rate = 10.0 Hz

Base Station Equipment

Primary Magnetometer: Fugro CF1 using Scintrex cesium (CS-3) vapour sensor with Marconi GPS card and antenna for measurement synchronization to GPS. The base station also collects barometric pressure and outside temperature.

Magnetometer Operating Range: 15,000 to 100,000 nT
Barometric Operating Range: 55kPa to 108 kPa
Temperature Operating Range: -40°C to 75°C
Sample Rate: 1.0 Hz

GPS Receiver: NovAtel OEM4 Card with an Aero antenna

Real-Time Accuracy:
1.8m CEP (L1)
Sample Rate: 1.0 Hz

Secondary Magnetometer: Scintrex cesium (CS-3) vapour sensor

Magnetometer Operating Range: 15,000 to 100,000 nT
Barometric Operating Range: 55kPa to 108 kPa
Temperature Operating Range: -40°C to 75°C
Sample Rate: 1.0 Hz

Quality Control and In-Field Processing

Digital data for each flight were transferred to the field workstation, in order to verify data quality and completeness. A database was created and updated using Geosoft Oasis Montaj and proprietary Fugro Atlas software. This allowed the field personnel to calculate, display and verify both the positional (flight path) and geophysical data. The initial database was examined as a preliminary assessment of the data acquired for each flight.

In-field processing of Fugro survey data consists of differential corrections to the airborne GPS data, verification of EM calibrations, drift correction of the raw airborne EM data, spike rejection and filtering of all geophysical and ancillary data, verification of the digital flight path recordings, calculation of preliminary resistivity data, and diurnal correction of magnetic data.

All data, including base station records, were checked on a daily basis to ensure compliance with the survey contract specifications. Re-flights were required if any of the following specifications were not met.

Navigation

A specialized GPS system provided in-flight navigation control. The system determined the absolute position of the helicopter by monitoring the range information of twelve channels (satellites). The Novatel OEM4 receiver was used for this application. In North America, the OEM4 receiver is WAAS-enabled (Wide Area Augmentation System) providing better real-time positioning.

A Novatel OEM4 GPS base station was used to record pseudo-range, carrier phase, ephemeris, and timing information of all available GPS satellites in view at a one second interval. These data are used to improve the conversion of aircraft raw ranges to differentially corrected aircraft position. The GPS antenna was set-up in a location that allowed for clear sight of the satellites above. The set-up of the antenna also considered surfaces that could cause signal reflection around the antenna that could be a source of error to the received data measurements.

Flight Path

Flight lines did not deviate from the intended flight path by more than 25% of the planned flight path over a distance of more than 1 kilometre. Flight specifications were based on GPS positional data recorded at the helicopter.

Clearance

The survey elevation is defined as the measurement of the helicopter radar altimeter to the tallest obstacle in the helicopter path. An obstacle is any structure or object which will impede the path of the helicopter to the ground and is not limited to and includes tree canopy, towers and power lines.

Survey elevations may vary based on the pilot's judgement of safe flying conditions around man-made structures or in rugged terrain.

The average survey elevation achieved for the helicopter and instrumentation during data collection was:

Helicopter	60 metres
Spectrometer	60 metres
Magnetometer	35 metres
DIGHEM EM sensor	35 metres

Survey elevations did not deviate by more than 20% over a distance of 2 km from the contracted elevation.

The achieved survey height average was impacted by steep terrain flying.

Flying Speed

Average calculated groundspeed was 68 km/h. The aircraft calculated groundspeed was between 3.6 to 147 km/h. This resulted in an equivalent ground sample interval of approximately 0.1 to 4.1 metres at a 10 Hz sampling rate. Variance in the survey speed was due to climbing and descending over steep terrain.

Airborne High Sensitivity Magnetometer

To assess the noise quality of the collected airborne magnetic data, Fugro monitors the 4th difference results during flight which is verified post flight by the processor. The contracted specification for the collected airborne magnetic data was that the non-normalized 4th difference would not exceed 1.6 nT over a continuous distance of 1 kilometre excluding areas where this specification was exceeded due to natural anomalies.

Magnetic Base Station

Ground magnetic base stations were set-up to measure the total intensity of the earth's magnetic field. The base stations were placed in a magnetically quiet area, away from power lines and moving metallic objects. The contracted specification for the collected ground magnetic data was the non-linear variations in the magnetic data were not to exceed 10 nT per minute. Throughout the period of the survey the earth's magnetic activity was calm. Fugro's standard of setting up the base station within 50 km from the centre of the survey block allowed for successful removal of the active magnetic events on the collected airborne magnetic data.

Electromagnetic Data

The contracted specification for the EM channels was a peak to peak noise envelope not to exceed the specified tolerance (Table 5) continuously over a horizontal distance of 2,000 metres under normal survey conditions.

The effects of spheric pulses were monitored on the EM channels by visual assessment of the data and monitoring of two spheric channels during flight operations. Spheric pulses may occur having strong peaks but narrow widths. Flying was not performed when spheric pulses became sufficiently intense and frequent that digital data processing techniques could not recover useful data.

The acceptable noise limits of the EM channels are stated below:

Frequency	Coil Orientation	Peak to Peak Noise Envelope (ppm)
1,000 Hz	vertical coaxial	5.0
900 Hz	horizontal coplanar	10.0
5,500 Hz	vertical coaxial	10.0
7,200 Hz	horizontal coplanar	20.0
56,000 Hz	horizontal coplanar	40.0

Table 6 EM System Noise Specifications

In-Flight EM System Calibration

Calibration of the system during the survey uses the Fugro AutoCal automatic, internal calibration process. At the beginning and end of each flight, and at intervals during the flight, the system is flown up to high altitude to remove it from any "ground effect" (response from the earth). Any remaining signal from the receiver coils (base level) is measured as the zero level, and is removed from the data collected until the time of the next calibration. Following the zero level setting, internal calibration coils, for which the response phase and amplitude have been determined at the factory, are automatically triggered – one for each frequency. The on-time of the coils is sufficient to determine an accurate response through any ambient noise. The receiver response to each calibration coil "event" is compared to the expected response (from the factory calibration) for both phase angle and amplitude, and any phase and gain corrections are automatically applied to bring the data to the correct value.

In addition, the outputs of the transmitter coils are continuously monitored during the survey, and the gains are adjusted to correct for any change in transmitter output.

Because the internal calibration coils are calibrated at the factory (on a resistive half-space) ground calibrations using external calibration coils on-site are not necessary for system calibration. A check calibration may be carried out on-site to ensure all systems are working correctly. All system calibrations will be carried out in the air, at sufficient altitude that there will be no measurable response from the ground.

The internal calibration coils are rigidly positioned and mounted in the system relative to the transmitter and receiver coils. In addition, when the internal calibration coils are calibrated at the factory, a rigid jig is employed to ensure accurate response from the external coils.

Using real time Fast Fourier Transforms and the calibration procedures outlined above, the data are processed in real time, from measured total field at a high sampling rate, to in-phase and quadrature values at 10 samples per second.

Data Processing

Flight Path Recovery

To check the quality of the positional data the speed of the bird is calculated using the differentially corrected x, y and z data. Any sharp changes in the speed are used to flag possible problems with the positional data. Where speed jumps occur, the data are inspected to determine the source of the error. The erroneous data are deleted and splined if less than two seconds in length. If the error is greater than two seconds the raw data are examined and if acceptable, may be shifted and used to replace the bad data. The gps z component is the most common source of error. When it shows problems that cannot be corrected by recalculating the differential correction, the barometric altimeter is used as a guide to assist in making the appropriate correction. The corrected WGS84 longitude and latitude coordinates were transformed to NAD83 using the following parameters.

Datum:	NAD83
Ellipsoid:	Clarke 1866
Projection:	UTM Zone 9N
Central meridian:	129° West
False Easting:	500000 metres
False Northing:	0 metres
Scale factor:	0.9996
WGS84 to Local Conversion:	Molodensky
Dx,Dy,Dz:	0, 0, 0

Recorded video flight path may also be linked to the data and used for verification of the flight path. Fiducial numbers are recorded continuously and are displayed on the margin of each digital image. This procedure ensures accurate correlation of data with respect to visible features on the ground. The fiducials appearing on the video frames and the corresponding fiducials in the digital profile database originate from the data acquisition system and are based on incremental time from start-up. Along with the acquisition system time, UTC time is also recorded in parallel and displayed (Figure 3).

Altitude Data

Radar altimeter data are despiked by applying a 1.5 second median and smoothed using a 1.5 second Hanning filter. The radar altimeter data are then subtracted from the GPS elevation to create a digital elevation model that is gridded and used in conjunction with profiles of the radar altimeter and flight path video to detect any spurious values.

Laser altimeter data are despiked and filtered using an alphatrim filter. The laser altimeter data are then subtracted from the GPS elevation to create a digital elevation model that is examined in grid format for spurious values. The laser does a better job of piercing the tree canopy than the radar altimeter, and was used in the resistivity/depth calculation.

Figure 3 Flight path video

Magnetic Base Station Diurnal

The raw diurnal data are sampled at 1 Hz and imported into a database. The data are filtered with a 51-point median filter and then a 51-point Hanning filter to remove spikes and smooth short wavelength variations. A non linear variation is then calculated and a flag channel is created to indicate where the variation exceeds the survey tolerance. Acceptable diurnal data are interpolated to a 10 Hz sample rate and the local regional field value, calculated from the average of the first day's diurnal data, is removed to leave the diurnal variation. This diurnal variation is then ready to be used in the processing of the airborne magnetic data.

Residual Magnetic Intensity

The Total Magnetic Field (TMF) data collected in flight were profiled on screen along with a fourth difference channel calculated from the TMF. Spikes were removed manually where indicated by the fourth difference. The despiked data were then corrected for lag by 3.1 seconds. The diurnal variation that was extracted from the filtered ground station data was then removed from the despiked and lagged TMF and an average magnetic base value of 57379.0 was added back. The IGRF was calculated using the 2010 IGRF model for the specific survey location, date and altitude of the sensor and removed from the TMF to obtain the Residual Magnetic Intensity (RMI). The results were then levelled using tie and traverse line intercepts. Manual adjustments were applied to any lines that required levelling, as indicated by shadowed images of the gridded magnetic data. The manually levelled data were then subjected to a microlevelling filter.

Magnetic First Vertical Derivative

The levelled, Residual Magnetic Intensity grid was subjected to a processing algorithm that enhances the response of magnetic bodies in the upper 500 metres and attenuates the response of deeper bodies. The resulting calculated vertical gradient grid (CVG) provides better definition and resolution of near-surface magnetic units. It also identifies weak magnetic features that may not be quite as evident in the RMI data. Regional magnetic variations and changes in lithology, however, may be better defined on the Residual Magnetic Intensity.

Electromagnetic Data

EM data are processed at the recorded sample rate of 10 Hz. Profiles of the data were examined on a flight by flight basis on screen to check in-flight calibrations and high altitude background removal. A lag of 1.0 seconds was applied and then a 9-point median and a 9-point Hanning filter were used to reduce noise to acceptable levels. Flights were then displayed and corrected for drift. Following that individual lines were displayed and further levelling corrections were applied while referencing the calculated apparent resistivity.

The EM data are examined to allow the interpreter to select the most appropriate EM anomaly picking controls for a given survey area. The EM picking parameters depend on several factors but are primarily based on the dynamic range of the resistivities within the survey area, and the types and expected geophysical responses of the targets being sought.

Apparent Resistivity

The apparent resistivities in ohm·m are generated from the in-phase and quadrature EM components for all of the coplanar frequencies, using a pseudo-layer half-space model. The inputs to the resistivity algorithm are the in-phase and quadrature amplitudes of the secondary field. The algorithm calculates the apparent resistivity in ohm·m, and the apparent height of the bird above the conductive source. Any difference between the apparent height and the true height, as measured by the laser altimeter, is called the pseudo-layer and reflects the difference between the real geology and a homogeneous halfspace. This difference is often attributed to the presence of a highly resistive upper layer. Any errors in the altimeter reading, caused by heavy tree cover, are included in the pseudo-layer and do not affect the resistivity calculation. The apparent depth estimates, however, will reflect the altimeter errors. Apparent resistivities calculated in this manner may differ from those calculated using other models.
In areas where the effects of magnetic permeability or dielectric permittivity have suppressed the in-phase responses, the calculated resistivities will be erroneously high. Various algorithms and inversion techniques can be used to partially correct for the effects of permeability and permittivity.

Apparent resistivity maps portray all of the information for a given frequency over the entire survey area. The large dynamic range afforded by the multiple frequencies makes the apparent resistivity parameter an excellent mapping tool.

The preliminary apparent resistivity images are carefully inspected to identify any lines or line segments that might require base level adjustments. Subtle changes between in-flight calibrations of the system can result in line-to-line differences that are more recognizable in resistive (low signal amplitude) areas. If required, manual level adjustments are carried out on the EM data to eliminate or minimize resistivity differences that can be attributed, in part, to changes in operating temperatures. These levelling

adjustments are usually very subtle, and do not result in the degradation of discrete anomalies.

After the manual levelling process is complete, revised resistivity grids are created. The resulting grids can be subjected to a microlevelling technique in order to smooth the data for contouring. The coplanar resistivity parameter has a broad 'footprint' that requires very little filtering.

Electromagnetic Anomalies

Anomalous electromagnetic responses are selected and analysed by computer to provide a preliminary electromagnetic anomaly map. The automatic selection algorithm is intentionally oversensitive to assure that no meaningful responses are missed. Using the preliminary picks in conjunction with the profile data, the interpreter then classifies the anomalies according to their source and eliminates those that are not substantiated by the data. The final interpreted EM anomalies include bedrock, surficial and cultural conductors, based on the typical HEM anomaly shapes shown in Figure 24. The types of conductors interpreted from the EM data are given below in Table 7.

Interpretation Symbol	Conductor Model
D	Narrow bedrock conductor (“vertical or dipping thin dyke”)
B	Bedrock conductor
S	Conductive cover (“horizontal thin sheet”)
H	Broad conductive rock unit, deep conductive weathering, thick conductive cover (“half space”)
E	Edge of broad conductor (“edge of a half space”)
L	Culture, e.g. power line, metal building or fence
“?”	Indicates some degree of uncertainty as to which is the most appropriate EM source model, but does not question the validity of the EM anomaly

Table 7 EM Anomaly Interpretation

EM anomalies are based on a near-vertical, half plane model. This model best reflects "discrete" bedrock conductors. Wide bedrock conductors or flat-lying conductive units, whether from surficial or bedrock sources, may give rise to very broad anomalous responses on the EM profiles. These broad conductors, which more closely approximate a half-space model, will be maximum coupled to the horizontal (coplanar) coil-pair and should be more evident on the resistivity parameter. Resistivity maps, therefore, may be more valuable than the electromagnetic anomaly maps, in areas where broad or flat-lying conductors are considered to be of importance.

Excellent resolution and discrimination of conductors was accomplished by using a fast sampling rate of 0.1 sec and by employing a “common” frequency (5500/7200 Hz) on two orthogonal coil-pairs (coaxial and coplanar). The resulting in-phase and quadrature difference channel parameters (DIFI and DIFQ) often permit differentiation of bedrock and surficial conductors, even though they may exhibit similar conductance values. For any Fugro multi-component helicopter frequency domain EM system (HFEM), the difference channel is a calculated product to assist interpretation of discrete conductor targets.

The difference channel is a parameter used to quantify the difference between the coaxial and

coplanar responses. It helps to distinguish which conductivity changes are caused by flat-lying conductors (like swamps) or changes in the layered earth (with a 1:4 ratio between CX and CP), and which anomalies are caused by discrete conductive bodies. The difference between the CP and CX for both in-phase and quadrature EM data is calculated everywhere, weighted to adjust the response for the geometric difference as well as differences in coil separation. For a flat-lying or halfspace (thick, flat-lying) conductor, the difference channel (DIFI or DIFQ) will be near zero, as it will over background areas (a layered earth). For a discrete conductor like a vertical thin dike, the difference channel will have a positive value. In practice the value will be somewhat variable, depending on the shape and thickness of the conductor and the conductivity of the host rock.

Anomalies that occur near the ends of the survey lines (i.e., outside the survey area) should be viewed with caution. Some of the weaker anomalies could be due to aerodynamic noise, i.e., bird bending, which is created by abnormal stresses to which the bird is subjected during the climb and turn of the aircraft between lines. Such aerodynamic noise is usually manifested by an anomaly on the coaxial in-phase channel only, although severe stresses can affect the coplanar in-phase channels as well.

EM anomalies may be grouped into three general categories. The first type consists of discrete, well-defined anomalies that yield marked inflections on the difference channels. These anomalies are usually attributed to conductive sulphides or graphite and are generally given a "B" (bedrock), "D" (vertical or dipping thin dyke) or "T" (vertical or dipping thick dyke) interpretive symbol, all denoting a bedrock source. EM anomalies that do not display the classic anomaly shape of the “thin dyke” model, but are considered to reflect sources at depth are generally given a “B” interpretation. The “T” anomaly is a very specific anomaly type, and is generally not used unless the specific criteria defined in Figure 24 are met.

The second class of anomalies comprises moderately broad responses that exhibit the characteristics of a half-space and do not yield well-defined inflections on the difference channels. Anomalies in this category are usually given an "S" or "H" interpretive symbol. The lack of a difference channel response usually implies a broad or flat-lying conductive source such as overburden. Some of these anomalies could reflect conductive rock units, zones of deep weathering, or the weathered tops of kimberlite pipes, all of which can yield “non-discrete” signatures.

The effects of conductive overburden are evident over portions of the survey area. Although the difference channels (DIFI and DIFQ) are extremely valuable in detecting bedrock conductors that are partially masked by conductive overburden, sharp undulations in the bedrock/overburden interface can yield anomalies in the difference channels which may be interpreted as possible bedrock conductors. Such anomalies usually fall into the "S?" or "B?" classification but may also be given an "E" interpretive symbol, denoting a resistivity contrast at the edge of a conductive unit.

The "?" symbol does not question the validity of an anomaly, but instead indicates some degree of uncertainty as to which is the most appropriate EM source model. This ambiguity results from the combination of effects from two or more conductive sources, such as overburden and bedrock, gradational changes, or moderately shallow dips. The presence of a conductive upper layer has a tendency to mask or alter the characteristics of bedrock conductors, making interpretation difficult. This problem is further exacerbated in the presence of magnetite.

In areas where EM responses are evident primarily on the quadrature components, zones of poor conductivity are indicated. Where these responses are coincident with magnetic anomalies, it is

possible that the in-phase component amplitudes have been suppressed by the effects of magnetite. Poorly-conductive magnetic features can give rise to resistivity anomalies that are only slightly below or slightly above background. If it is expected that poorly-conductive economic mineralization could be associated with magnetite-rich units, most of these weakly anomalous features will be of interest. In areas where magnetite causes the in-phase components to become negative, the apparent conductance and depth of EM anomalies will be unreliable. Magnetite effects usually give rise to overstated (higher) resistivity values and understated (shallow) depth calculations.

The third class of anomalies consists of cultural anomalies, which are usually given the symbol "L" or "L?". Anomalies in this category can include telephone or power lines, pipelines, railways, fences, metal bridges or culverts, buildings and other metallic structures.

Radiometrics

All radiometric data reductions performed by Fugro rigorously follow the procedures described in the IAEA Technical Report[1].

All processing of radiometric data was undertaken at the natural sampling rate of the spectrometer, i.e., one second. The data were not interpolated to match the fundamental 0.1 second interval of the EM and magnetic data.

Pre-filtering

Four parameters were filtered, but not returned to the database:

- Radar altimeter, pressure and temperature were smoothed with a 3-point Hanning filter
- Cosmic was smoothed with a 9-point Hanning filter

Live Time Correction

The spectrometer, a Radiation Solutions RS-500, uses the notion of "live time" to express the relative period of time the instrument was able to register new pulses per sample interval. This is the opposite of the traditional "dead time", which is an expression of the relative period of time the system was unable to register new pulses per sample interval.

The GR-820 measures the live time electronically, and outputs the value in milliseconds. The live time correction is applied to the total count, potassium, uranium, thorium, upward uranium and cosmic channels. The formula used to apply the correction is as follows:

$$C_{lt} = C_{raw} * \frac{1000.0}{L}$$

where: C_{lt} is the live time corrected channel in counts per second
C_{raw} is the raw channel data in counts per second
L is the live time in milliseconds

Aircraft and Cosmic Background

Aircraft background and cosmic stripping corrections were applied to the total count, potassium, uranium, thorium and upward uranium channels using the following formula:

[1] Exploranium, I.A.E.A. Report, Airborne Gamma-Ray Spectrometer Surveying, Technical Report No. 323, 1991

$$C_{ac} = C_{lt} - (a_c + b_c * \mathrm{Cos}_f)$$

where: C_{ac} is the background and cosmic corrected channel
C_{lt} is the live time corrected channel
a_c is the aircraft background for this channel
b_c is the cosmic stripping coefficient for this channel
Cos_f is the filtered Cosmic channel

Compton Stripping

Following the radon correction, the potassium, uranium and thorium are corrected for spectral overlap. First, α,β and γ the stripping ratios, are modified according to altitude. Then an adjustment factor based on a, the reversed stripping ratio, uranium into thorium, is calculated. (Note: the stripping ratio altitude correction constants are expressed in change per metre. A constant of 0.3048 is required to conform to the internal usage of height in feet):

$$\alpha_h = \alpha + h_{ef} * 0.00049$$

$$\alpha_r = \frac{1.0}{1.0 - a * \alpha_h}$$

$$\beta_h = \beta + h_{ef} * 0.00065$$

$$\gamma_h = \gamma + h_{ef} * 0.00069$$

where: α, β, γ are the Compton stripping coefficients
α_h, β_h, γ_h are the height corrected Compton stripping coefficients
h_{ef} is the height above ground in metres
α_r is the scaling factor correcting for back scatter
a is the reverse stripping ratio

The stripping corrections are then carried out using the following formulas:

$$Th_c = (Th_{rc} - a * U_{rc}) * \alpha_r$$
$$K_c = K_{rc} - \gamma_h * U_c - \beta_h * Th_c$$
$$U_c = (U_{rc} - \alpha_h * Th_{\gamma c}) * \alpha_\gamma$$

where: U_c, Th_c and K_c are corrected uranium, thorium and potassium
α_h,β_h,γ_h are the height corrected Compton stripping coefficients
U_{rc}, Th_{rc} and K_{rc} are radon-corrected uranium, thorium and potassium
α_r is the backscatter correction

Attenuation Corrections

The total count, potassium, uranium and thorium data are then corrected to a nominal survey altitude, in this case 60 m. This is done according to the equation:

$$C_a = C * e^{\mu(h_{ef} - ho)}$$

where: C_a is the output altitude corrected channel
C is the input channel
e^{μ} is the attenuation correction for that channel
h_{ef} is the effective altitude
h_0 is the nominal survey altitude to correct to

The radiometric correction parameters used for this survey were:

Cosmic Correction: TC	1.305126	22.782973
Cosmic Correction: K	0.085464	3.716780
Cosmic Correction: U	0.063507	-0.485623
Cosmic Correction: Th	0.069926	-1.059239
Cosmic Correction: UpU	0.014321	0.646759
Compton Stripping: Alpha	0.289	
Compton Stripping: Beta	0.421	
Compton Stripping: Gamma	0.782	
Compton Stripping: AlphaPerMetre	0.00049	
Compton Stripping: BetaPerMetre	0.00065	
Compton Stripping: GammaPerMetre	0.00069	
Compton Stripping: GrastyBackscatter_a	0.036	
Compton Stripping: GrastyBackscatter_b	-0.004	
Compton Stripping: GrastyBackscatter_g	-0.001	
Altitude Attenuation: TC	-0.006700	
Altitude Attenuation: K	-0.007953	
Altitude Attenuation: U	-0.007239	
Altitude Attenuation: Th	-0.006587	
Radon Correction Parameter: TC	14.99	702.17
Radon Correction Parameter: K	0.91	90.01
Radon Correction Parameter: Th	0.003	27.60
Radon Correction Parameter: UpU	0.3414	-6.062
A1=0.065215 A2=0.032072		

Table 8 Radiometric parameters

Conversion to Concentration and Ratios

The final leveled counts data was converted to ground concentration using the following conversion factors:

Element	Conversion Factor
Potassium Counts	58.2 cps/%
Uranium Counts	6.48 cps/ppm
Thorium Counts	3.87 cps/ppm

Table 9: Conversion factors for CPS to Equivalence

The concentration values were then gridded using a minimum curvature method and an algorithm was applied to create the three ratio grids.

Digital Elevation

The laser altimeter values (ALTL – aircraft to ground clearance) are subtracted from the differentially corrected and de-spiked GPS-Z values to produce profiles of the height above mean sea level along the survey lines. These values are gridded to produce contour maps showing approximate elevations within the survey area. Any subtle line-to-line discrepancies are manually removed. After the manual corrections are applied, the digital terrain data are filtered with a microlevelling algorithm.

The accuracy of the elevation calculation is directly dependent on the accuracy of the two input parameters, ALTL and GPS-Z. The GPS-Z value is primarily dependent on the number of available satellites. Although post-processing of GPS data will yield X and Y accuracies in the order of 1-2 metres, the accuracy of the Z value is usually much less, sometimes in the ±5 metre range. Further inaccuracies may be introduced during the interpolation and gridding process.

Because of the inherent inaccuracies of this method, no guarantee is made or implied that the information displayed is a true representation of the height above sea level. Although this product may be of some use as a general reference, THIS PRODUCT MUST NOT BE USED FOR NAVIGATION PURPOSES.

Contour, Colour and Shadow Map Displays

The magnetic and resistivity data are interpolated onto a regular grid using a modified Akima spline technique. The resulting grid is suitable for image processing and generation of contour maps. The grid cell size is 20% of the line interval. Radiometric data grids are created using a minimum curvature algorithm with a grid cell size equal to 25% of the line interval.

Colour maps are produced by interpolating the grid down to the pixel size. The parameter is then incremented with respect to specific amplitude ranges to provide colour "contour" maps.

Final Products

This section lists the final maps and products that have been provided under the terms of the survey agreement. Other products can be prepared from the existing dataset, if requested. These include magnetic enhancements or derivatives, percent magnetite, resistivities corrected for magnetic permeability and/or dielectric permittivity, digital terrain, resistivity-depth sections, inversions, and overburden thickness. Most parameters can be displayed as contours, profiles, or in colour.

Maps

Base maps of the survey area were produced by scanning published topographic maps to a bitmap (.bmp) format. This process provides a relatively accurate, distortion-free base that facilitates correlation of the navigation data to the map coordinate system. The topographic files were combined with geophysical data for plotting some of the final maps. All maps were created using the following parameters:

Projection Description:

Datum:	NAD83
Ellipsoid:	GRS80
Projection:	UTM Zone 9N
Central meridian:	129° West
False Easting:	500000 metres
False Northing:	0 metres
Scale factor:	0.9996
WGS84 to Local Conversion:	Molodensky
Dx,Dy,Dz:	0, 0, 0

Maps depicting the survey results have been plotted and provided as a PDF (or .MAP) at a scale of 1:20,000 as listed in Table 10. Each parameter is plotted on one map sheet.

Final Map Products	No. of Map Sets Plotted
EM Anomalies	2
Residual Magnetic Intensity	2
Calculated Vertical Magnetic Gradient	2
Apparent Resistivity 900 Hz	2
Apparent Resistivity 7,200 Hz	2
Total Count	2
Potassium	2
Uranium	2
Thorium	2
Uranium/Thorium Ratio	2
Uranium/Potassium Ratio	2
Thorium/Potassium Ratio	2

Table 10 Final Map Products

Digital Archives

Line and grid data in the form of a Geosoft database (*.gdb) and XYZ file and Geosoft grids (*.grd) have been written to DVD. The formats and layouts of these archives are further described in Appendix B (Data Archive Description).

Report

Two paper copies of this Geophysical Survey Report plus a digital copy in PDF format.

Flight Path Videos

All survey flights in BIN/BDX format with a viewer.

SURVEY RESULTS

General Overview

The geophysical signature for carbonatite related REE deposits can vary greatly depending upon many factors which include, but not limited to, carbonatite type, alteration, and host and adjacent lithologies[2]. (Hoover, 1992).

The magnetic data may be used as a direct identification for follow-up targets if the deposits within the survey area contain sufficient quantities of magnetite or other magnetic minerals. Anomalous radiometric highs can also be used as an exploration guide, in particular high thorium and uranium concentrations. Carbonatite and other REE generally do not yield a distinctive EM anomaly but the resistivity data, along with the magnetic and radiometric datasets, can be useful in highlighting changes in lithologies, alteration zones and mapping structural features within the survey area.

Images of the survey area with respect to the magnetic, conductive and radiometric properties are displayed in Figure 4.

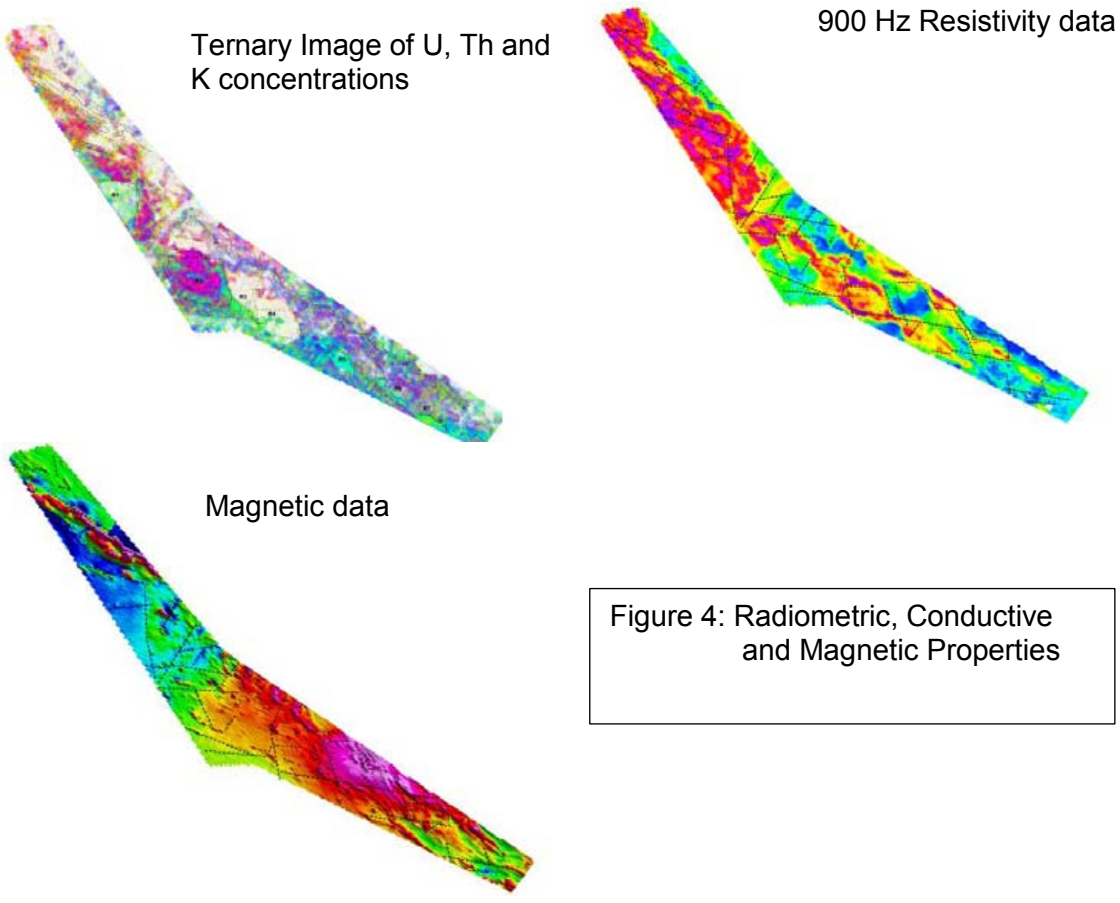

Figure 4: Radiometric, Conductive and Magnetic Properties

[2] [2] Hoover, D.B., compiler, 1992, Geophysical model of carbonatite, in Hoover, D.B., Heran,W.D., and Hill, P.L., eds., The geophysical expression of selected mineral deposit models: U.S. Geological Survey Open-File Report 92-557, p80-84.

The radiometric data in Figure 4 is presented as a ternary image with red colours representing potassium, blue representing Thorium and yellow representing Uranium concentration. Higher relative concentrations of thorium and uranium yield green colours, orange colours represent higher potassium (red) and Uranium (Yellow), and purple represents higher Potassium (red) and Thorium (blue). The darker colours represent region of higher concentrations while the lighter colours and white areas represent regions of low counts.

The ternary image in Figure 4 indicates that the northern portion of the survey block generally yields lower radiometric concentrations (lighter colours) than those within the southern part of the block (darker colours). There also appears to be relatively higher Potassium and Uranium concentrations (more red, orange and yellow colours) in the north while the southern area contains relatively higher Th and U than K (more yellow, blue and green colours).

The magnetic patterns generally exhibit a NW/SE trend direction across the block as evident within the gridded RMI data and calculated vertical magnetic gradient data. Most linear magnetic anomalies appear quite narrow with strike lengths ranging from a few hundred metres to over a few kilometers in length. These well-defined discrete anomaly shapes indicate these features are near surface and are therefore more enhanced within the calculated vertical magnetic gradient data.

Within the northern limb of the survey area, a large conductive unit dominates the region which consists of numerous interpreted bedrock conductors. The calculated resistivities within this zone generally become more conductive at depth as evident by the correlation between the decrease in transmitted frequency form the Dighem system and resistivity. Resistivities of less than 10 ohm-m are commonly displayed by the 900 Hz resistivity data. This conductive zone is truncated in the south by a weakly conductive NE-SW trending river valley identified within Figure 5. Along an inferred break in close proximity to the north side of the valley, the data suggest a slight increase in relative Uranium concentrations.

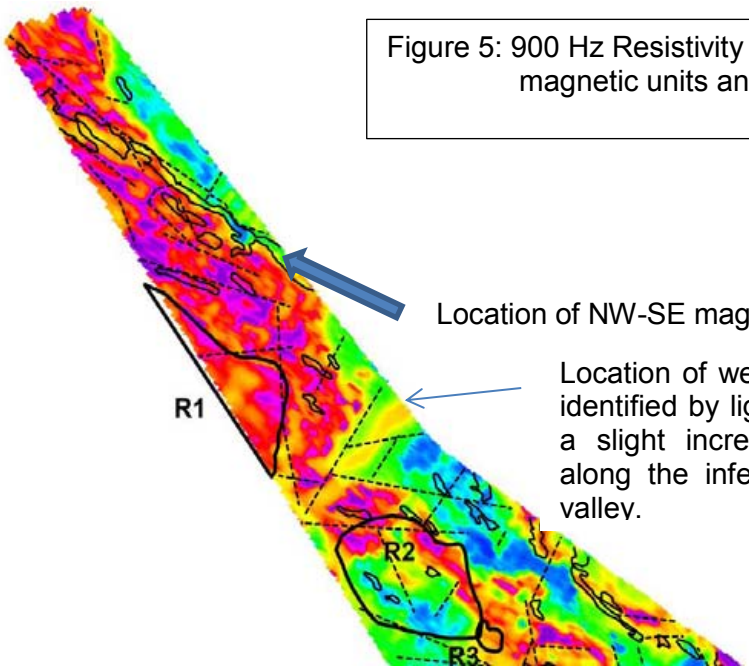

Figure 5: 900 Hz Resistivity data with outlines of magnetic units and breaks.

Figures 6 and 7 indicate the relationship between the magnetic units, the inferred breaks, and the radiometric data in the northern region of the survey block. A wide curvy linear NW/SE trending magnetic unit, refer to Figure 7, has been mapped within the northern section of the block. It is situated within a zone of low radiometric counts with more potassium rich units mapped to the south. There are some small zones indicating an increase in relative uranium concentrations along its strike length. There is no obvious conductive trend associated with this magnetic unit.

The stronger more pronounced magnetic units which are outlined in Figures 6 and 7 are generally situated within zones of low radiometric counts. However, many of the magnetic outlines follow the general trends within the ternary image.

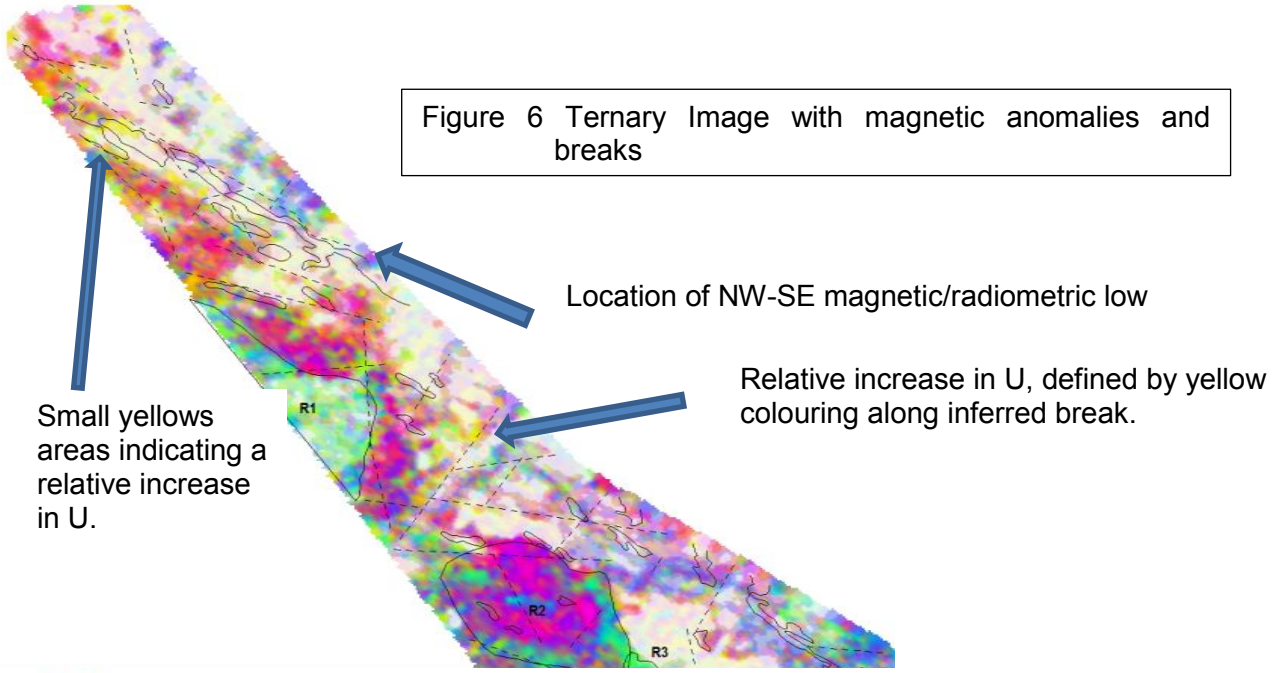

Figure 6 Ternary Image with magnetic anomalies and breaks

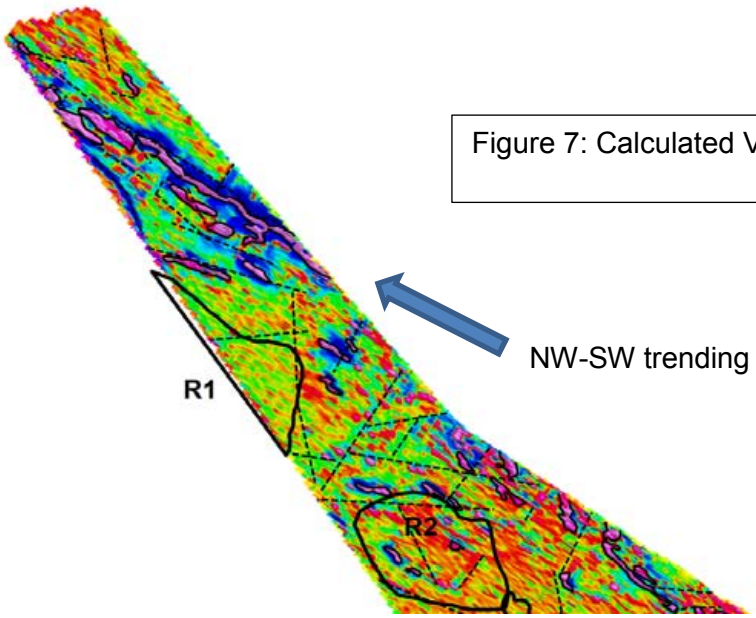

Figure 7: Calculated Vertical Magnetic Gradient

Two large radiometric anomalous zones have been labelled as R1 and R2. Zone R1, (refer to Figure 6) is a large zone displaying low counts within the 3 radiometric element windows of K, Th, and U. Within this zone, there is a slight relative increase in Th and U as indicated by the green-blue colouring within the ternary image and as a high within the Th/K ratio data displayed in Figure 9. Along the eastern boundary of this zone is a relative increase of potassium counts as indicated by the red colouring in the ternary data. There is little evidence of Zone R1 within the 900 Hz resistivity data however there is excellent agreement with a zone of increased resistivities as mapped by the 56 kHz data. Refer to Figure 8. This may be of interest as both the 56kHz resistivity data and the radiometric data map near surface features with the radiometric data limited to mapping only the top few inches of the earth and the 56kHz mapping the top 5 meters or so across Zone R1. There is no obvious corresponding anomalous magnetic unit associated with Zone R1.

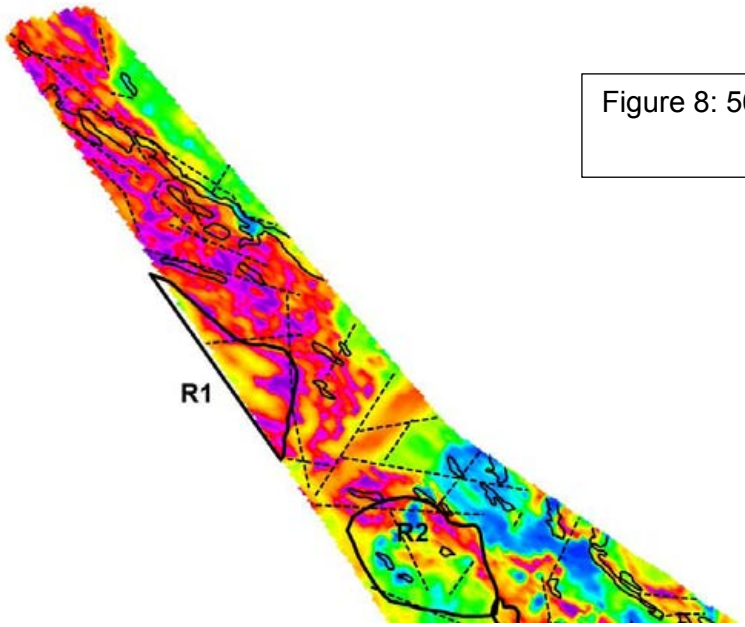

Figure 8: 56kHz Resistivity Data

Zone R2 (Refer to Figure 6) represents a large circular shaped relative potassium high. It appears as a low within the Th/K ratio data (Figure 9). Within the center of Zone R2, there is a small anomalous area of higher Th counts. This is suggested in the ternary image by the blue coloured region, as high within the Th/K ratio data, as a low within the U/Th ratio data and it is not evident within the U/K ratio data. There is also a slight corresponding increase in conductivity. There is little evidence of this small center feature within the magnetic data.

Along the southern and eastern boundary of zone R2 there is a slight relative increase in Th and U as evident by the blue-green coloured zones within the ternary image. The eastern area corresponds to a conductive unit. Both the eastern conductive and radiometric zone extends further to the south and may be related to Zones R3 and R4 discussed later in this report.

The southern limb of the survey block differs from the northern portion as there is an overall increase in background resistivity values. There are some discrete EM conductors highlighted but not to the same degree as towards the northern portion. As well, there appears to be higher thorium and uranium

concentrations and an increase in the magnetic amplitudes towards the south.

Table 11 summarizes the discrete EM anomaly responses interpreted from the survey data with respect to conductance grade and interpretation for the survey area. The anomalies are archived in CSV format on the final archive DVD. Although EM conductors may not be a strong indicator for the presence of rare earth elements, they do provide additional information regarding the geological and conductive mineralization within the area.

Table 11 EM Anomaly Statistics

Xeno Project, Dease lake Area, BC

Conductor Grade	Conductor Range Siemens (mhos)	No. of Responses
7	> 100	9
6	50 -100	14
5	20 – 50	91
4	10 – 20	173
3	5 -10	286
2	1 – 5	819
1	< 1	205
*	indeterminate	102
Total		1699

Conductor Model	Most likely source	No. of Responses
L	Culture	0
D	Thin bedrock conductor	747
/	Dipping thin bedrock conductor	16
\	Dipping thin bedrock conductor	15
T	Thick bedrock conductor	0
B	Discrete bedrock conductor	657
H	Rock unit or thick cover	17
S	Conductive cover	247
E	Edge of wide conductor	0
Total		1699

Potential Zones of Interest

The potential zones of interest were picked primarily upon an identifiable thorium and/or uranium anomaly within the ternary and ratio images. Their setting within the magnetic and resistivity datasets is also noted. As mentioned previously, zones with a magnetic signature may be of more interest if the REE deposits are associated with magnetite or other magnetic minerals.

Five zones of interest are clearly outlined within the Th/K ratio data and within the ternary image. These zones are labelled R3 through R7 on Figure 9 below. The geophysical signatures of each target zone are listed in Tables12 and 13.

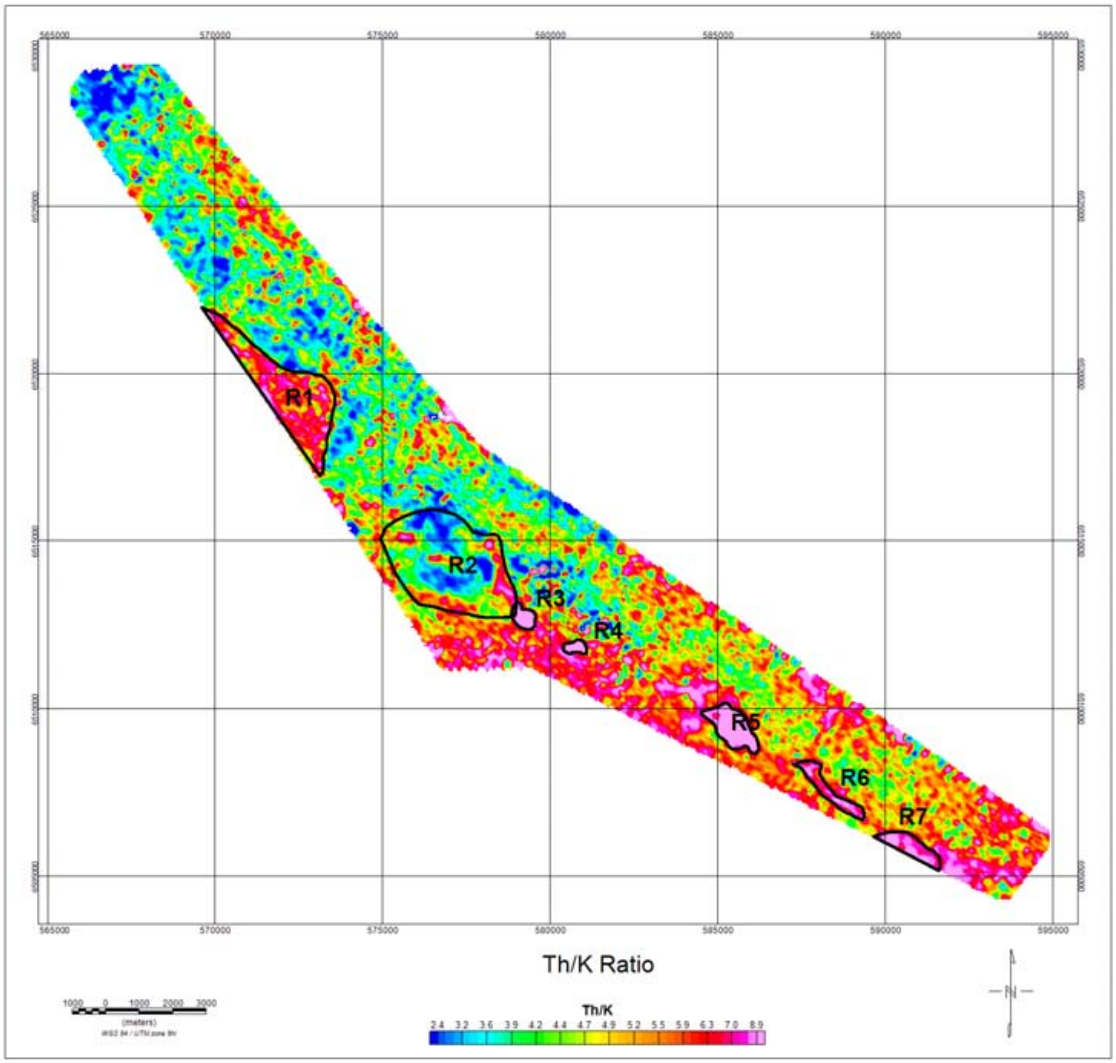

Figure 9: Th/K ratio data

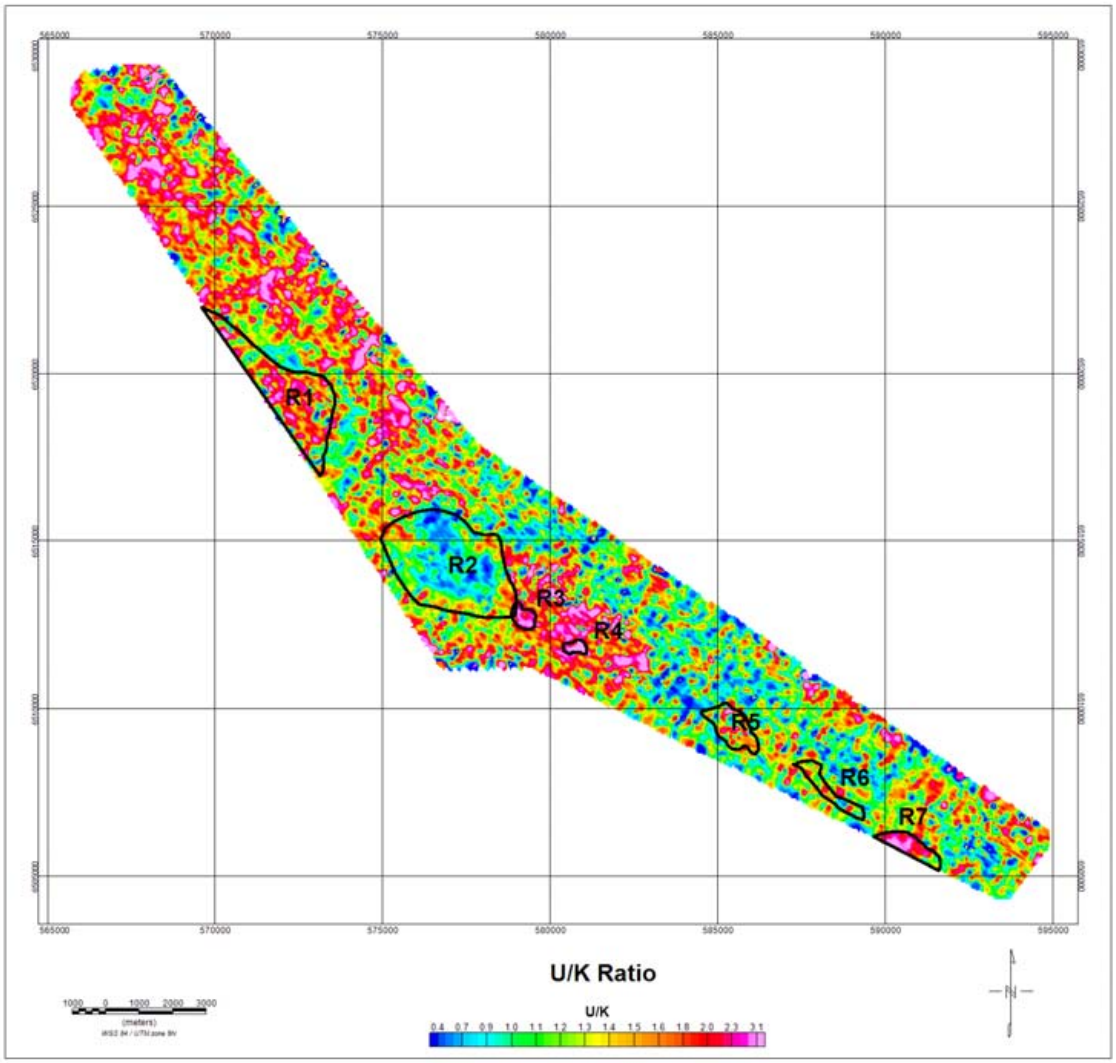

Figure 10 U/K ratio

Zone	Th/K ratio	U/K ratio	U/Th ratio	Mag	EM
R3	Well defined high: values 10-12	Poorly defined within larger high: values 2-3	Poorly defined values <0.2	Nil	Within moderately conductive unit, no distinct zone
R4	Well defined high values 11-14	Within larger high values 3-4	Poorly defined low values <0.4	Located along break	Similar to R3

Table 12: Geophysical Signature for Targets R3 and R5

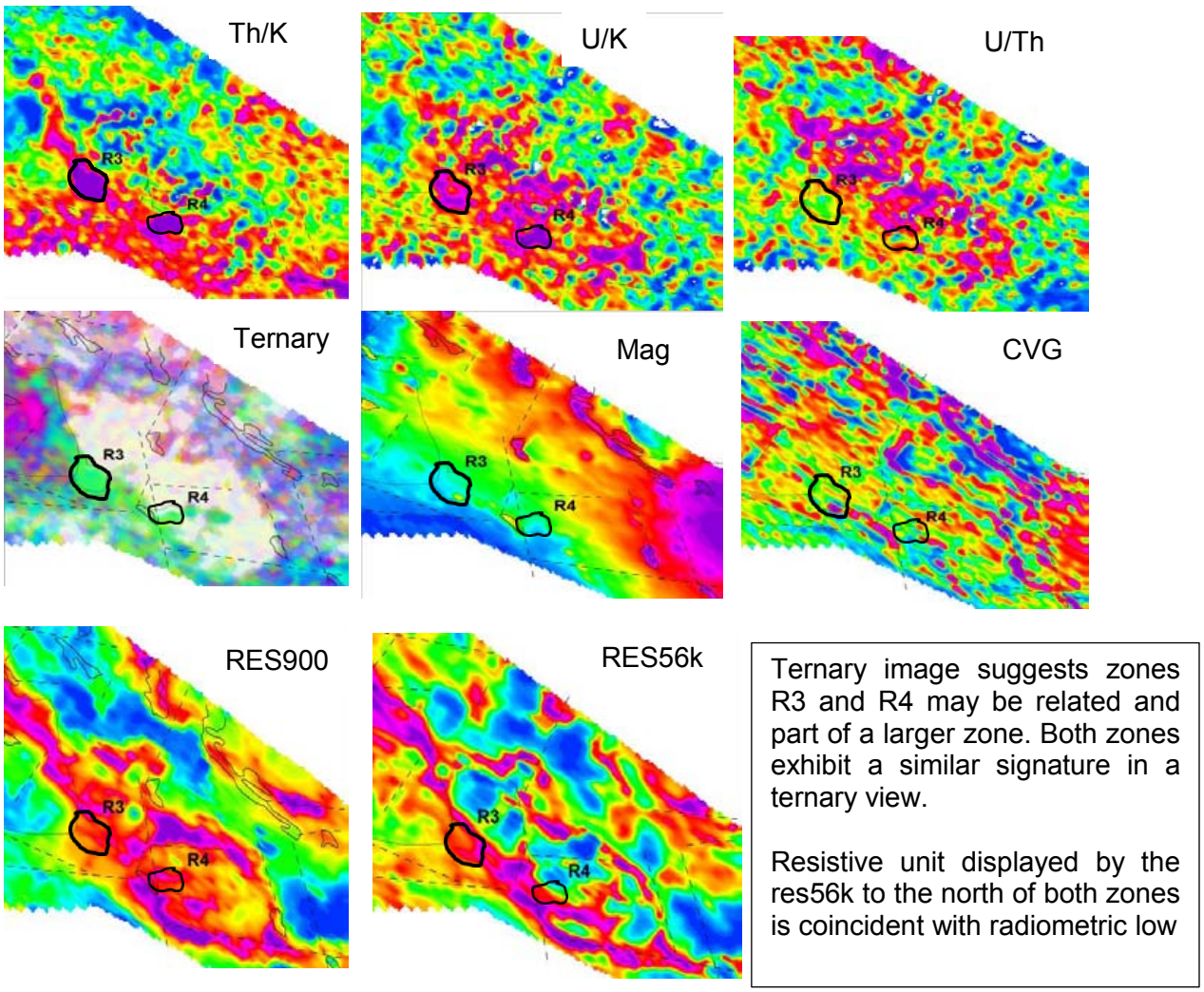

Figure 11: Potential Targets R3 and R4

Zone	Th/K ratio	U/K ratio	U/Th ratio	Mag	EM
R5	Well-defined high values 9-15	Poorly defined zone values <1	Poorly defined low values >0.3	Magnetic trends along margins	Variable across zone, west is conductive, east is resistive. No distinct zone
R6	Moderately well-defined high values 6-9	Nil	Nil	Thin mag high along southern margins	Situated within larger resistive trend
R7	Moderately well-defined high values 7-10	Well defined zone High values 2-3	Nil	Thin mag high along Northern margin	Within a larger resistive unit.

Table 13: Geophysical Signature of Targets R5, R6 and R7

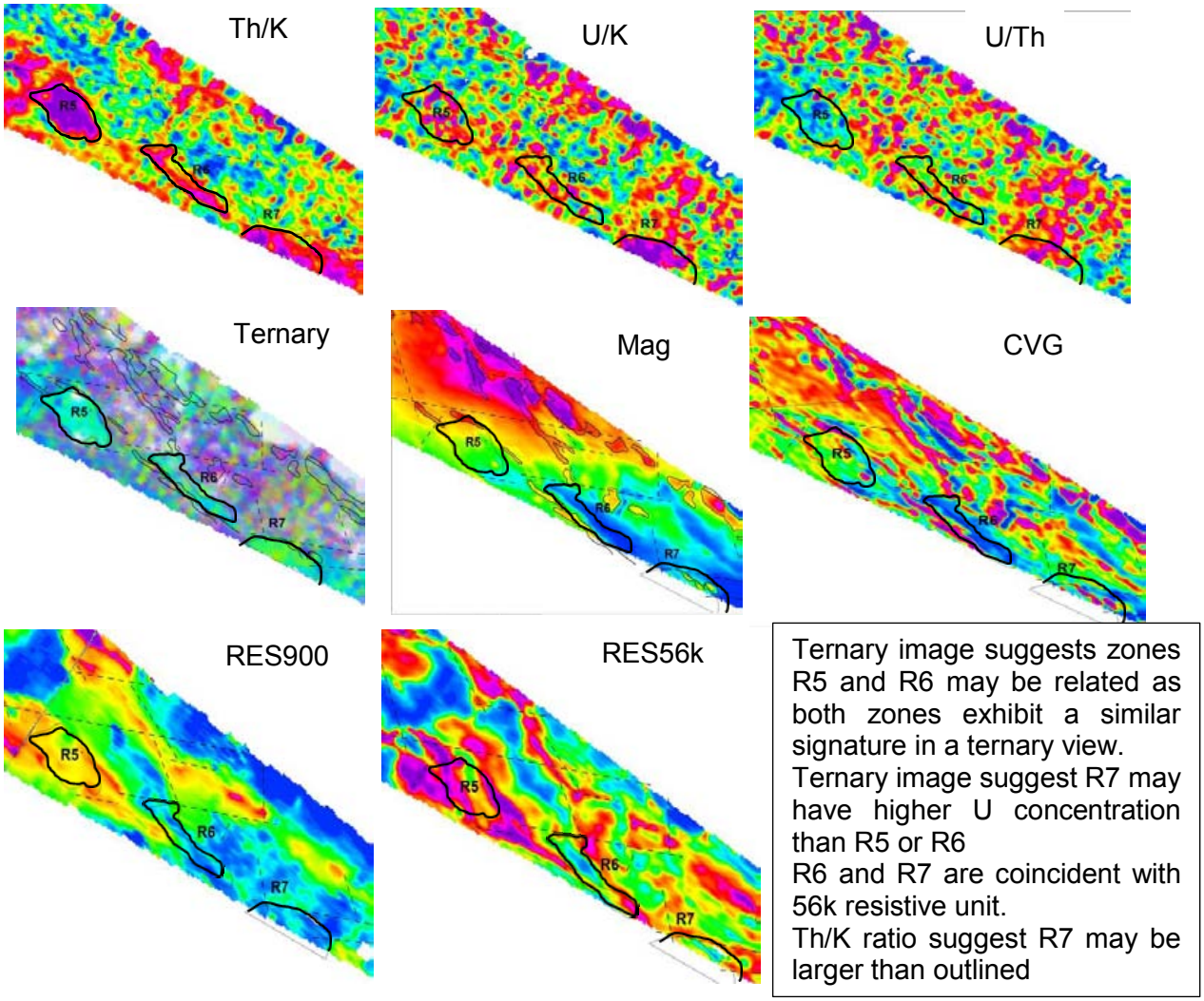

Figure 12: Potential Targets R 5, R6 & R7

Zones R3, R4 and R7 can be differentiated from zones R5 and R6 as there appears to be an increase in relative U as indicated by the shading in the ternary data, i.e. appears greener in colour.

CONCLUSIONS AND RECOMMENDATIONS

This report provides a very brief description of the survey results and describes the equipment, data processing procedures and logistics of the airborne survey over the Xeno Project, Dease lake Area, BC, near Dease Lake, British Columbia. The various maps included with this report display the magnetic, radiometric and conductive properties of the survey area.

It is recommended that the survey results be assessed and fully evaluated in conjunction with all other available geophysical, geological and geochemical information. In particular, structural analysis of the data should be undertaken and areas of interest should be selected. It is important that careful examination of these areas be carried out on the ground in order to eliminate possible man-made sources of the EM anomalies. An attempt should be made to determine the geophysical "signatures" over any known zones of mineralization in the survey areas or their vicinity.

The anomalous zones defined by the survey should be subjected to further investigation using appropriate surface exploration techniques. Anomalous zones that are currently considered to be of moderately low priority may require upgrading if follow-up results are favourable, or if they occur in areas of favourable geology.

It is also recommended that image processing of existing geophysical data be considered, in order to extract the maximum amount of information from the survey results. Current software and imaging techniques often provide valuable information on structure and lithology, which may not be clearly evident on the contour and colour maps. These techniques can yield images that define subtle, but significant, structural details.

Respectfully submitted,

FUGRO AIRBORNE SURVEYS CORP.

R11075

Appendix A

List of Personnel

List of Personnel:

The following personnel were involved in the acquisition, processing, interpretation and presentation of data, relating to a DIGHEM airborne geophysical survey carried out for Rara Terra Minerals Corp over the Xeno Project, Dease lake Area, BC near Dease Lake, British Columbia.

Duane Griffith	Manager, Geophysical Services
Lesley Minty	Project Manager
Chris Sawyer	Flight Planner
Terry Lacey	Electronics Technician
Alex Zlojutro	Field Data Processor
Amar Neku	Field Data Processor
Al Sweet	Pilot (Questral Helicopters)
Joseph Sutton	AME (Questral Helicopters)
Doug Garrie	Interpretation
Sean Plener	Data Processor

All personnel were employees of Fugro Airborne Surveys, except where indicated.

Appendix B

Data Archive Description

Data Archive Description:

Survey Details:

Survey Area Name:	Xeno Project, Dease lake Area, BC
Project number:	11075
Client:	Rara Terra Minerals Corp
Survey Company Name:	Fugro Airborne Surveys
Flown Dates:	July 8 to July 14, 2012
Archive Creation Date:	September 12, 2012

Geodetic Information for map products:

Datum:	NAD83
Ellipsoid:	GRS80
Projection:	UTM Zone 17N
Central meridian:	129° West
False Easting:	500000 metres
False Northing:	0 metres
Scale factor:	0.9996
WGS84 to Local Conversion:	Molodensky
Dx,Dy,Dz:	0, 0, 0

Grid Archive:

Geosoft Grids:

File	Description	Units
RMI	Residual Magnetic Intensity	nT
CVG	Calculated Magnetic Vertical Gradient	nT/m
res7200	Apparent Resistivity 7,200 Hz	ohm·m
res900	Apparent Resistivity 900 Hz	ohm·m
TC	Total Count	cps
K	Potassium	cps
U	Uranium	cps
Th	Thorium	Cps
U_over_K	Uranium/Potassium Ratio	Ratio
U_over_Th	Uranium/Thorium Ratio	Ratio
Th_over_K	Thorium/Potassium Ratio	Ratio

Linedata Archive:

Geosoft Database Layout:

Field	Variable	Description	Units
1	X_Bird	Bird Easting NAD83	m
2	Y_Bird	Bird Northing NAD83	m
3	X_Heli	Helicopter Easting NAD83	m
	Y_Heli	Helicopter Northing NAD83	m

4	fid	fiducial	-
5	Lon_Bird	Bird Longitude WGS84	degrees
6	Lat_Bird	Bird Latitude WGS84	degrees
7	Lon_Heli	Helicopter Longitude WGS84	degrees
8	Lat_Heli	Helicopter Latitude WGS84	degrees
9	flight	Flight number	-
10	date	Flight date	ddmmyy
11	altrad_heli	Helicopter height above surface from radar altimeter	m
12	altrad_bird	Bird height above surface from radar altimeter	m
13	altlas_bird	Bird height above surface from laser altimeter	m
14	gpsz	Helicopter height above geoid	m
15	dem	Digital elevation model (above geoid)	m
16	diurnal	Measured ground magnetic intensity	nT
17	diurnal_cor	Diurnal correction – base removed	nT
18	mag_raw	Total magnetic field – spike rejected	nT
19	mag_lag	Total magnetic field - corrected for lag	nT
20	mag_diu	Total magnetic field – diurnal variation removed	nT
21	igrf	international geomagnetic reference field	nT
22	mag_rmi	Residual magnetic intensity	nT
23	cpi900_filt	Coplanar inphase 900 Hz – unlevelled	ppm
24	cpq900_filt	Coplanar quadrature 900 Hz – unlevelled	ppm
25	cxi1000_filt	Coplanar inphase 1000 Hz – unlevelled	ppm
26	cxq1000_filt	Coplanar quadrature 1000 Hz – unlevelled	ppm
27	cxi5500_filt	Coaxial inphase 5500 Hz – unlevelled	ppm
28	cxq5500_filt	Coaxial quadrature 5500 Hz – unlevelled	ppm
29	cpi7200_filt	Coplanar inphase 7200 Hz – unlevelled	ppm
30	cpq7200_filt	Coplanar quadrature 7200 Hz – unlevelled	ppm
31	cpi56k_filt	Coplanar inphase 56 kHz – unlevelled	ppm
32	cpq56k_filt	Coplanar quadrature 56 kHz – unlevelled	ppm
33	cpi900_llev	Coplanar inphase 900 Hz – levelled	ppm
34	cpq900_llev	Coplanar quadrature 900 Hz – levelled	ppm
35	cxi1000_llev	Coplanar inphase 1000 Hz – levelled	ppm
36	cxq1000_llev	Coplanar quadrature 1000 Hz – levelled	ppm
37	cxi5500_llev	Coaxial inphase 5500 Hz – levelled	ppm
38	cxq5500_llev	Coaxial quadrature 5500 Hz – levelled	ppm
39	cpi7200_llev	Coplanar inphase 7200 Hz – levelled	ppm
40	cpq7200_llev	Coplanar quadrature 7200 Hz – levelled	ppm
41	cpi56k_llev	Coplanar inphase 56 kHz – levelled	ppm
42	cpq56k_llev	Coplanar quadrature 56 kHz – levelled	ppm
43	res56k	Apparent Resistivity 56,000 Hz	ohm·m
44	res7200	Apparent Resistivity 7,200 Hz	ohm·m
45	res900	Apparent Resistivity 900 Hz	ohm·m
46	dep56k	Apparent Depth 56,000 Hz	m
47	dep7200	Apparent Depth 7,200 Hz	m

48	dep900	Apparent Depth 900 Hz	m
49	cppl	Coplanar powerline monitor	
50	cpsp	Coplanar spherics monitor	
51	cxsp	Coaxial spherics monitor	
52	difi	Difference channel – cxi5500/cpi7200	
53	difq	Difference channel – cxq5500/cpq7200	
54	tc_raw	Total Count - uncorrected	cps
55	k_raw	Potassium - uncorrected	cps
56	u_raw	Uranium – uncorrected	cps
57	th_raw	Thorium – uncorrected	cps
58	u_up_raw	Upward-looking Uranium - uncorrected	cps
59	cosmic	Cosmic – uncorrected	cps
60	livetime	Live time	ms
61	effectiveheight	Height at standard temperature and pressure	m
62	kpa	pressure	kpa
63	temp_ext	external temperature	ºC
64	tc	Total Count	cps
65	k	Potassium	cps
66	u	Uranium	cps
67	th	Thorium	cps
68	eU	Uranium Concentration	ppm
69	eTh	Thorium Concentration	Ppm
70	eK	Potassium Concentration	%
71	spec256_down	Full downward-looking spectrum (GDB only)	

Note – The null values in the GDB and XYZ archives are displayed as *.

Anomaly CSV Layout :

Field	Variable	Description	Units
1	easting	Easting NAD83	m
2	northing	Northing NAD83	m
3	fid	Fiducial	-
4	flt	Flight number	-
5	mhos	Conductance (see report for model used)	seimens
6	depth	Depth (see report for model used)	m
7	mag	Mag correlation, local amplitude	nT
8	cxi1	In-phase coaxial 5,500 Hz, local amplitude	ppm
9	cxq1	Quadrature coaxial 5,500 Hz, local amplitude	ppm
10	cpi1	In-phase coplanar 7,200 Hz, local amplitude	ppm
11	cpq1	Quadrature coplanar 7,200 Hz, local amplitude	ppm
12	cpi2	In-phase coplanar 900 Hz, local amplitude	ppm
13	cpq2	Quadrature coplanar 900 Hz, local amplitude	ppm
14	let	Anomaly Identifier	-
15	sym	Anomaly interpretation symbol	-
16	grd	Anomaly Grade	-

Georeferenced vector plot of EM anomalies in DXF13 format.

Anomaly.dxf

Maps:

PDF files of final maps at a scale of 1:20,000. One map set consists of three map sheets.

File	Description	Units
aem	EM Anomalies	-
mag	Residual Magnetic Intensity	nT
cvg	Calculated Vertical Magnetic Gradient	nT/m
res7200	Apparent Resistivity 7200 Hz	ohm·m
res900	Apparent Resistivity 900 Hz	ohm·m
tc	Total Count	cps
k	Potassium	cps
u	Uranium	cps
th	Thorium	cps

Report:

A logistics and processing report for Project #11075 in PDF format:

R11075.pdf

Video:

Digital video in BIN/BDX format are archived for all survey flights. To view the files, two video viewers are included. The first viewer is a stand alone program and can be used by everyone. The second viewer requires Oasis Montaj and is version specific. Documentation is included with more information.

Digital Flight Path.pdf

FASSurveyReplay (Stand alone)
FugroDVD_MontajViewer72 (Oasis Montaj)

Appendix C

Map Product Grids

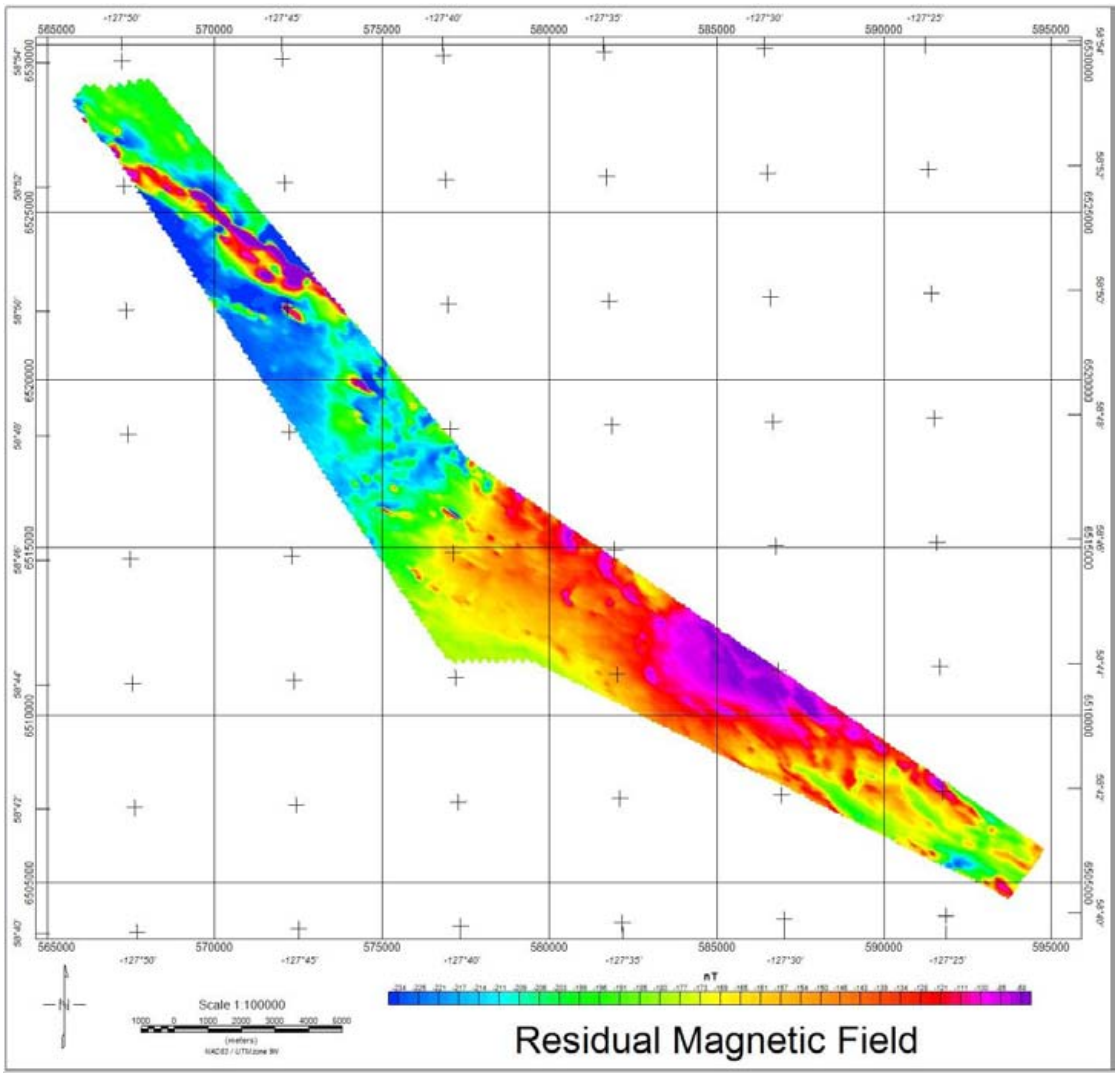

Figure 13 Residual Magnetic Field

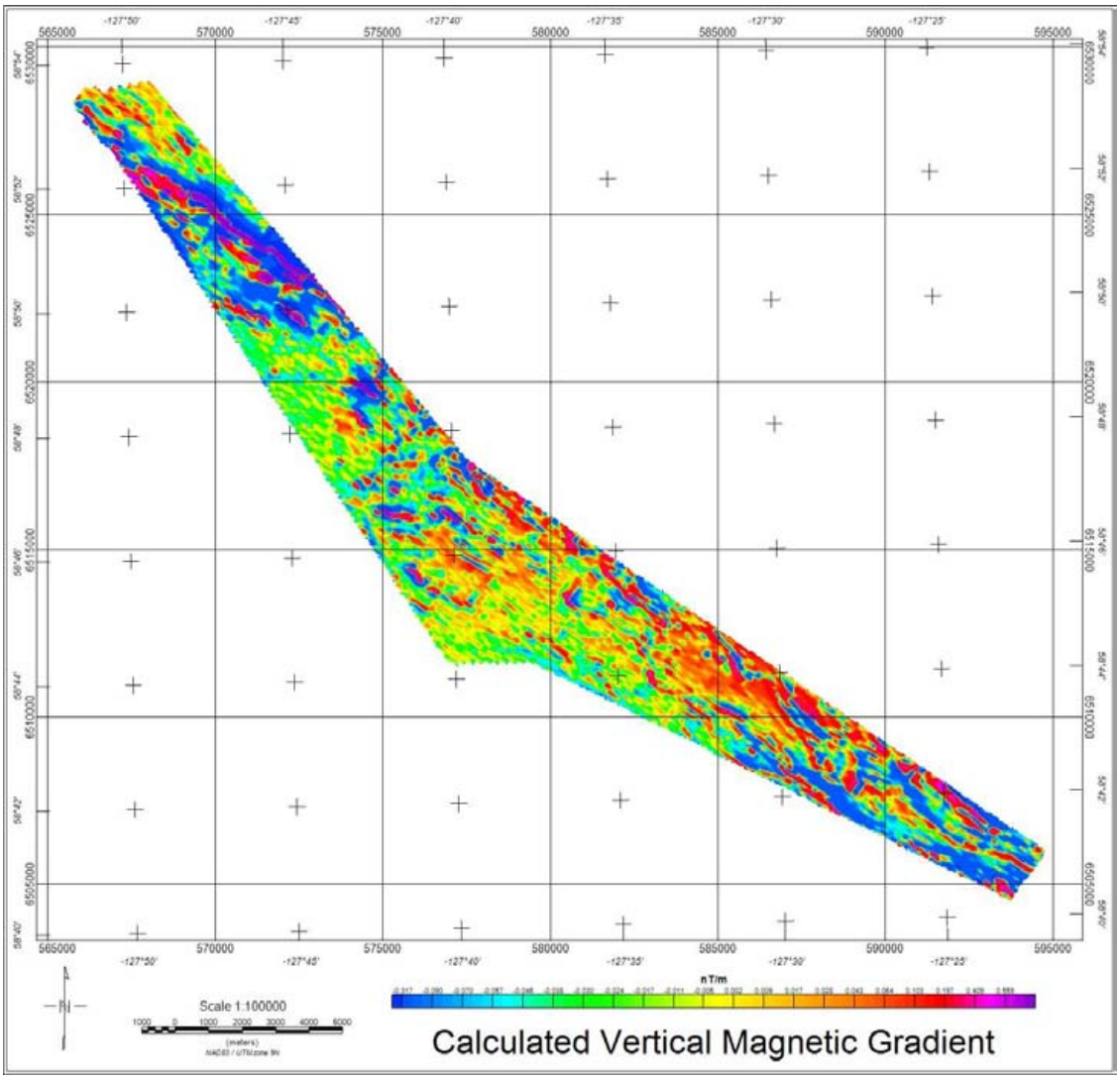

Figure 14 Calculated Vertical Magnetic Gradient

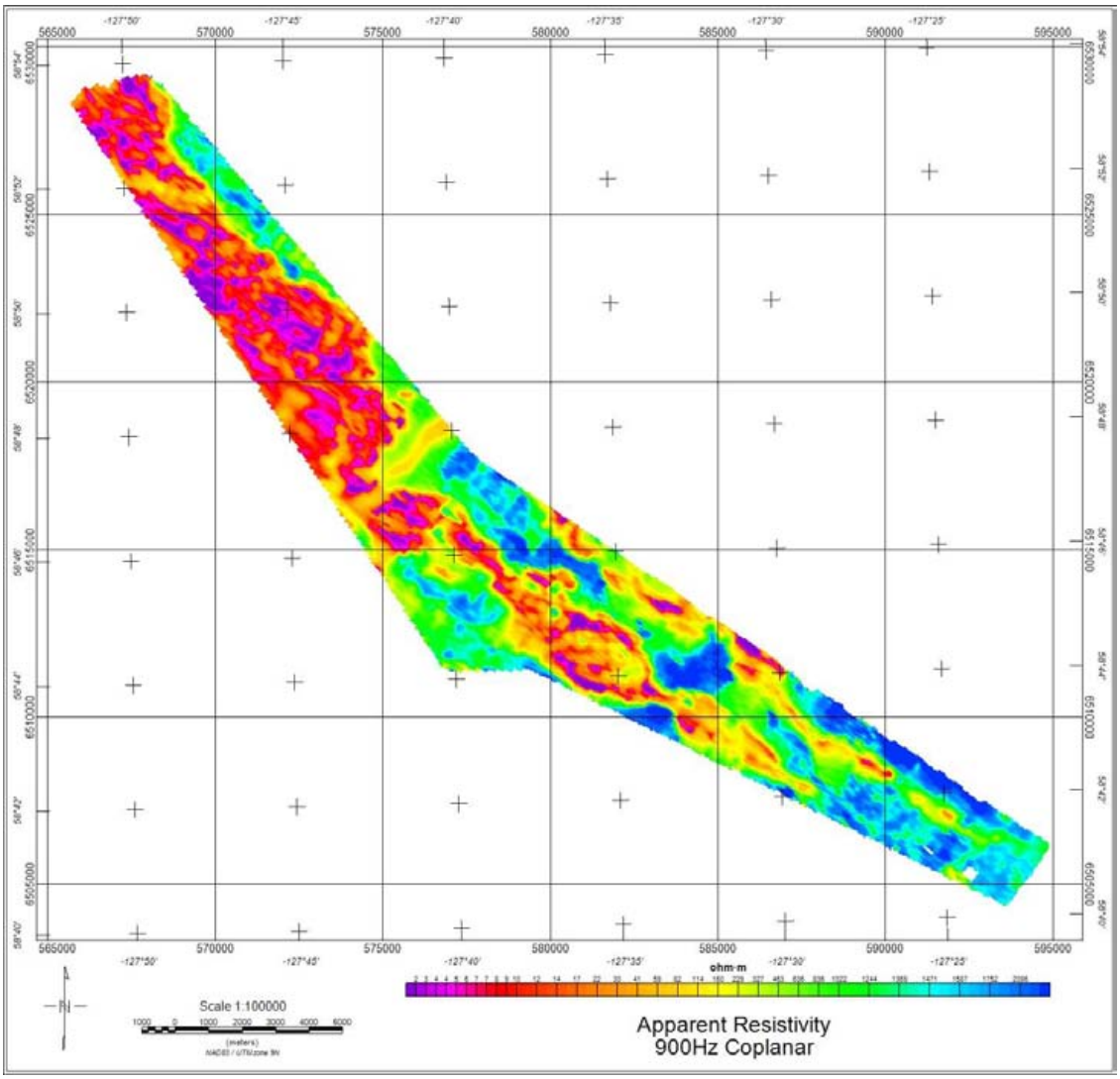

Figure 15 Apparent Resistivity 900 Hz

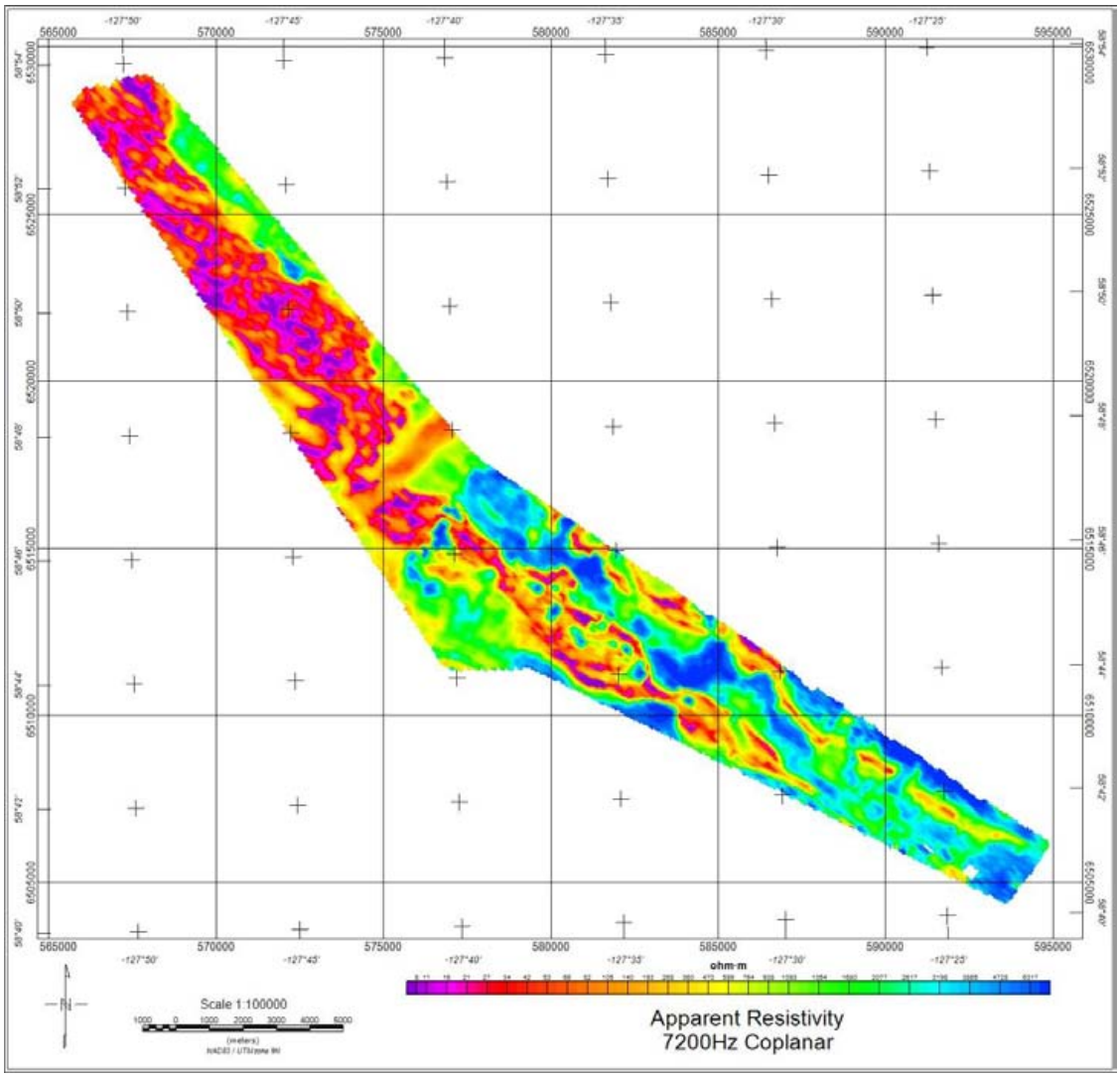

Figure 16: Apparent Resistivity 7200 Hz

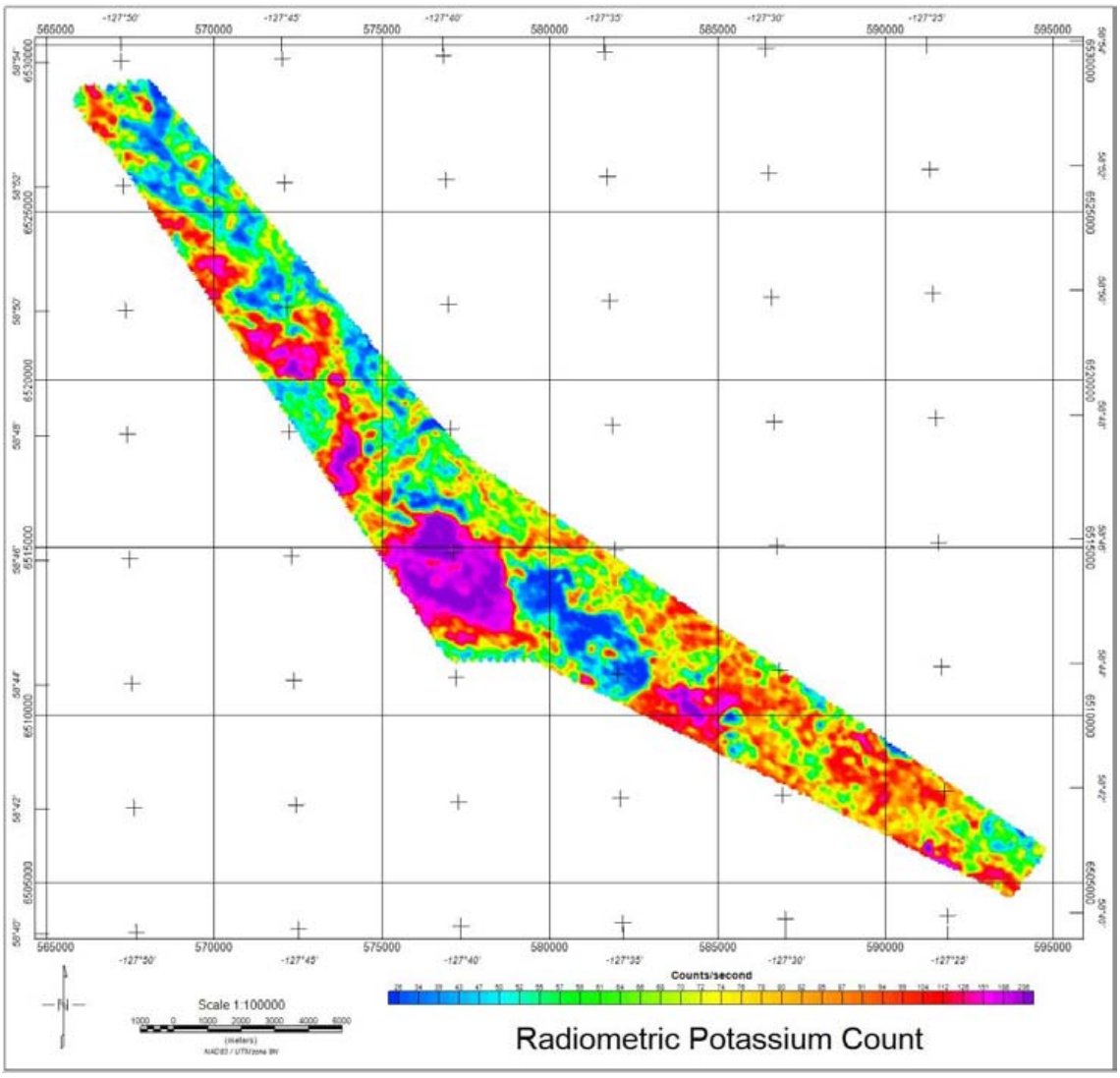

Figure 17: Radiometric Potassium Count

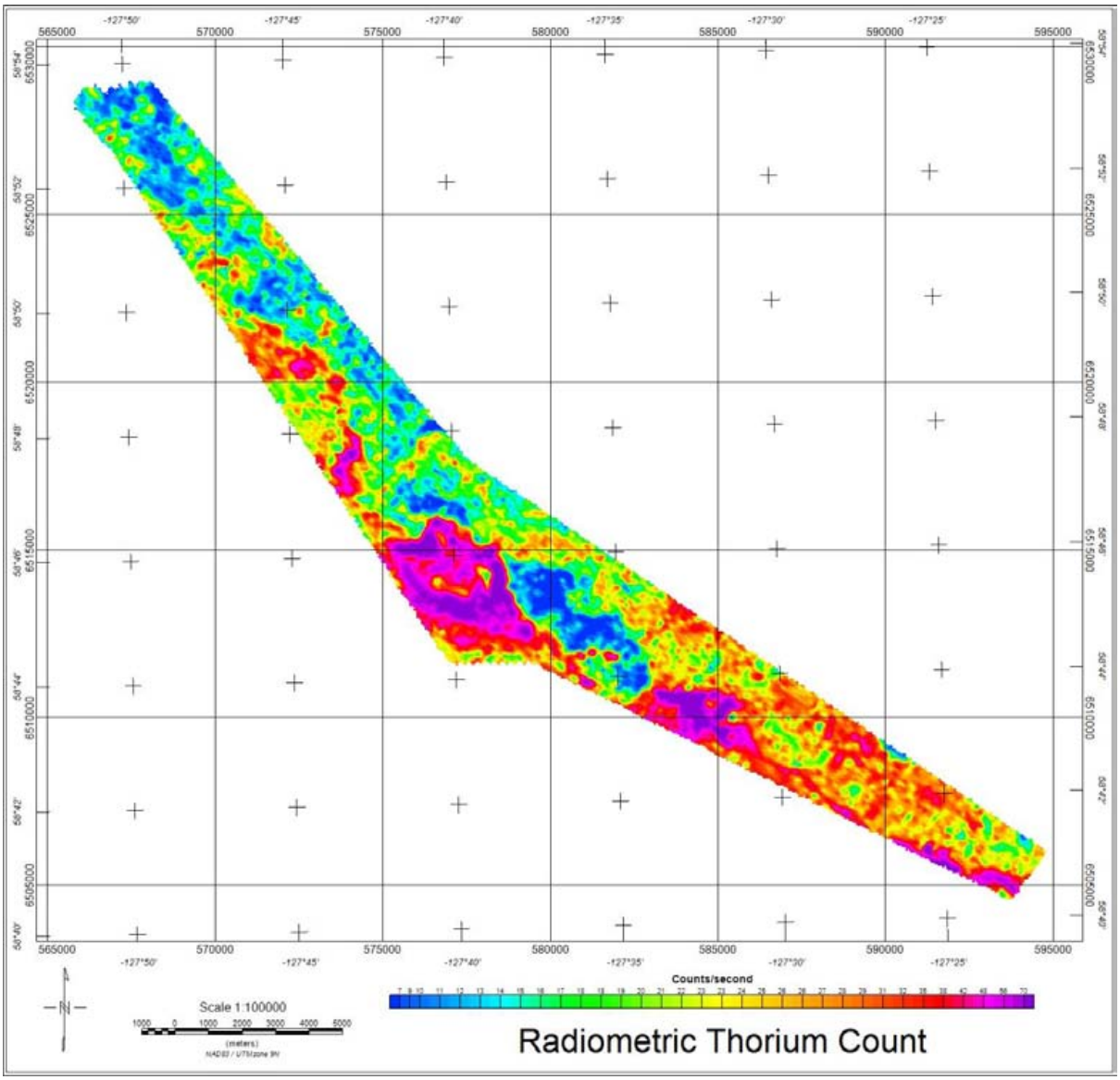

Figure 18: Radiometric Thorium Count

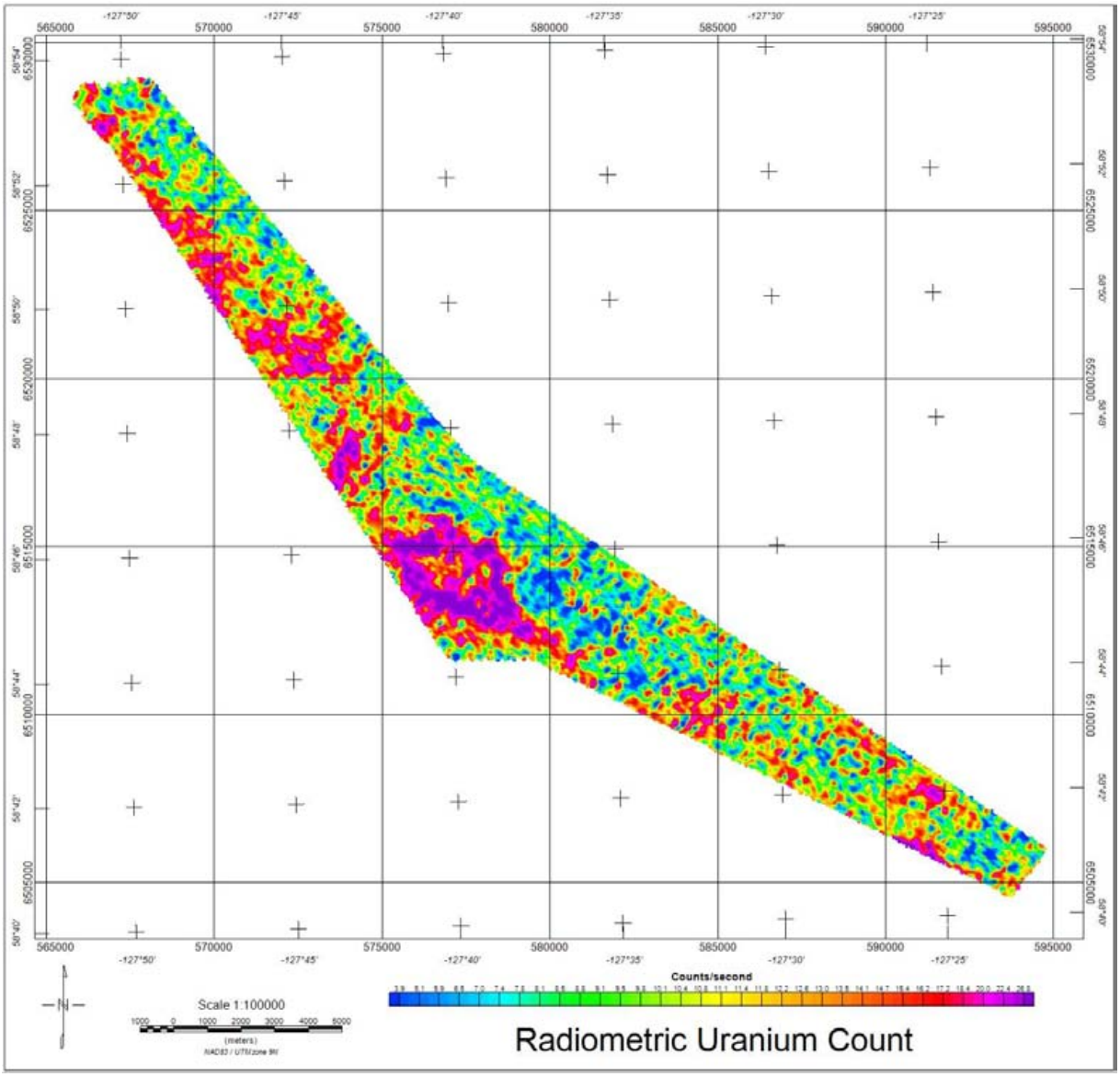

Figure 19: Radiometric Uranium Count

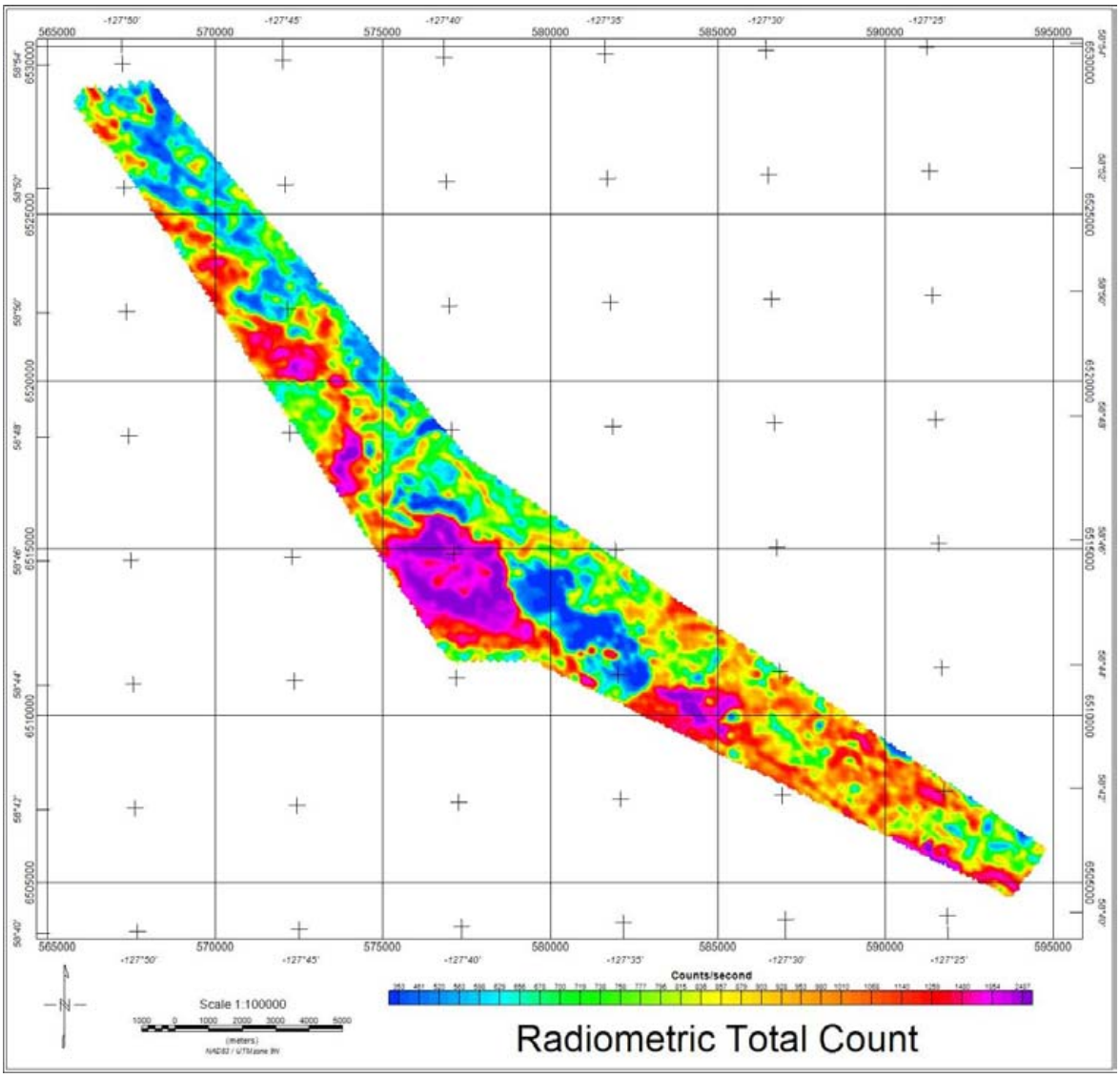

Figure 20: Radiometric Total Count

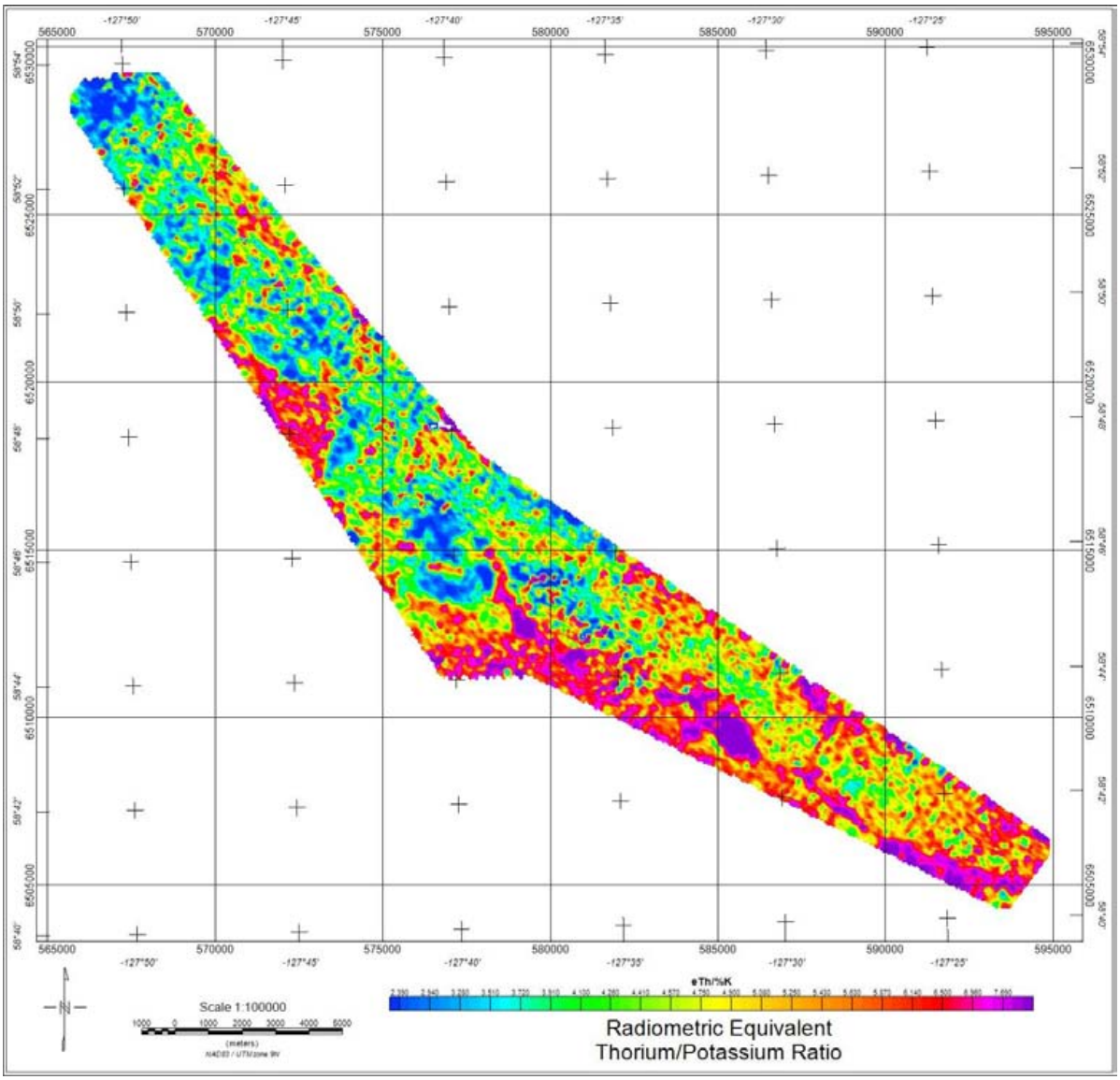

Figure 21: Radiometric Equivalent Thorium/Potassium Ratio

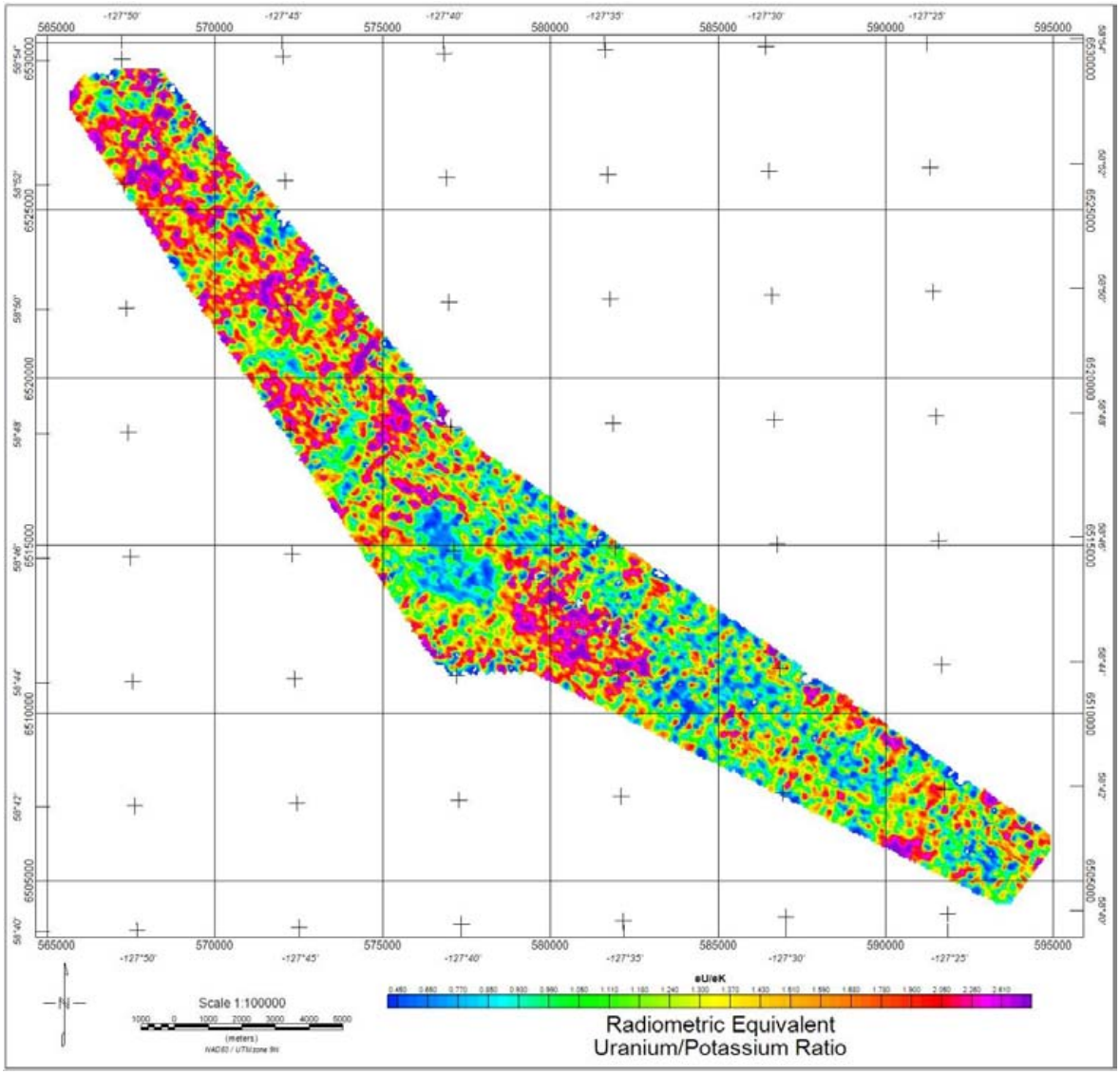

Figure 22: Radiometric Equivalent Uranium/Potassium Ratio

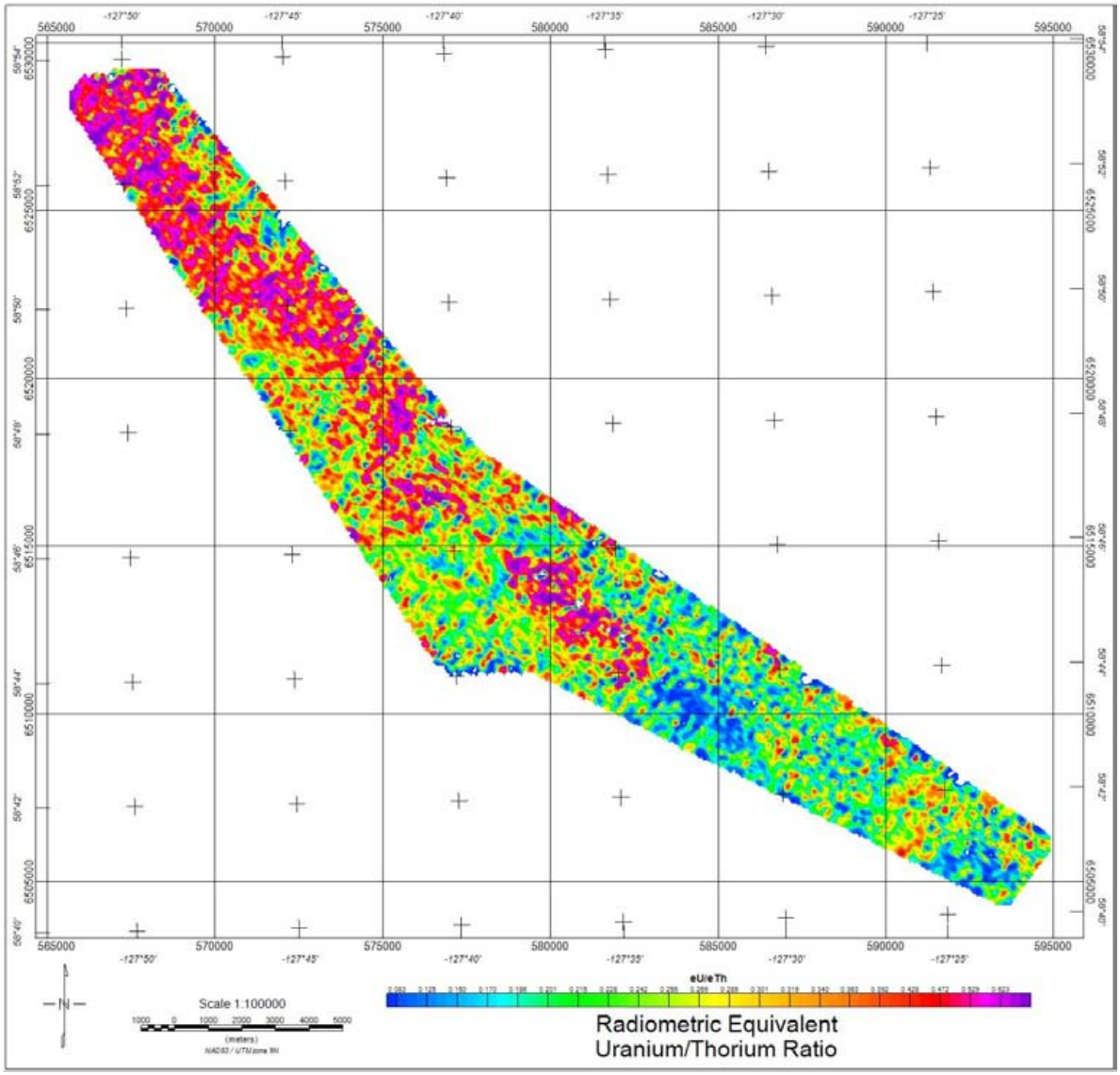

Figure 23: Radiometric Equivalent Uranium/Thorium Ratio

Appendix D

Calibration and Tests

Magnetics Lag Test

Project Number: 11075

Date Flown: 05/07/2012
Flight Number: 4002

Survey Type: HFEM / MAGNETICS / RADIOMETRICS
Aircraft Registration: C-GHKM

Correction Lag Applied: 3.1 seconds

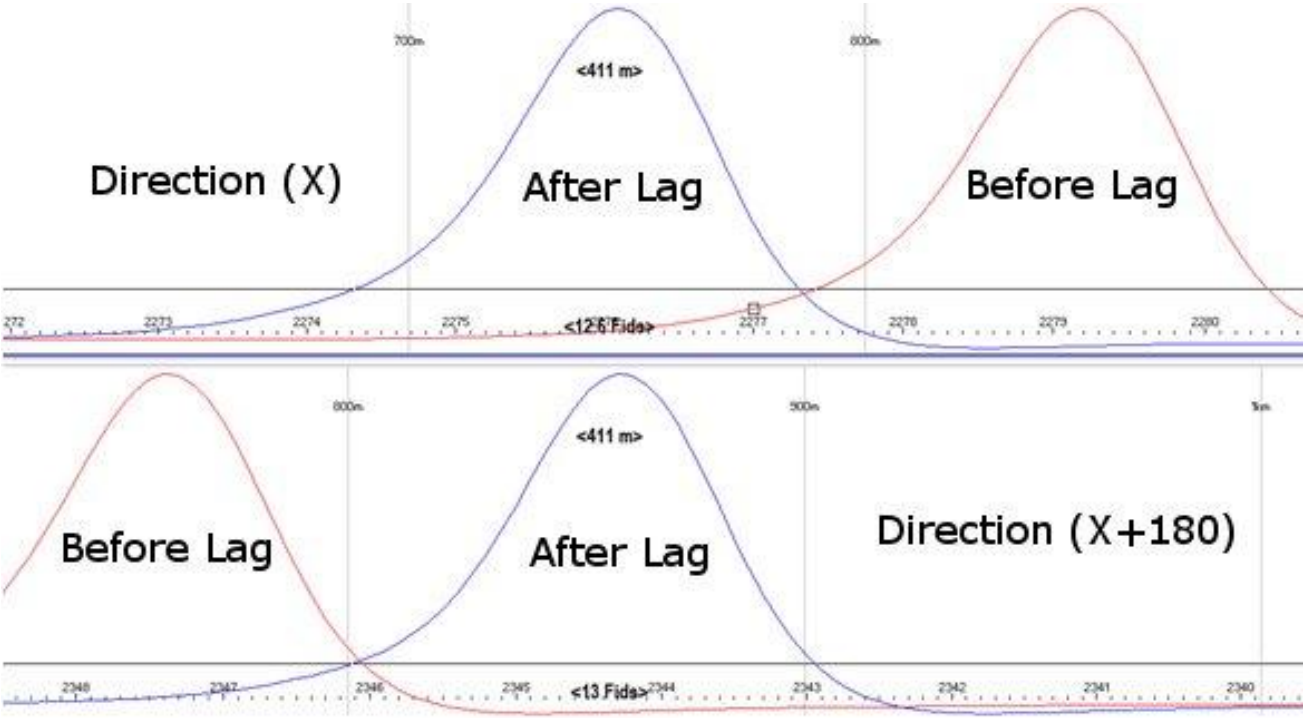

Electromagnetics Lag Test

Project Number: 11075

Date Flown: 05/07/2012
Flight Number: 4002

Survey Type: HFEM / MAGNETICS / RADIOMETRICS
Aircraft Registration: C-GHKM

Correction Lag Applied: 0.8 seconds

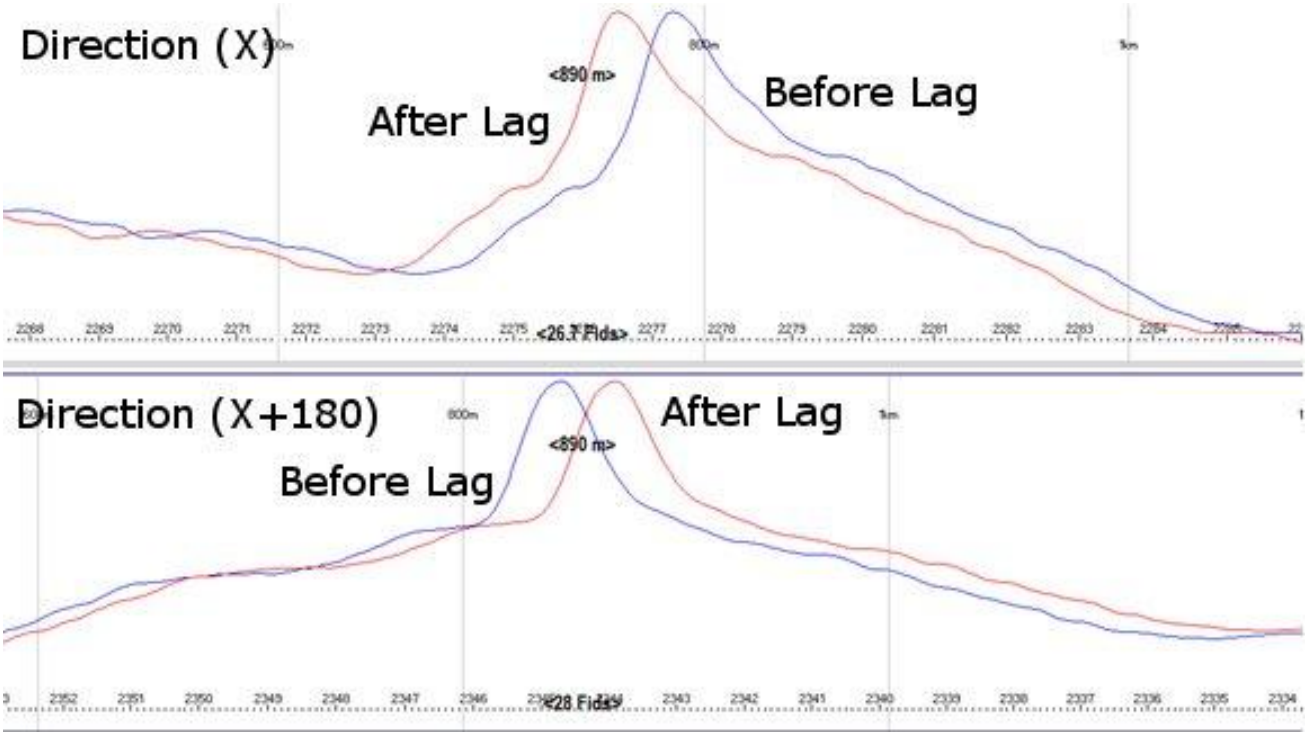

ALTIMETER CALIBRATION

Project Number: 11075

Survey Type: HFEM / MAGNETICS / RADIOMETRICS

Date Flown: 06/07/2012

Aircraft Registration: C-GHKM

Flight Number: 4003

LINE	TARGET RADAR (ft)	ZHG_HELI	ZHG_BIRD	ALTRAD_FT	ALTLASLP_M	ALTBAR_M
1	0	393.5	389.9	8.0	0.0	270.1
200	200	456.8	425.4	208.3	34.4	358.5
250	250	473.0	441.4	261.7	50.7	373.1
300	300	485.8	454.5	302.9	63.9	389.1
350	350	502.3	470.8	356.5	80.2	404.1

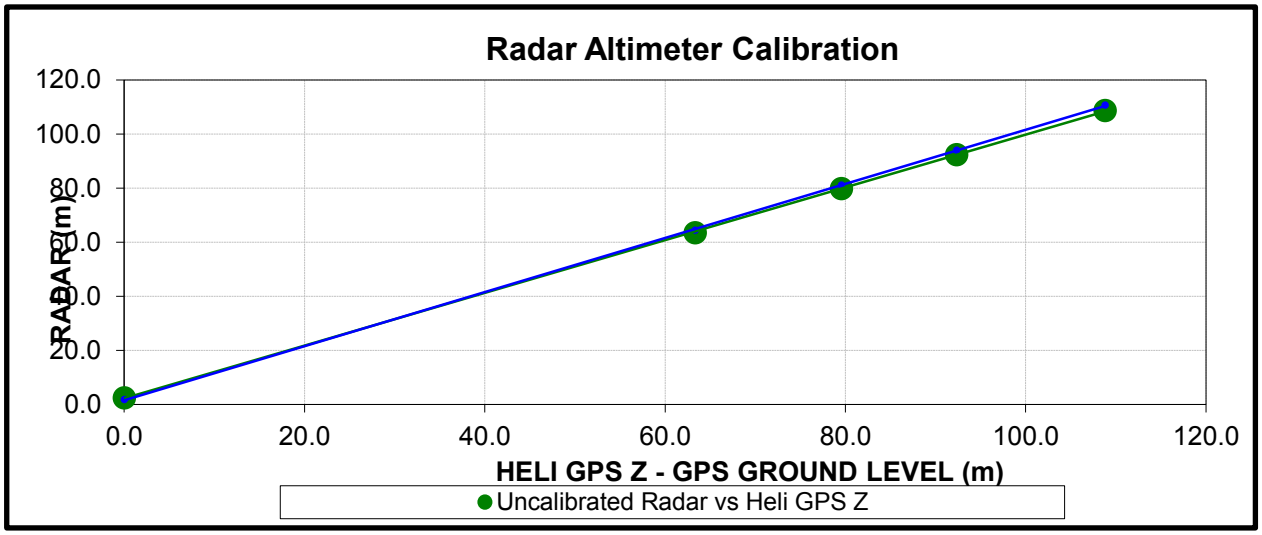

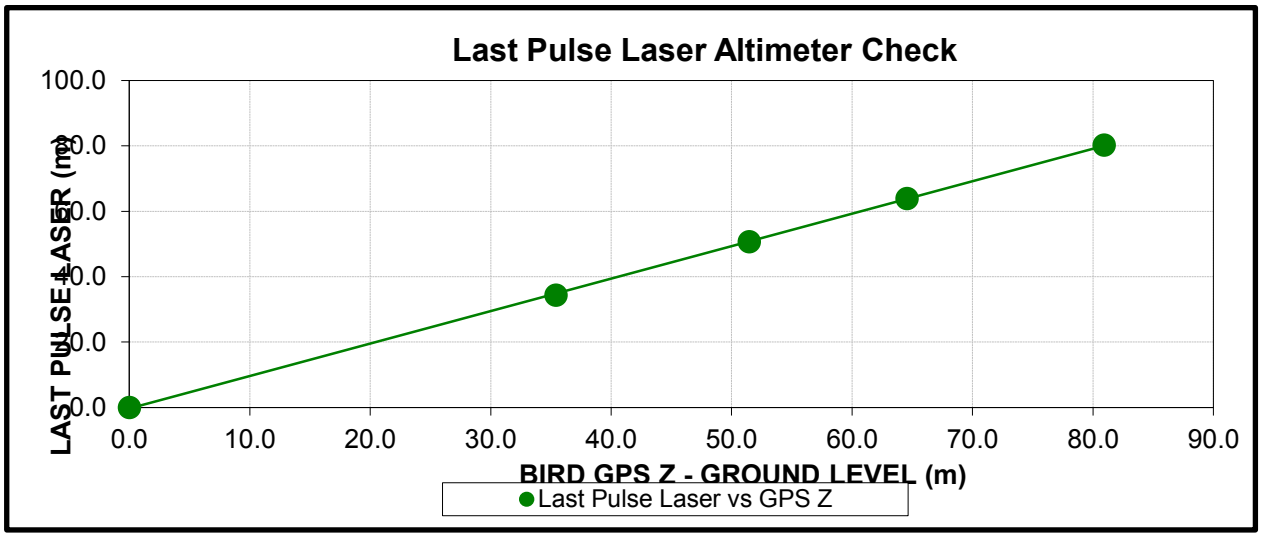
Last Pulse Laser Altimeter Check
LAST PULSE LASER (m)
100.0
0.0
10.0
20.0
30.0
40.0
50.0
60.0
70.0
80.0
90.0
BIRD GPS Z - GROUND LEVEL (m)
Last Pulse Laser vs GPS Z

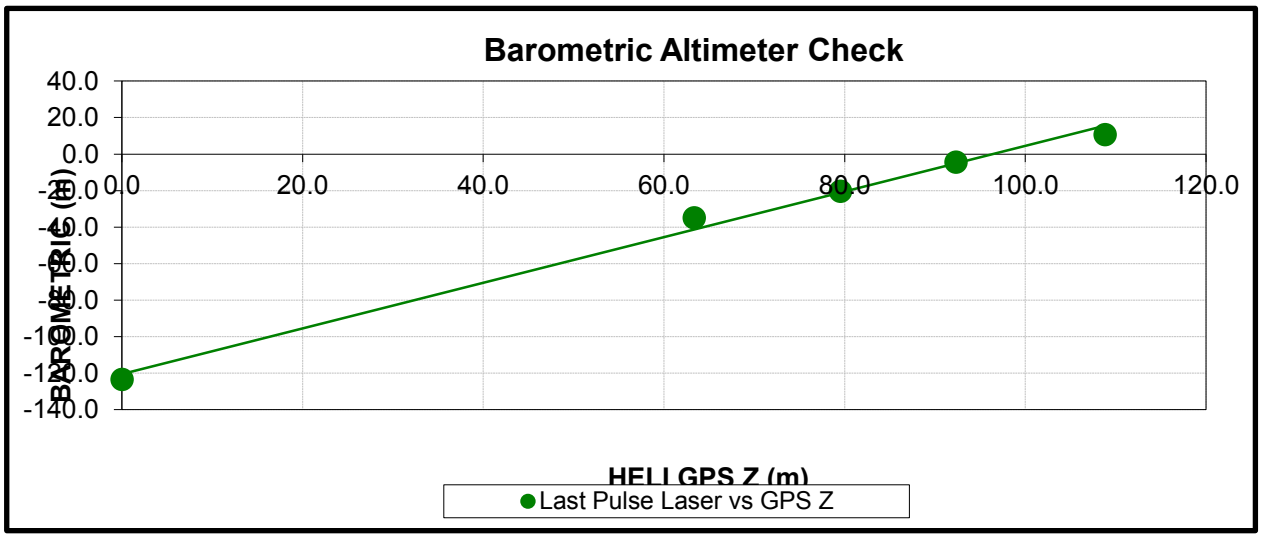
Barometric Altimeter Check
BAROMETRIC (m)
40.0
20.0
0.0
-20.0
-40.0
-60.0
-80.0
-100.0
-120.0
-140.0
0.0
20.0
40.0
60.0
80.0
100.0
120.0
HELI GPS Z (m)
Last Pulse Laser vs GPS Z

COSMIC CORRECTION COEFFICENTS

Project Number:
Date Flown:
Flight Number:

Spec Pack(s) Serial Number:
Spec Console Type:
Spec Console Serial Number:

LINE	AVERAGE TC_DOWN	AVERAGE K_DOWN	AVERAGE U_DOWN	AVERAGE TH_DOWN	AVERAGE U_UP	AVERAGE COSMIC
7500	331.509	24.14	14.718	15.37	4.014	237.829
8000	357.055	25.942	16.193	17.189	4.328	253.771
8500	384.728	27.395	17.846	18.018	4.645	275.38
9000	409.512	29.352	18.273	20.073	4.782	294.197
9500	444.549	31.354	20.226	21.776	5.312	320.991
10000	473.283	33.197	20.226	23.659	5.561	344.796

Cosmic Correction Coefficents		
	Cosmic Stripping (Slope)	Aircraft Background (Intercept)
TC	1.305126	22.782973
K	0.085464	3.716780
U	0.063507	-0.485623
Th	0.069926	-1.059239
U Up	0.014321	0.646759

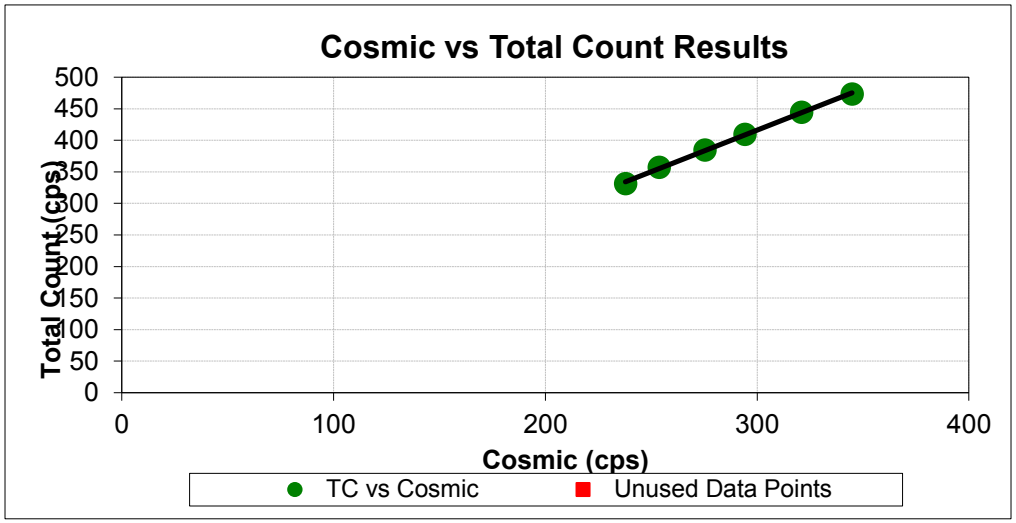
Cosmic vs Total Count Results
Total Count (cps)
500
450
400
350
300
250
200
150
100
50
0
0
100
200
300
400
Cosmic (cps)
TC vs Cosmic
Unused Data Points

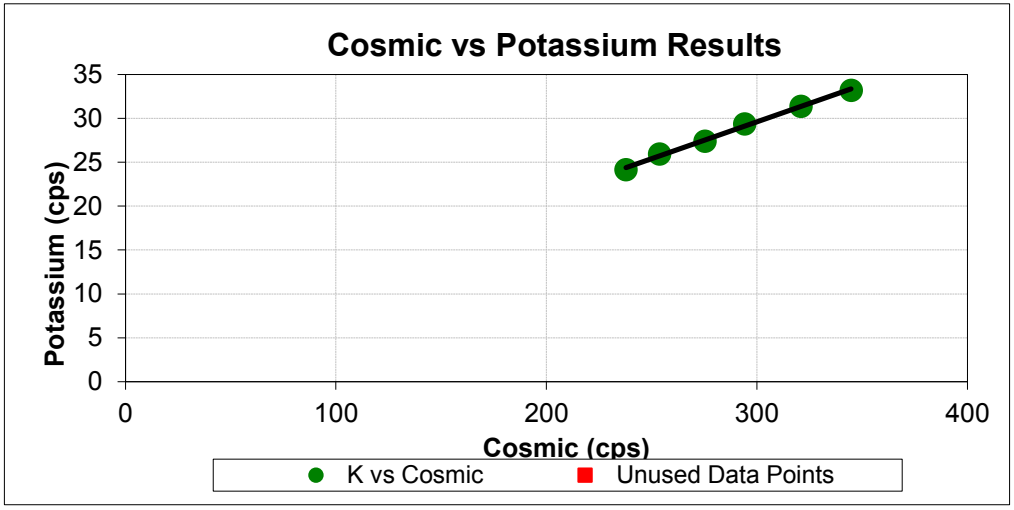
Cosmic vs Potassium Results
Potassium (cps)
35
30
25
20
15
10
5
0
0
100
200
300
400
Cosmic (cps)
K vs Cosmic
Unused Data Points

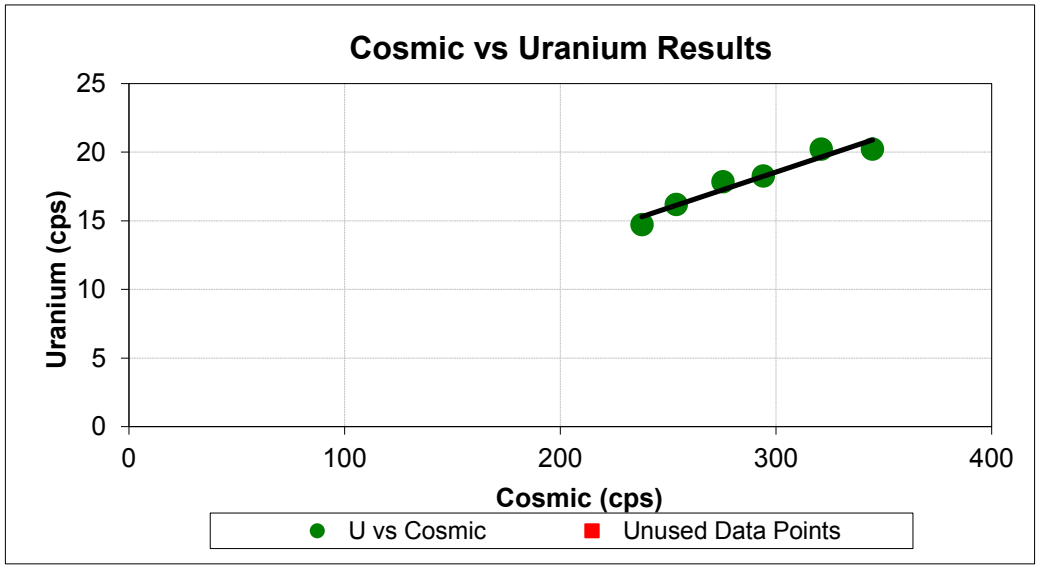
Cosmic vs Uranium Results
Uranium (cps)
25
20
15
10
5
0
0
100
200
300
400
Cosmic (cps)
U vs Cosmic
Unused Data Points

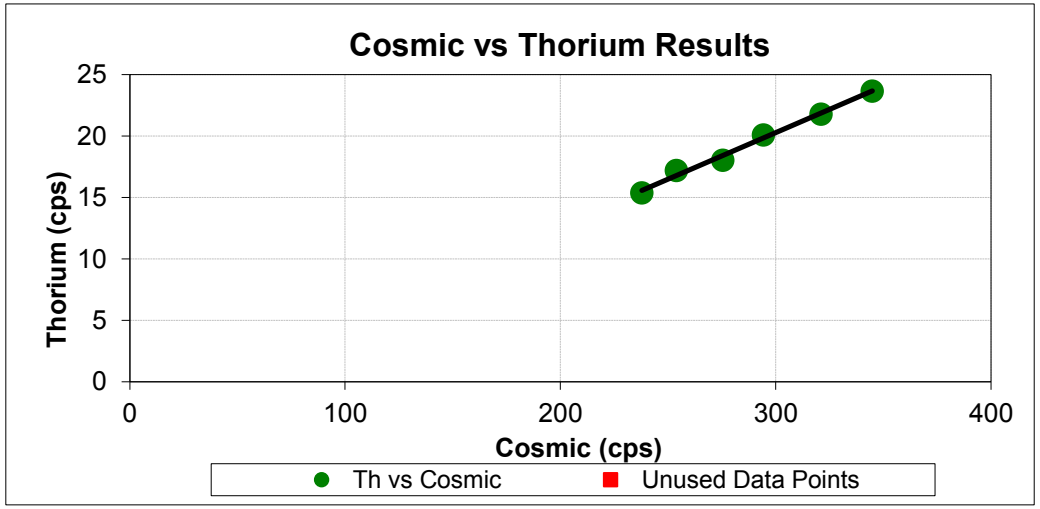
Cosmic vs Thorium Results
Thorium (cps)
25
20
15
10
5
0
0
100
200
300
400
Cosmic (cps)
Th vs Cosmic
Unused Data Points

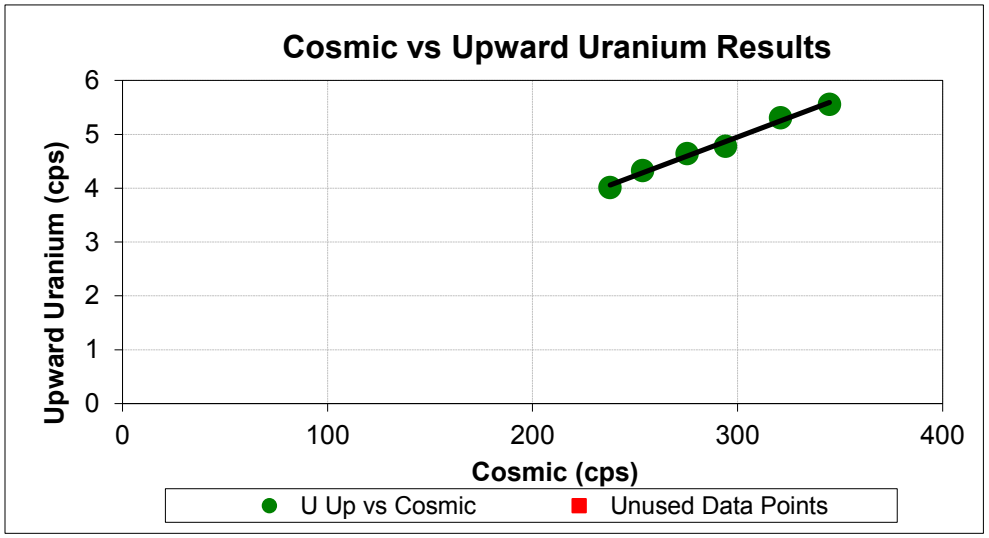

ALTITUDE ATTENUATION COEFFICENTS

Project Number:
Date Flown:
Flight Number:

Spec Pack(s) Serial Number:
Spec Console Type:
Spec Console Serial Number:

LINE	AVERAGE TC_DOWN_ ATTENCOR	AVERAGE K_DOWN_ ATTENCOR	AVERAGE U_DOWN_ ATTENCOR	AVERAGE TH_DOWN_ ATTENCOR	AVERAGE EFFECTIVE HEIGHT
100					
200	1055.87300	87.17700	14.50900	29.08600	57.36700
300	890.40400	71.18600	12.62700	23.65500	81.04300
400	738.32000	55.48300	9.92600	20.39600	105.97100
500	604.90400	44.24900	7.87600	16.78200	138.15100
1000	255.82700	15.45700	2.72100	7.63500	268.40400

Summary of Altitude Attenuation Coefficents (Must Be Negative)	
TC	-0.006700
K	-0.007953
U	-0.007239
Th	-0.006587

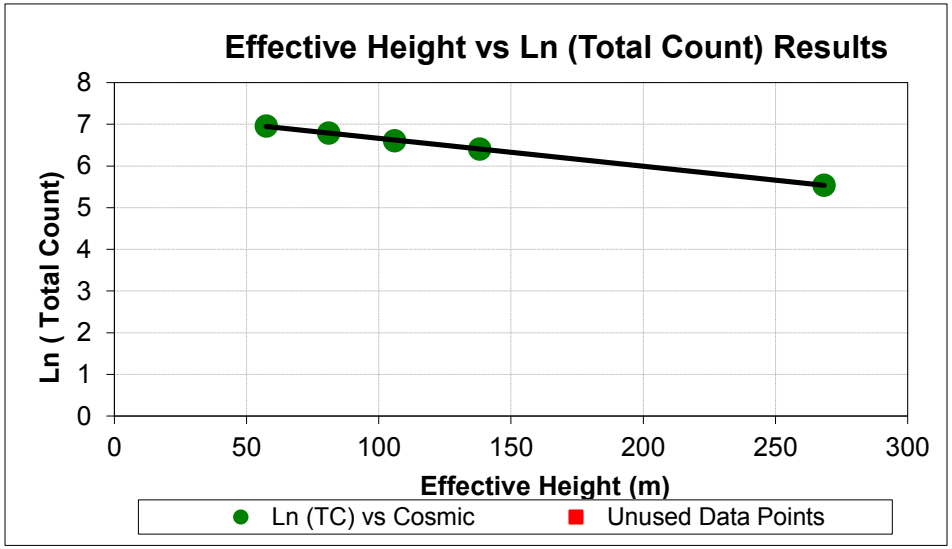
Effective Height vs Ln (Total Count) Results
Ln (Total Count)
0
1
2
3
4
5
6
7
8
0
50
100
150
200
250
300
Effective Height (m)
Ln (TC) vs Cosmic
Unused Data Points

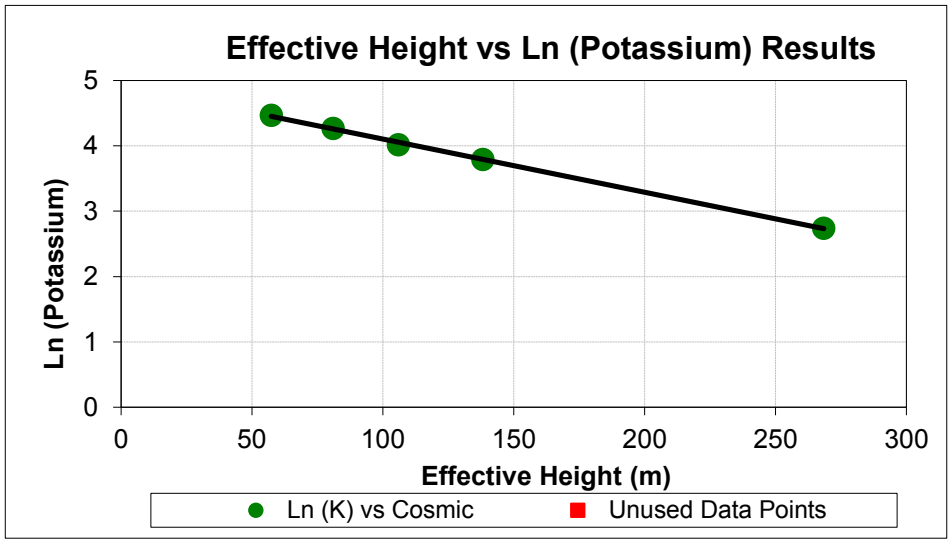
Effective Height vs Ln (Potassium) Results
Ln (Potassium)
0
1
2
3
4
5
0
50
100
150
200
250
300
Effective Height (m)
Ln (K) vs Cosmic
Unused Data Points

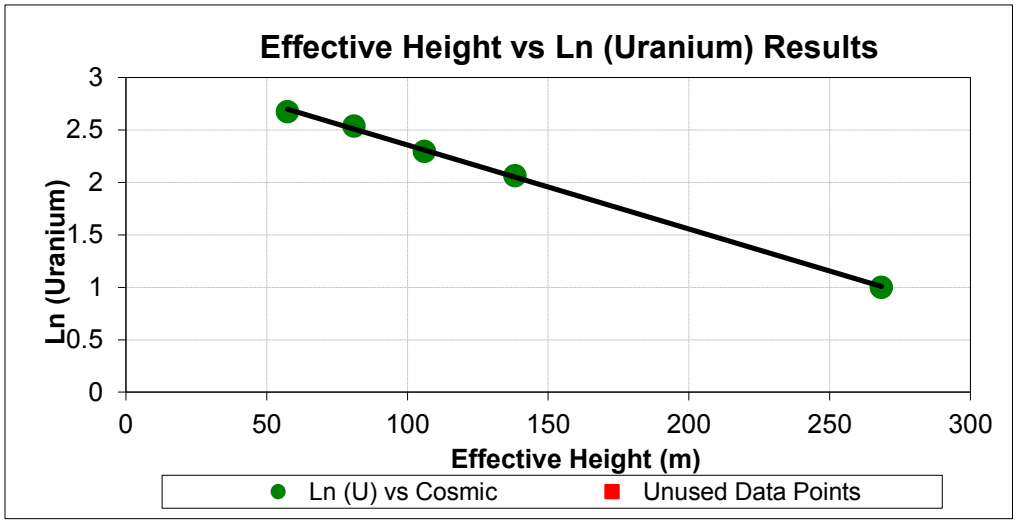
Effective Height vs Ln (Uranium) Results
Ln (Uranium)
3
2.5
2
1.5
1
0.5
0
0
50
100
150
200
250
300
Effective Height (m)
Ln (U) vs Cosmic
Unused Data Points

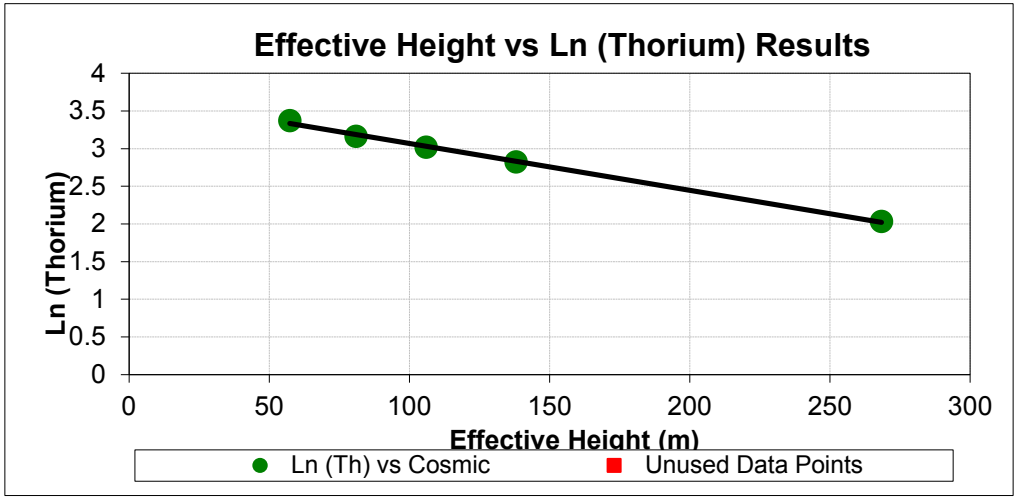
Effective Height vs Ln (Thorium) Results
Ln (Thorium)
4
3.5
3
2.5
2
1.5
1
0.5
0
0
50
100
150
200
250
300
Effective Height (m)
Ln (Th) vs Cosmic
Unused Data Points

Appendix E

Background Information

Electromagnetics

Fugro electromagnetic responses fall into two general classes, discrete and broad. The discrete class consists of sharp, well-defined anomalies from discrete conductors such as sulphide lenses and steeply dipping sheets of graphite and sulphides. The broad class consists of wide anomalies from conductors having a large horizontal surface such as flatly dipping graphite or sulphide sheets, saline water-saturated sedimentary formations, conductive overburden and rock, kimberlite pipes and geothermal zones. A vertical conductive slab with a width of 200 m would straddle these two classes.

The vertical sheet (half plane) is the most common model used for the analysis of discrete conductors. All anomalies plotted on the geophysical maps are analyzed according to this model. The following section entitled **Discrete Conductor Analysis** describes this model in detail, including the effect of using it on anomalies caused by broad conductors such as conductive overburden.

The conductive earth (half-space) model is suitable for broad conductors. Resistivity contour maps result from the use of this model. A later section entitled **Resistivity Mapping** describes the method further, including the effect of using it on anomalies caused by discrete conductors such as sulphide bodies.

Geometric Interpretation

The geophysical interpreter attempts to determine the geometric shape and dip of the conductor. Figure 24 shows typical HEM anomaly shapes which are used to guide the geometric interpretation.

Discrete Conductor Analysis

The EM anomalies appearing on the electromagnetic map are analyzed by computer to give the conductance (i.e., conductivity-thickness product) in siemens (mhos) of a vertical sheet model. This is done regardless of the interpreted geometric shape of the conductor. This is not an unreasonable procedure, because the computed conductance increases as the electrical quality of the conductor increases, regardless of its true shape. DIGHEM anomalies are divided into seven grades of conductance, as shown in Table 14. The conductance in siemens (mhos) is the reciprocal of resistance in ohms.

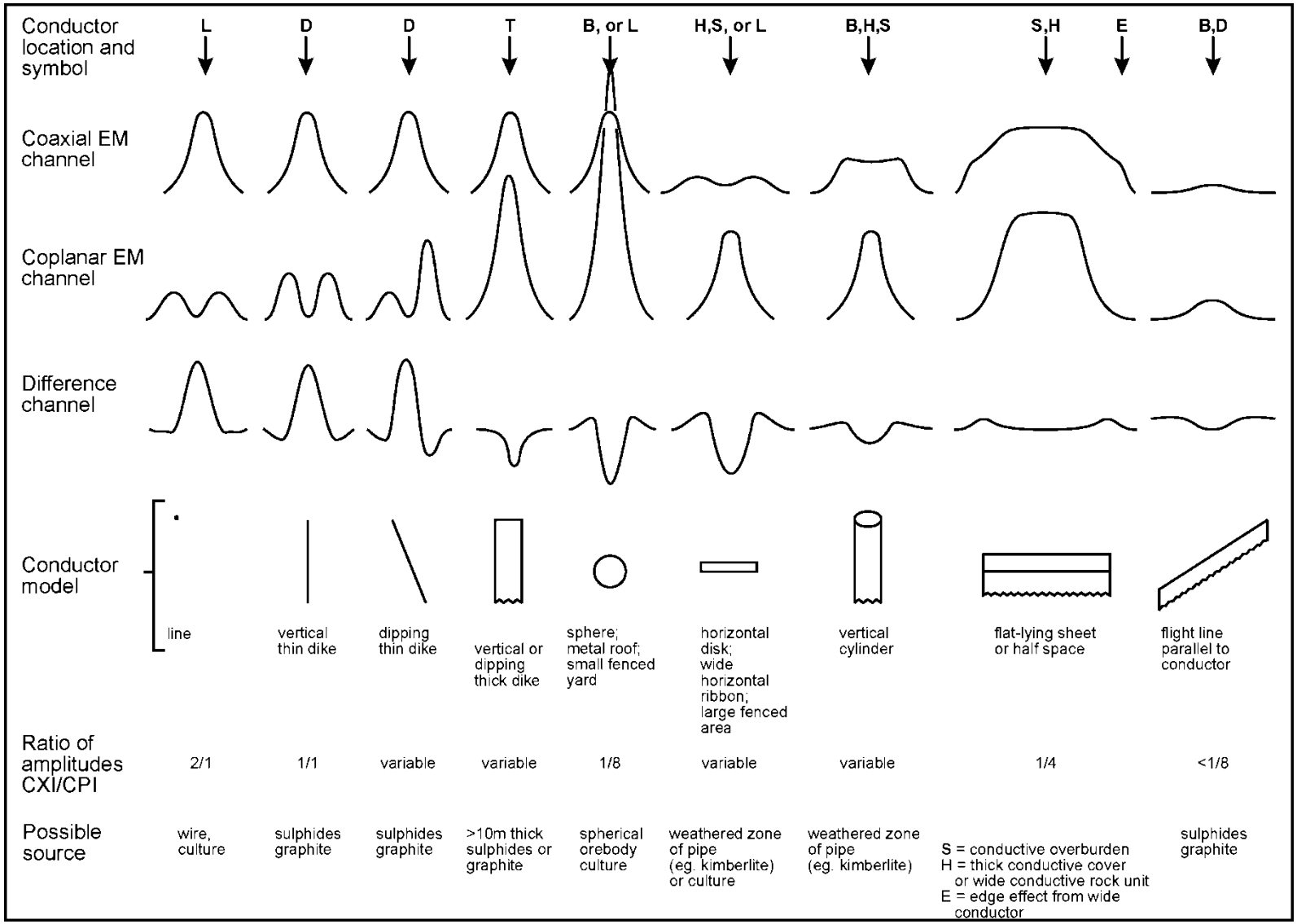

Typical HEM anomaly shapes

Figure 24 EM Anomaly Shapes

The conductance value is a geological parameter because it is a characteristic of the conductor alone. It generally is independent of frequency, flying height or depth of burial, apart from the averaging over a greater portion of the conductor as height increases. Small anomalies from deeply buried strong conductors are not confused with small anomalies from shallow weak conductors because the former will have larger conductance values.

Anomaly Grade	Siemens
7	> 100
6	50 - 100
5	20 - 50
4	10 - 20
3	5 - 10
2	1 - 5
1	< 1

Table 14 EM Anomaly Grades

Conductive overburden generally produces broad EM responses which may not be shown as anomalies on the geophysical maps. However, patchy conductive overburden in otherwise resistive areas can yield discrete anomalies with a conductance grade (cf. Table 14) of 1, 2 or even 3 for conducting clays which have resistivities as low as 50 ohm-m. In areas where ground resistivities are below 10 ohm-m, anomalies caused by weathering variations and similar causes can have any conductance grade. The anomaly shapes from the multiple coils often allow such conductors to be recognized, and these are indicated by the letters S, H, and sometimes E on the geophysical maps (see EM legend on maps).

For bedrock conductors, the higher anomaly grades indicate increasingly higher conductances. Examples: the New Insco copper discovery (Noranda, Canada) yielded a grade 5 anomaly, as did the neighbouring copper-zinc Magusi River ore body; Mattabi (copper-zinc, Sturgeon Lake, Canada) and Whistle (nickel, Sudbury, Canada) gave grade 6; and the Montcalm nickel-copper discovery (Timmins, Canada) yielded a grade 7 anomaly. Graphite and sulphides can span all grades but, in any particular survey area, field work may show that the different grades indicate different types of conductors.

Strong conductors (i.e., grades 6 and 7) are characteristic of massive sulphides or graphite. Moderate conductors (grades 4 and 5) typically reflect graphite or sulphides of a less massive character, while weak bedrock conductors (grades 1 to 3) can signify poorly connected graphite or heavily disseminated sulphides. Grades 1 and 2 conductors may not respond to ground EM equipment using frequencies less than 2000 Hz.

The presence of sphalerite or gangue can result in ore deposits having weak to moderate conductances. As an example, the three million ton lead-zinc deposit of Restigouche Mining Corporation near Bathurst, Canada, yielded a well-defined grade 2 conductor. The 10 percent by volume of sphalerite occurs as a coating around the fine grained massive pyrite, thereby inhibiting electrical conduction. Faults, fractures and shear zones may produce anomalies that typically have low conductances (e.g., grades 1 to 3). Conductive rock formations can yield anomalies of any

conductance grade. The conductive materials in such rock formations can be salt water, weathered products such as clays, original depositional clays, and carbonaceous material.

For each interpreted electromagnetic anomaly on the geophysical maps, a letter identifier and an interpretive symbol are plotted beside the EM grade symbol. In areas where anomalies are crowded, the letter identifiers and interpretive symbols may be obliterated. The EM grade symbols, however, will always be discernible, and the obliterated information can be obtained from the anomaly listing on the final data archive.

Dip symbols are used to indicate the direction of dip of conductors. These symbols are used only when the anomaly shapes are unambiguous, which usually requires a fairly resistive environment.

A further interpretation is often presented on the EM map by means of a line-to-line correlation of bedrock anomalies, which is based on a comparison of anomaly shapes on adjacent lines. This provides conductor axes that may define the geological structure over portions of the survey area. The absence of conductor axes in an area implies that anomalies could not be correlated from line to line with reasonable confidence.

The electromagnetic anomalies are designed to provide a correct impression of conductor quality by means of the conductance grade symbols. The symbols can stand alone with geology when planning a follow-up program. The actual conductance values are printed in the attached anomaly list for those who wish quantitative data. The map provides an interpretation of conductors in terms of length, strike and dip, geometric shape, conductance, and thickness. The accuracy is comparable to an interpretation from a high quality ground EM survey having the same line spacing.

The appended EM anomaly list provides a tabulation of anomalies in ppm, conductance, and depth for the vertical sheet model. No conductance or depth estimates are shown for weak anomalous responses that are not of sufficient amplitude to yield reliable calculations.

Since discrete bodies normally are the targets of EM surveys, local base (or zero) levels are used to compute local anomaly amplitudes. This contrasts with the use of true zero levels which are used to compute true EM amplitudes for resistivity calculations. Local anomaly amplitudes are shown in the EM anomaly list and these are used to compute the vertical sheet parameters of conductance and depth.

Questionable Anomalies

The EM maps may contain anomalous responses that are displayed as asterisks (*). These responses denote weak anomalies of indeterminate conductance, which may reflect one of the following: a weak conductor near the surface, a strong conductor at depth (e.g., 100 to 120 m below surface) or to one side of the flight line, or aerodynamic noise. Those responses that have the appearance of valid bedrock anomalies on the flight profiles are indicated by appropriate interpretive symbols (see EM legend on maps). The others probably do not warrant further investigation unless their locations are of considerable geological interest.

The Thickness Parameter

A comparison of coaxial and coplanar shapes can provide an indication of the thickness of a steeply dipping conductor. The amplitude of the coplanar anomaly (e.g., CPI channel) increases relative to the coaxial anomaly (e.g., CXI) as the apparent thickness increases, i.e., the thickness in the horizontal plane. (The thickness is equal to the conductor width if the conductor dips at 90 degrees and strikes at right angles to the flight line.) This report refers to a conductor as thin when the thickness is likely to be less than 3 m, and thick when in excess of 10 m. Thick conductors are indicated on the EM map by parentheses "( )". For base metal exploration in steeply dipping geology, thick conductors can be high priority targets because many massive sulphide ore bodies are thick. The system cannot sense the thickness when the strike of the conductor is subparallel to the flight line, when the conductor has a shallow dip, when the anomaly amplitudes are small, or when the resistivity of the environment is below 100 ohm-m.

Resistivity Mapping

Resistivity mapping is useful in areas where broad or flat lying conductive units are of interest. One example of this is the clay alteration which is associated with Carlin-type deposits in the south west United States. The resistivity parameter was able to identify the clay alteration zone over the Cove deposit. The alteration zone appeared as a strong resistivity low on the 900 Hz resistivity parameter. The 7,200 Hz and 56,000 Hz resistivities showed more detail in the covering sediments, and delineated a range front fault. This is typical in many areas of the south west United States, where conductive near surface sediments, which may sometimes be alkalic, attenuate the higher frequencies.

Resistivity mapping has proven successful for locating diatremes in diamond exploration. Weathering products from relatively soft kimberlite pipes produce a resistivity contrast with the unaltered host rock. In many cases weathered kimberlite pipes were associated with thick conductive layers that contrasted with overlying or adjacent relatively thin layers of lake bottom sediments or overburden.

Areas of widespread conductivity are commonly encountered during surveys. These conductive zones may reflect alteration zones, shallow-dipping sulphide or graphite-rich units, saline ground water, or conductive overburden. In such areas, EM amplitude changes can be generated by decreases of only 5 m in survey altitude, as well as by increases in conductivity. The typical flight record in conductive areas is characterized by in-phase and quadrature channels that are continuously active. Local EM peaks reflect either increases in conductivity of the earth or decreases in survey altitude. For such conductive areas, apparent resistivity profiles and contour maps are necessary for the correct interpretation of the airborne data. The advantage of the resistivity parameter is that anomalies caused by altitude changes are virtually eliminated, so the resistivity data reflect only those anomalies caused by conductivity changes. The resistivity analysis also helps the interpreter to differentiate between conductive bedrock and conductive overburden. For example, discrete conductors will generally appear as narrow lows on the contour map and broad conductors (e.g., overburden) will appear as wide lows.

The apparent resistivity is calculated using the pseudo-layer (or buried) half-space model defined by Fraser (1978)[3]. This model consists of a resistive layer overlying a conductive half-space. The depth channels give the apparent depth below surface of the conductive material. The apparent depth is simply the apparent thickness of the overlying resistive layer. The apparent depth (or thickness) parameter will be positive when the upper layer is more resistive than the underlying material, in which case the apparent depth may be quite close to the true depth.

The apparent depth will be negative when the upper layer is more conductive than the underlying material, and will be zero when a homogeneous half-space exists. The apparent depth parameter must be interpreted cautiously because it will contain any errors that might exist in the measured altitude of the EM bird (e.g., as caused by a dense tree cover). The inputs to the resistivity algorithm are the in-phase and quadrature components of the coplanar coil-pair. The outputs are the apparent resistivity of the conductive half-space (the source) and the sensor-source distance. The flying height is not an input variable, and the output resistivity and sensor-source distance are independent of the flying height when the conductivity of the measured material is sufficient to yield significant in-phase as well as quadrature responses. The apparent depth, discussed above, is simply the sensor-source distance minus the measured altitude or flying height. Consequently, errors in the measured altitude will affect the apparent depth parameter but not the apparent resistivity parameter.

The apparent depth parameter is a useful indicator of simple layering in areas lacking a heavy tree cover. Depth information has been used for permafrost mapping, where positive apparent depths were used as a measure of permafrost thickness. However, little quantitative use has been made of negative apparent depths because the absolute value of the negative depth is not a measure of the thickness of the conductive upper layer and, therefore, is not meaningful physically. Qualitatively, a negative apparent depth estimate usually shows that the EM anomaly is caused by conductive overburden. Consequently, the apparent depth channel can be of significant help in distinguishing between overburden and bedrock conductors.

[3] Resistivity mapping with an airborne multicoil electromagnetic system: Geophysics, v. 43, p.144-172

Interpretation in Conductive Environments

Environments having low background resistivities (e.g., below 30 ohm-m for a 900 Hz system) yield very large responses from the conductive ground. This usually prohibits the recognition of discrete bedrock conductors. However, Fugro data processing techniques produce three parameters that contribute significantly to the recognition of bedrock conductors in conductive environments. These are the in-phase and quadrature difference channels (DIFI and DIFQ, which are available only on systems with "common" frequencies on orthogonal coil pairs), and the resistivity and depth channels (RES and DEP) for each coplanar frequency.

The EM difference channels (DIFI and DIFQ) eliminate most of the responses from conductive ground, leaving responses from bedrock conductors, cultural features (e.g., telephone lines, fences, etc.) and edge effects. Edge effects often occur near the perimeter of broad conductive zones. This can be a source of geologic noise. While edge effects yield anomalies on the EM difference channels, they do not produce resistivity anomalies. Consequently, the resistivity channel aids in eliminating anomalies due to edge effects. On the other hand, resistivity anomalies will coincide with the most highly conductive sections of conductive ground, and this is another source of geologic noise. The recognition of a bedrock conductor in a conductive environment therefore is based on the anomalous responses of the two difference channels (DIFI and DIFQ) and the resistivity channels (RES). The most favourable situation is where anomalies coincide on all channels.

The DEP channels, which give the apparent depth to the conductive material, also help to determine whether a conductive response arises from surficial material or from a conductive zone in the bedrock. When these channels ride above the zero level on the depth profiles (i.e., depth is negative), it implies that the EM and resistivity profiles are responding primarily to a conductive upper layer, i.e., conductive overburden. If the DEP channels are below the zero level, it indicates that a resistive upper layer exists, and this usually implies the existence of a bedrock conductor. If the low frequency DEP channel is below the zero level and the high frequency DEP is above, this suggests that a bedrock conductor occurs beneath conductive cover.

Reduction of Geologic Noise

Geologic noise refers to unwanted geophysical responses. For purposes of airborne EM surveying, geologic noise refers to EM responses caused by conductive overburden and magnetic permeability. It was mentioned previously that the EM difference channels (i.e., channel DIFI for in-phase and DIFQ for quadrature) tend to eliminate the response of conductive overburden.

Magnetite produces a form of geological noise on the in-phase channels. Rocks containing less than 1% magnetite can yield negative in-phase anomalies caused by magnetic permeability. When magnetite is widely distributed throughout a survey area, the in-phase EM channels may continuously rise and fall, reflecting variations in the magnetite percentage, flying height, and overburden thickness. This can lead to difficulties in recognizing deeply buried bedrock conductors, particularly if conductive overburden also exists. However, the response of broadly distributed magnetite generally vanishes on the in-phase difference channel DIFI. This feature can be a significant aid in the recognition of conductors that occur in rocks containing accessory magnetite.

EM Magnetite Mapping

The information content of HEM data consists of a combination of conductive eddy current responses and magnetic permeability responses. The secondary field resulting from conductive eddy current flow is frequency-dependent and consists of both in-phase and quadrature components, which are positive in sign. On the other hand, the secondary field resulting from magnetic permeability is independent of frequency and consists of only an in-phase component which is negative in sign. When magnetic permeability manifests itself by decreasing the measured amount of positive in-phase, its presence may be difficult to recognize. However, when it manifests itself by yielding a negative in-phase anomaly (e.g., in the absence of eddy current flow), its presence is assured. In this latter case, the negative component can be used to estimate the percent magnetite content.

A magnetite mapping technique, based on the low frequency coplanar data, can be complementary to magnetometer mapping in certain cases. Compared to magnetometry, it is far less sensitive but is more able to resolve closely spaced magnetite zones, as well as providing an estimate of the amount of magnetite in the rock. The method is sensitive to ¼% magnetite by weight when the EM sensor is at a height of 30 m above a magnetitic half-space. It can individually resolve steep dipping narrow magnetite-rich bands which are separated by 60 m. Unlike magnetometry, the EM magnetite method is unaffected by remanent magnetism or magnetic latitude.

The EM magnetite mapping technique provides estimates of magnetite content which are usually correct within a factor of 2 when the magnetite is fairly uniformly distributed. EM magnetite maps can be generated when magnetic permeability is evident as negative in-phase responses on the data profiles.

Like magnetometry, the EM magnetite method maps only bedrock features, provided that the overburden is characterized by a general lack of magnetite. This contrasts with resistivity mapping which portrays the combined effect of bedrock and overburden.

The Susceptibility Effect

When the host rock is conductive, the positive conductivity response will usually dominate the secondary field, and the susceptibility effect[4] will appear as a reduction in the in-phase, rather than as a negative value. The in-phase response will be lower than would be predicted by a model using zero susceptibility. At higher frequencies the in-phase conductivity response also gets larger, so a negative magnetite effect observed on the low frequency might not be observable on the higher frequencies, over the same body. The susceptibility effect is most obvious over discrete magnetite-rich zones, but also occurs over uniform geology such as a homogeneous half-space.

High magnetic susceptibility will affect the calculated apparent resistivity, if only conductivity is considered. Standard apparent resistivity algorithms use a homogeneous half-space model, with

[4] Magnetic susceptibility and permeability are two measures of the same physical property. Permeability is generally given as relative permeability, μ_r, which is the permeability of the substance divided by the permeability of free space ($4\ \pi\ x\ 10^{-7}$). Magnetic susceptibility k is related to permeability by $k=\mu^r-1$. Susceptibility is a unitless measurement, and is usually reported in units of 10^{-6}. The typical range of susceptibilities is –1 for quartz, 130 for pyrite, and up to $5\ x\ 10^5$ for magnetite, in 10^{-6} units (Telford et al, 1986).

zero susceptibility. For these algorithms, the reduced in-phase response will, in most cases, make the apparent resistivity higher than it should be. It is important to note that there is nothing wrong with the data, nor is there anything wrong with the processing algorithms. The apparent difference results from the fact that the simple geological model used in processing does not match the complex geology.

Measuring and Correcting the Magnetite Effect

Theoretically, it is possible to calculate (forward model) the combined effect of electrical conductivity and magnetic susceptibility on an EM response in all environments. The difficulty lies, however, in separating out the susceptibility effect from other geological effects when deriving resistivity and susceptibility from EM data.

Over a homogeneous half-space, there is a precise relationship between in-phase, quadrature, and altitude. These are often resolved as phase angle, amplitude, and altitude. Within a reasonable range, any two of these three parameters can be used to calculate the half space resistivity. If the rock has a positive magnetic susceptibility, the in-phase component will be reduced and this departure can be recognized by comparison to the other parameters.

The algorithm used to calculate apparent susceptibility and apparent resistivity from HEM data, uses a homogeneous half-space geological model. Non half-space geology, such as horizontal layers or dipping sources, can also distort the perfect half-space relationship of the three data parameters. While it may be possible to use more complex models to calculate both rock parameters, this procedure becomes very complex and time-consuming. For basic HEM data processing, it is most practical to stick to the simplest geological model.

Magnetite reversals (reversed in-phase anomalies) have been used for many years to calculate an “FeO” or magnetite response from HEM data (Fraser, 1981). However, this technique could only be applied to data where the in-phase was observed to be negative, which happens when susceptibility is high and conductivity is low.

Applying Susceptibility Corrections

Resistivity calculations done with susceptibility correction may change the apparent resistivity. High-susceptibility conductors, that were previously masked by the susceptibility effect in standard resistivity algorithms, may become evident. In this case the susceptibility corrected apparent resistivity is a better measure of the actual resistivity of the earth. However, other geological variations, such as a deep resistive layer, can also reduce the in-phase by the same amount. In this case, susceptibility correction would not be the best method. Different geological models can apply in different areas of the same data set. The effects of susceptibility, and other effects that can create a similar response, must be considered when selecting the resistivity algorithm.

Susceptibility from EM vs Magnetic Field Data

The response of the EM system to magnetite may not match that from a magnetometer survey. First, HEM-derived susceptibility is a rock property measurement, like resistivity. Magnetic data show the total magnetic field, a measure of the potential field, not the rock property. Secondly, the shape of an anomaly depends on the shape and direction of the source magnetic field. The electromagnetic field of HEM is much different in shape from the earth's magnetic field. Total field magnetic anomalies are different at different magnetic latitudes; HEM susceptibility anomalies have the same shape regardless of their location on the earth.

In far northern latitudes, where the magnetic field is nearly vertical, the total magnetic field measurement over a thin vertical dike is very similar in shape to the anomaly from the HEM-derived susceptibility (a sharp peak over the body). The same vertical dike at the magnetic equator would yield a negative magnetic anomaly, but the HEM susceptibility anomaly would show a positive susceptibility peak.

Effects of Permeability and Dielectric Permittivity

Resistivity algorithms that assume free-space magnetic permeability and dielectric permittivity, do not yield reliable values in highly magnetic or highly resistive areas. Both magnetic polarization and displacement currents cause a decrease in the in-phase component, often resulting in negative values that yield erroneously high apparent resistivities. The effects of magnetite occur at all frequencies, but are most evident at the lowest frequency. Conversely, the negative effects of dielectric permittivity are most evident at the higher frequencies, in resistive areas.

Table 15 below shows the effects of varying permittivity over a resistive (10,000 ohm-m) half space, at frequencies of 56,000 Hz (DIGHEM) and 102,000 Hz (RESOLVE).

Apparent Resistivity Calculations

Freq (Hz)	Coil	Sep (m)	Thres (ppm)	Alt (m)	In Phase	Quad Phase	App Res	App Depth (m)	Permittivity
56,000	CP	6.3	0.1	30	7.3	35.3	10118	-1.0	1 Air
56,000	CP	6.3	0.1	30	3.6	36.6	19838	-13.2	5 Quartz
56,000	CP	6.3	0.1	30	-1.1	38.3	81832	-25.7	10 Epidote
56,000	CP	6.3	0.1	30	-10.4	42.3	76620	-25.8	20 Granite
56,000	CP	6.3	0.1	30	-19.7	46.9	71550	-26.0	30 Diabase
56,000	CP	6.3	0.1	30	-28.7	52.0	66787	-26.1	40 Gabbro
102,000	CP	7.86	0.1	30	32.5	117.2	9409	-0.3	1 Air
102,000	CP	7.86	0.1	30	11.7	127.2	25956	-16.8	5 Quartz
102,000	CP	7.86	0.1	30	-14.0	141.6	97064	-26.5	10 Epidote
102,000	CP	7.86	0.1	30	-62.9	176.0	83995	-26.8	20 Granite
102,000	CP	7.86	0.1	30	-107.5	215.8	73320	-27.0	30 Diabase
102,000	CP	7.86	0.1	30	-147.1	259.2	64875	-27.2	40 Gabbro

Table 15 Effects of Permittivity on In-phase/Quadrature/Resistivity

Methods have been developed (Huang and Fraser, 2000, 2001) to correct apparent resistivities for the effects of permittivity and permeability. The corrected resistivities yield more credible values than if the effects of permittivity and permeability are disregarded.

Recognition of Culture

Cultural responses include all EM anomalies caused by man-made metallic objects. Such anomalies may be caused by inductive coupling or current gathering. The concern of the interpreter is to recognize when an EM response is due to culture. Points of consideration used by the interpreter, when coaxial and coplanar coil-pairs are operated at a common frequency, are as follows:

1. Channels CXPL and CPPL monitor 60 Hz radiation. An anomaly on these channels shows that the conductor is radiating power. Such an indication is normally a guarantee that the conductor is cultural. However, care must be taken to ensure that the conductor is not a geologic body that strikes across a power line, carrying leakage currents.

2. A flight that crosses a "line" (e.g., fence, telephone line, etc.) yields a centre-peaked coaxial anomaly and an m-shaped coplanar anomaly.[5] When the flight crosses the cultural line at a high angle of intersection, the amplitude ratio of coaxial/coplanar response is 2. Such an EM anomaly can only be caused by a line. The geologic body that yields anomalies most closely resembling a line is the vertically dipping thin dike. Such a body, however, yields an amplitude ratio of 1 rather than 2. Consequently, an m-shaped coplanar anomaly with a CXI/CPI amplitude ratio of 2 is virtually a guarantee that the source is a cultural line.

3. A flight that crosses a sphere or horizontal disk yields centre-peaked coaxial and coplanar anomalies with a CXI/CPI amplitude ratio (i.e., coaxial/coplanar) of $^1/_8$. In the absence of geologic bodies of this geometry, the most likely conductor is a metal roof or small fenced yard.[6] Anomalies of this type are virtually certain to be cultural if they occur in an area of culture.

4. A flight that crosses a horizontal rectangular body or wide ribbon yields an m-shaped coaxial anomaly and a centre-peaked coplanar anomaly. In the absence of geologic bodies of this geometry, the most likely conductor is a large fenced area.[5] Anomalies of this type are virtually certain to be cultural if they occur in an area of culture.

5. EM anomalies that coincide with culture, as seen on the camera film or video display, are usually caused by culture. However, care is taken with such coincidences because a geologic conductor could occur beneath a fence, for example. In this example, the fence would be expected to yield an m-shaped coplanar anomaly as in case #2 above. If, instead, a centre-peaked coplanar anomaly occurred, there would be concern that a thick geologic conductor coincided with the cultural line.

---

[5] See Figure 24 presented earlier.

[6] It is a characteristic of EM that geometrically similar anomalies are obtained from: (1) a planar conductor, and (2) a wire which forms a loop having dimensions identical to the perimeter of the equivalent planar conductor.

6. The above description of anomaly shapes is valid when the culture is not conductively coupled to the environment. In this case, the anomalies arise from inductive coupling to the EM transmitter. However, when the environment is quite conductive (e.g., less than 100 ohm-m at 900 Hz), the cultural conductor may be conductively coupled to the environment. In this latter case, the anomaly shapes tend to be governed by current gathering. Current gathering can completely distort the anomaly shapes, thereby complicating the identification of cultural anomalies. In such circumstances, the interpreter can only rely on the radiation channels and on the camera film or video records.

Magnetic Responses

The measured total magnetic field provides information on the magnetic properties of the earth materials in the survey area. The information can be used to locate magnetic bodies of direct interest for exploration, and for structural and lithological mapping.

The total magnetic field response reflects the abundance of magnetic material in the source. Magnetite is the most common magnetic mineral. Other minerals such as ilmenite, pyrrhotite, franklinite, chromite, hematite, arsenopyrite, limonite and pyrite are also magnetic, but to a lesser extent than magnetite on average.

In some geological environments, an EM anomaly with magnetic correlation has a greater likelihood of being produced by sulphides than one which is non-magnetic. However, sulphide ore bodies may be non-magnetic (e.g., the Kidd Creek deposit near Timmins, Canada) as well as magnetic (e.g., the Mattabi deposit near Sturgeon Lake, Canada).

Iron ore deposits will be anomalously magnetic in comparison to surrounding rock due to the concentration of iron minerals such as magnetite, ilmenite and hematite.

Changes in magnetic susceptibility often allow rock units to be differentiated based on the total field magnetic response. Geophysical classifications may differ from geological classifications if various magnetite levels exist within one general geological classification. Geometric considerations of the source such as shape, dip and depth, inclination of the earth's field and remanent magnetization will complicate such an analysis.

In general, mafic lithologies contain more magnetite and are therefore more magnetic than many sediments which tend to be weakly magnetic. Metamorphism and alteration can also increase or decrease the magnetization of a rock unit.

Textural differences on a total field magnetic contour, colour or shadow map due to the frequency of activity of the magnetic parameter resulting from inhomogeneities in the distribution of magnetite within the rock, may define certain lithologies. For example, near surface volcanics may display highly complex contour patterns with little line-to-line correlation.

Rock units may be differentiated based on the plan shapes of their total field magnetic responses. Mafic intrusive plugs can appear as isolated "bulls-eye" anomalies. Granitic intrusives appear as sub-circular zones, and may have contrasting rings due to contact metamorphism. Generally, granitic terrain will lack a pronounced strike direction, although granite gneiss may display strike.

Linear north-south units are theoretically not well-defined on total field magnetic maps in equatorial regions due to the low inclination of the earth's magnetic field. However, most stratigraphic units will have variations in composition along strike that will cause the units to appear as a series of alternating magnetic highs and lows.

Faults and shear zones may be characterized by alteration that causes destruction of magnetite (e.g., weathering) that produces a contrast with surrounding rock. Structural breaks may be filled by magnetite-rich, fracture filling material as is the case with diabase dikes, or by non-magnetic felsic material.

Faulting can also be identified by patterns in the magnetic total field contours or colours. Faults and dikes tend to appear as lineaments and often have strike lengths of several kilometres. Offsets in narrow, magnetic, stratigraphic trends also delineate structure. Sharp contrasts in magnetic lithologies may arise due to large displacements along strike-slip or dip-slip faults.

Gamma Ray Spectrometry

Radioelement concentrations are measures of the abundance of radioactive elements in the rock. The original abundance of the radioelements in any rock can be altered by the subsequent processes of metamorphism and weathering.

Gamma radiation in the range that is measured in the thorium, potassium, uranium and total count windows is strongly attenuated by rock, overburden and water. Almost all of the total radiation measured from rock and overburden originates in the upper .5 metres. Moisture in soil and bodies of water will mask the radioactivity from underlying rock. Weathered rock materials that have been displaced by glacial, water or wind action will not reflect the general composition of the underlying bedrock. Where residual soils exist, they may reflect the composition of underlying rock except where equilibrium does not exist between the original radioelement and the products in its decay series.

Radioelement counts (expressed as counts per second) are the rates of detection of the gamma radiation from specific decaying particles corresponding to products in each radioelements decay series. The radiation source for uranium is bismuth (Bi-214), for thorium it is thallium (Tl-208) and for potassium it is potassium (K-40).

The uranium and thorium radioelement concentrations are dependent on a state of equilibrium between the parent and daughter products in the decay series. Some daughter products in the uranium decay are long lived and could be removed by processes such as leaching. One product in the series, radon (Rn-222), is a gas which can easily escape. Both of these factors can affect the degree to which the calculated uranium concentrations reflect the actual composition of the source rock. Because the daughter products of thorium are relatively short lived, there is more likelihood that the thorium decay series is in equilibrium.

Lithological discrimination can be based on the measured relative concentrations and total, combined, radioactivity of the radioelements. Feldspar and mica contain potassium. Zircon, sphene and apatite are accessory minerals in igneous rocks that are sources of uranium and thorium. Monazite, thorianite, thorite, uraninite and uranothorite are also sources of uranium and thorium which are found in granites and pegmatites.

In general, the abundance of uranium, thorium and potassium in igneous rock increases with acidity.

Pegmatites commonly have elevated concentrations of uranium relative to thorium. Sedimentary rocks derived from igneous rocks may have characteristic signatures that are influenced by their parent rocks, but these will have been altered by subsequent weathering and alteration.

Metamorphism and alteration will cause variations in the abundance of certain radioelements relative to each other. For example, alterative processes may cause uranium enrichment to the extent that a rock will be of economic interest. Uranium anomalies are more likely to be economically significant if they consist of an increase in the uranium relative to thorium and potassium, rather than a sympathetic increase in all three radioelements.

Faults can exhibit radioactive highs due to increased permeability which allows radon migration, or as lows due to structural control of drainage and fluvial sediments which attenuate gamma radiation from the underlying rocks. Faults can also be recognized by sharp contrasts in radiometric lithologies due to large strike-slip or dip-slip displacements. Changes in relative radioelement concentrations due to alteration will also define faults.

Similar to magnetics, certain rock types can be identified by their plan shapes if they also produce a radiometric contrast with surrounding rock. For example, granite intrusions will appear as sub-circular bodies, and may display concentric zonations. They will tend to imminent strike direction. Offsets of narrow, continuous, stratigraphic units with contrasting radiometric signatures can identify faulting, and folding of stratigraphic trends will also be apparent.

Appendix F

Data Processing Flowcharts

FDEM Data Processing Flow Chart

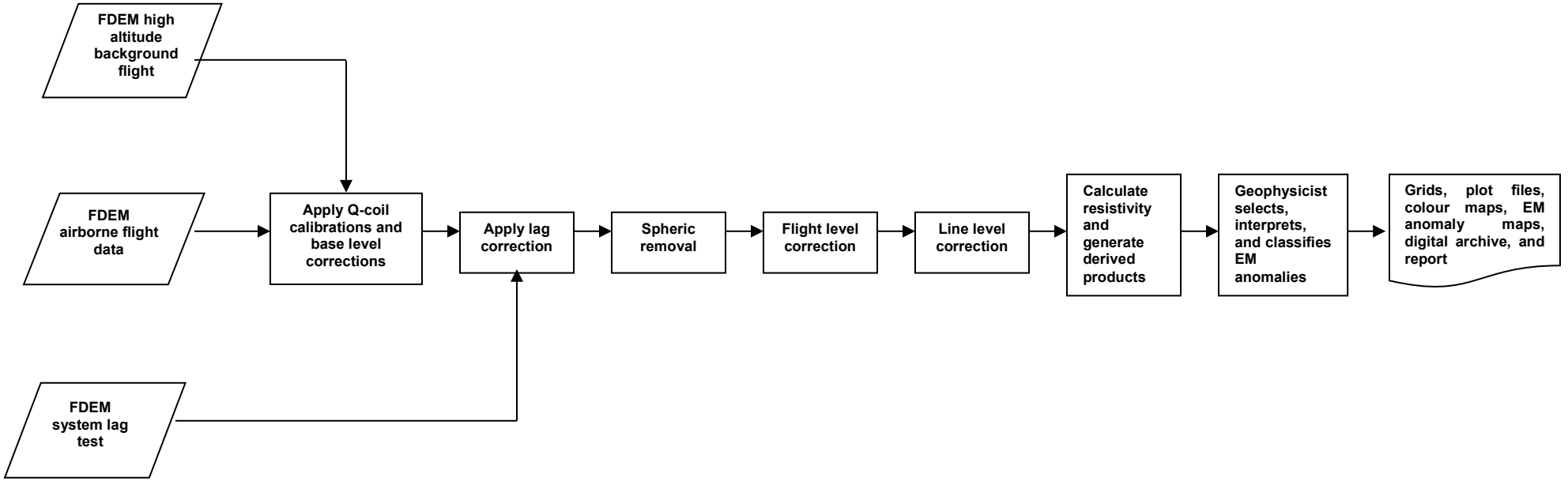

Magnetic Data Processing Flow Chart

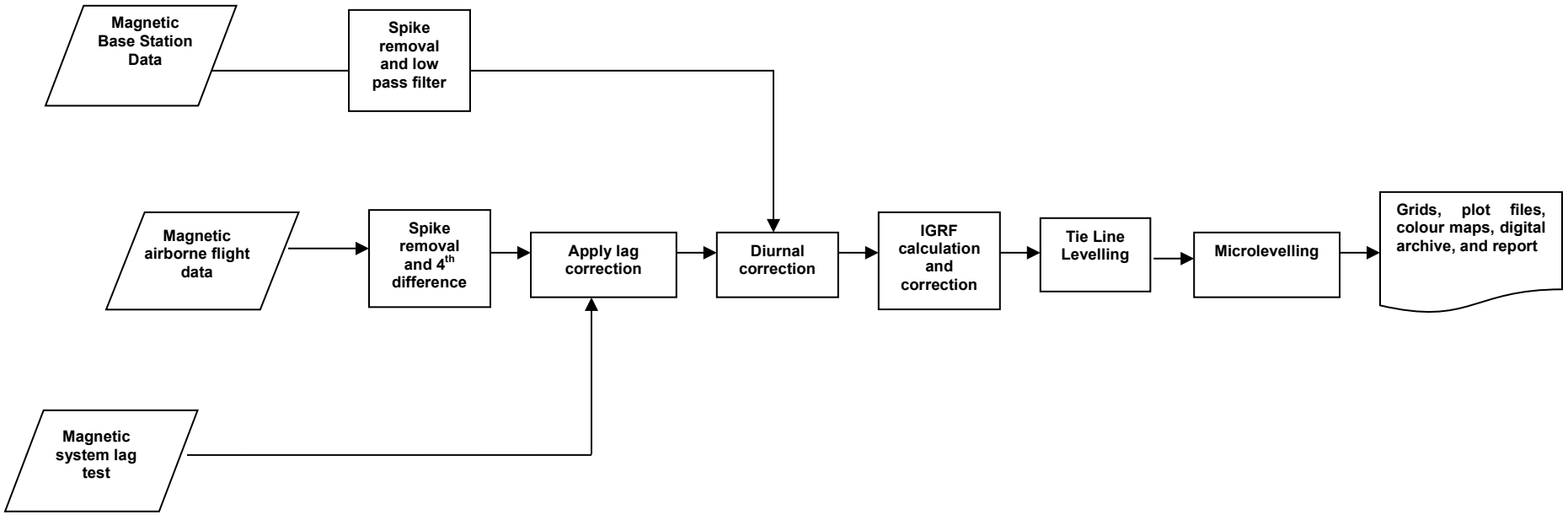

Radiometric Data Processing Flow Chart

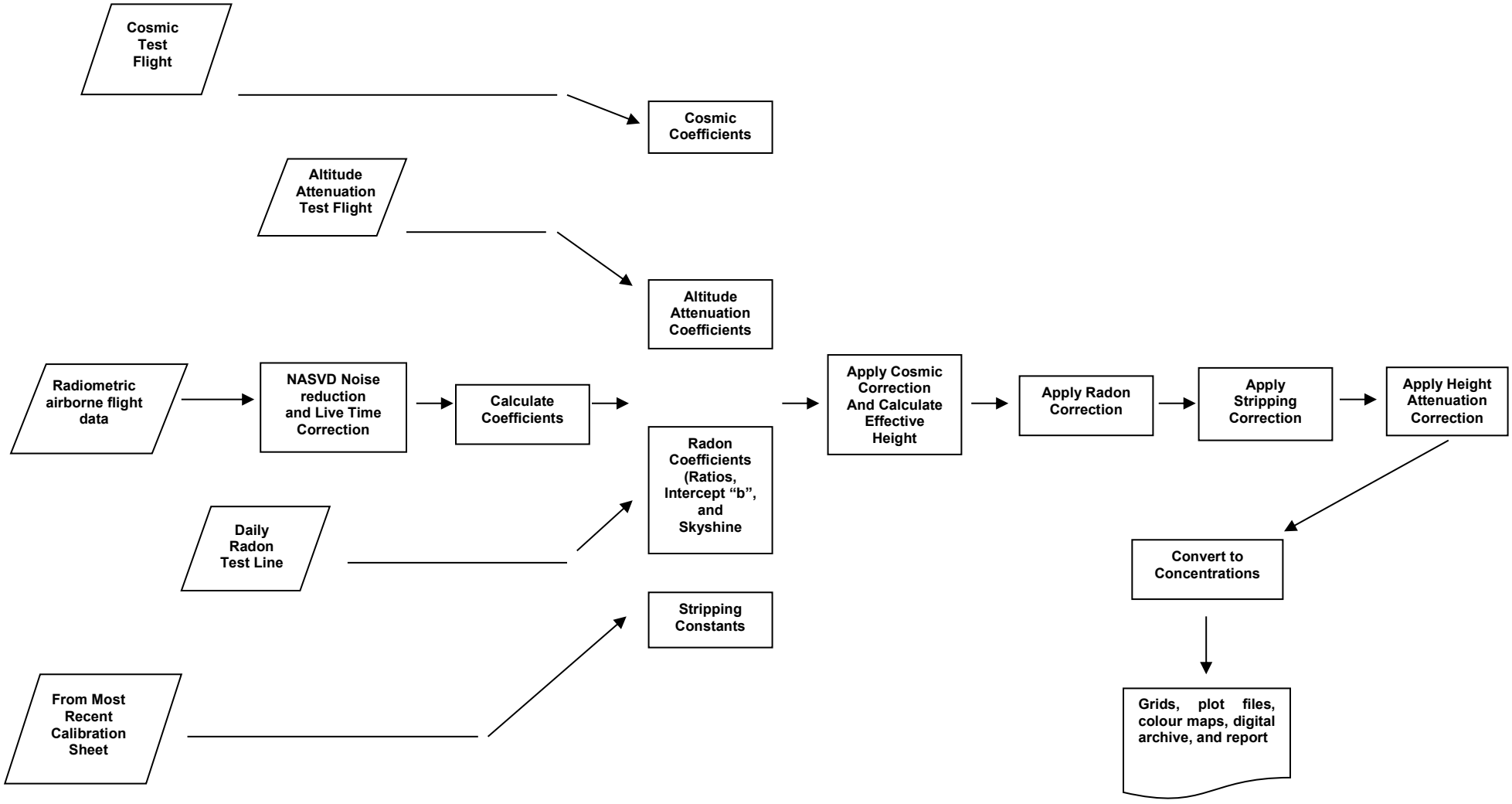

Appendix G

Glossary

FUGRO GLOSSARY OF AIRBORNE GEOPHYSICAL TERMS

accelerometer: an instrument that measures both acceleration (due to motion) and acceleration due to ***gravity***.

altitude attenuation: the absorption of gamma rays by the atmosphere between the earth and the detector. The number of gamma rays detected by a system decreases as the altitude increases.

AGG: Airborne ***gravity gradiometer.***

AGS: Airborne ***gamma-ray spectrometry***.

amplitude: The strength of the total electromagnetic field. In ***frequency domain*** it is most often the sum of the squares of ***in-phase*** and ***quadrature*** components. In multi-component electromagnetic surveys it is generally the sum of the squares of all three directional components.

analytic signal: The total amplitude of all the directions of magnetic ***gradient***. Calculated as the sum of the squares.

anisotropy: Having different ***physical parameters*** in different directions. This can be caused by layering or fabric in the geology. Note that a unit can be anisotropic, but still **homogeneous**.

anomaly: A localized change in the geophysical data characteristic of a discrete source, such as a conductive or magnetic body: something locally different from the **background**.

apparent- : the ***physical parameters*** of the earth measured by a geophysical system are normally expressed as apparent, as in "apparent ***resistivity*****"**. This means that the measurement is limited by assumptions made about the geology in calculating the response measured by the geophysical system. Apparent resistivity calculated with ***HEM***, for example, generally assumes that the earth is a ***homogeneous half-space*** – not layered.

attitude: the orientation of a geophysical system relative to the earth. Some surveys assume the instrument attitudes are constant, and other surveys measure the attitude and correct the data for the changes in response because of attitude.

B-field: In time-domain **electromagnetic** surveys, the magnetic field component of the (electromagnetic) **field**. This can be measured directly, although more commonly it is calculated by integrating the time rate of change of the magnetic field **dB/dt**, as measured with a receiver coil.

background: The "normal" response in the geophysical data – that response observed over most of the survey area. **Anomalies** are usually measured relative to the background. In airborne gamma-ray spectrometric surveys the term defines the **cosmic**, radon, and aircraft responses in the absence of a signal from the ground.

base-level: The measured values in a geophysical system in the absence of any outside signal. All geophysical data are measured relative to the system base level.

base frequency: The frequency of the pulse repetition for a ***time-domain electromagnetic*** system. Measured between subsequent positive pulses.

base magnetometer: A stationary magnetometer used to record the ***diurnal*** variations in the earth's magnetic field; to be used to correct the survey magnetic data.

bird: A common name for the pod towed beneath or behind an aircraft, carrying the geophysical sensor array.

bucking: The process of removing the strong ***signal*** from the ***primary field*** at the ***receiver*** from the data, to measure the ***secondary field***. It can be done electronically or mathematically. This is done in ***frequency-domain EM***, and to measure ***on-time*** in ***time-domain EM***.

calibration: a procedure to ensure a geophysical instrument is measuring accurately and repeatably. Most often applied in ***EM*** and ***gamma-ray spectrometry***.

calibration coil: A wire coil of known size and dipole moment, which is used to generate a field of known ***amplitude*** and ***phase*** or ***decay constant*** in the receiver, for system calibration. Calibration coils can be external, or internal to the system. Internal coils may be called Q-coils.

coaxial coils: **[CX]** Coaxial coils in an HEM system are in the vertical plane, with their axes horizontal and collinear in the flight direction. These are most sensitive to vertical conductive objects in the ground, such as thin, steeply dipping conductors perpendicular to the flight direction. Coaxial coils generally give the sharpest anomalies over localized conductors. (See also ***coplanar coils***)

coil: A multi-turn wire loop used to transmit or detect electromagnetic fields. Time varying ***electromagnetic*** fields through a coil induce a voltage proportional to the strength of the field and the rate of change over time.

compensation: Correction of airborne geophysical data for the changing effect of the aircraft. This process is generally used to correct data in ***fixed-wing time-domain electromagnetic*** surveys (where the transmitter is on the aircraft and the receiver is moving), and magnetic surveys (where the sensor is on the aircraft, turning in the earth's magnetic field.

component: In ***frequency domain electromagnetic*** surveys this is one of the two **phase** measurements – ***in-phase or quadrature***. In "multi-component" electromagnetic surveys it is also used to define the measurement in one geometric direction (vertical, horizontal in-line and horizontal transverse – the Z, X and Y components).

Compton scattering: gamma ray photons will bounce off electrons as they pass through the earth and atmosphere, reducing their energy and then being detected by ***radiometric*** sensors at lower energy levels. See also ***stripping***.

conductance: See ***conductivity thickness***

conductivity: [σ] The facility with which the earth or a geological formation conducts electricity. Conductivity is usually measured in milli-Siemens per metre (mS/m). It is the reciprocal of ***resistivity***.

conductivity-depth imaging: see ***conductivity-depth transform***.

conductivity-depth transform: A process for converting electromagnetic measurements to an approximation of the conductivity distribution vertically in the earth, assuming a ***layered earth***. (Macnae and Lamontagne, 1987; Wolfgram and Karlik, 1995)

conductivity thickness: [**σt**] The product of the ***conductivity***, and thickness of a large, tabular body. (It is also called the "conductivity-thickness product") In electromagnetic geophysics, the response of a thin plate-like conductor is proportional to the conductivity multiplied by thickness. For example a 10 metre thickness of 20 Siemens/m mineralization will be equivalent to 5 metres of 40 S/m; both have 200 S conductivity thickness. Sometimes referred to as conductance.

conductor: Used to describe anything in the ground more conductive than the surrounding geology. Conductors are most often clays or graphite, or hopefully some type of mineralization, but may also be man-made objects, such as fences or pipelines.

continuation: mathematical procedure applied to ***potential field*** geophysical data to approximate data collected at a different altitude. Data can be continued upward to a higher altitude or downward to a lower altitude.

coplanar coils: **[CP]** In HEM, the coplanar coils lie in the horizontal plane with their axes vertical, and parallel. These coils are most sensitive to massive conductive bodies, horizontal layers, and the ***halfspace***.

cosmic ray: High energy sub-atomic particles from outer space that collide with the earth's atmosphere to produce a shower of gamma rays (and other particles) at high energies.

counts (per second): The number of ***gamma-rays*** detected by a gamma-ray ***spectrometer.*** The rate depends on the geology, but also on the size and sensitivity of the detector.

culture: A term commonly used to denote any man-made object that creates a geophysical anomaly. Includes, but not limited to, power lines, pipelines, fences, and buildings.

current channelling: See current gathering.

current gathering: The tendency of electrical currents in the ground to channel into a conductive formation. This is particularly noticeable at higher frequencies or early time channels when the formation is long and parallel to the direction of current flow. This tends to enhance anomalies relative to inductive currents (see also ***induction***). Also known as current channelling.

daughter products: The radioactive natural sources of gamma-rays decay from the original "parent" element (commonly potassium, uranium, and thorium) to one or more lower-energy "daughter" elements. Some of these lower energy elements are also radioactive and decay further. ***Gamma-ray spectrometry*** surveys may measure the gamma rays given off by the original element or by the decay of the daughter products.

dB/dt: As the ***secondary electromagnetic field*** changes with time, the magnetic field [**B**] component induces a voltage in the receiving ***coil***, which is proportional to the rate of change of the magnetic field over time.

decay: In ***time-domain electromagnetic*** theory, the weakening over time of the ***eddy currents*** in the ground, and hence the ***secondary field*** after the ***primary field*** electromagnetic pulse is turned off. In ***gamma-ray spectrometry***, the radioactive breakdown of an element, generally potassium, uranium, thorium, into their ***daughter*** products.

decay constant: see time constant.

decay series: In ***gamma-ray spectrometry***, a series of progressively lower energy ***daughter products*** produced by the radioactive breakdown of uranium or thorium.

depth of exploration: The maximum depth at which the geophysical system can detect the target. The depth of exploration depends very strongly on the type and size of the target, the contrast of the target with the surrounding geology, the homogeneity of the surrounding geology, and the type of geophysical system. One measure of the maximum depth of exploration for an electromagnetic system is the depth at which it can detect the strongest conductive target – generally a highly conductive horizontal layer.

differential resistivity: A process of transforming ***apparent resistivity*** to an approximation of layer resistivity at each depth. The method uses multi-frequency HEM data and approximates the effect of shallow layer ***conductance*** determined from higher frequencies to estimate the deeper conductivities (Huang and Fraser, 1996)

dipole moment: [NIA] For a transmitter, the product of the area of a ***coil***, the number of turns of wire, and the current flowing in the coil. At a distance significantly larger than the size of the coil, the magnetic field from a coil will be the same if the dipole moment product is the same. For a receiver coil, this is the product of the area and the number of turns. The sensitivity to a magnetic field (assuming the source is far away) will be the same if the dipole moment is the same.

diurnal: The daily variation in a natural field, normally used to describe the natural fluctuations (over hours and days) of the earth's magnetic field.

dielectric permittivity: **[ε]** The capacity of a material to store electrical charge, this is most often measured as the relative permittivity [ε_r], or ratio of the material dielectric to that of free space. The effect of high permittivity may be seen in HEM data at high frequencies over highly resistive geology as a reduced or negative ***in-phase***, and higher ***quadrature*** data.

dose rate: see **exposure rate**.

drape: To fly a survey following the terrain contours, maintaining a constant altitude above the local ground surface. Also applied to re-processing data collected at varying altitudes above ground to simulate a survey flown at constant altitude.

drift: Long-time variations in the base-level or calibration of an instrument.

eddy currents: The electrical currents induced in the ground, or other conductors, by a time-varying ***electromagnetic field*** (usually the ***primary field***). Eddy currents are also induced in the aircraft's metal frame and skin; a source of ***noise*** in EM surveys.

electromagnetic: **[EM]** Comprised of a time-varying electrical and magnetic field. Radio waves are common electromagnetic fields. In geophysics, an electromagnetic system is one which transmits a time-varying ***primary field*** to induce ***eddy currents*** in the ground, and then measures the ***secondary field*** emitted by those eddy currents.

energy window: A broad spectrum of ***gamma-ray*** energies measured by a spectrometric survey. The energy of each gamma-ray is measured and divided up into numerous discrete energy levels, called windows.

equivalent (thorium or uranium): The amount of radioelement calculated to be present, based on the gamma-rays measured from a **daughter** element. This assumes that the ***decay series*** is in equilibrium – progressing normally.

exposure rate: in radiometric surveys, a calculation of the total exposure rate due to gamma rays at the ground surface. It is used as a measurement of the concentration of all the **radioelements** at the surface. Sometimes called “dose rate”.See also: **natural exposure rate**.

fiducial, or fid: Timing mark on a survey record. Originally these were timing marks on a profile or film; now the term is generally used to describe 1-second interval timing records in digital data, and on maps or profiles.

Figure of Merit: **(FOM)** A sum of the 12 distinct magnetic noise variations measured by each of four flight directions, and executing three aircraft attitude variations (yaw, pitch, and roll) for each direction. The flight directions are generally parallel and perpendicular to planned survey flight directions. The FOM is used as a measure of the **manoeuvre noise** before and after **compensation.**

fixed-wing: Aircraft with wings, as opposed to “rotary wing” helicopters.

flight: a continuous interval of survey data collection, generally between stops at base to refuel.

flight-line: a single line of data across the survey area. Surveys are generally comprised of many parallel flight lines to cover the survey area, with wider-spaced ***tie lines*** perpendicular. Flight lines are generally separated by ***turn-arounds*** when the aircraft is outside the survey area.

footprint: This is a measure of the area of sensitivity under the aircraft of an airborne geophysical system. The footprint of an ***electromagnetic*** system is dependent on the altitude of the system, the orientation of the transmitter and receiver and the separation between the receiver and transmitter, and the conductivity of the ground. The footprint of a ***gamma-ray spectrometer*** depends mostly on the altitude. For all geophysical systems, the footprint also depends on the strength of the contrasting ***anomaly***.

frequency domain: An ***electromagnetic*** system which transmits a harmonic ***primary field*** that oscillates over time (e.g. sinusoidal), inducing a similarly varying electrical current in the ground. These systems generally measure the changes in the ***amplitude*** and ***phase*** of the ***secondary field*** from the ground at different frequencies by measuring the **in-phase** and **quadrature** phase components. See also ***time-domain***.

full-stream data: Data collected and recorded continuously at the highest possible sampling rate. Normal data are stacked (see ***stacking***) over some time interval before recording.

gamma-ray: A very high-energy photon, emitted from the nucleus of an atom as it undergoes a change in energy levels.

gamma-ray spectrometry: Measurement of the number and energy of natural (and sometimes man-made) gamma-rays across a range of photon energies.

GGI: gravity gradiometer instrument. An airborne gravity gradiometer (AGG) consists of a GGI mounted in an inertial platform together with a temperature control system.

gradient: In magnetic surveys, the gradient is the change of the magnetic field over a distance, either vertically or horizontally in either of two directions. Gradient data can be measured, or calculated from the total magnetic field data because it changes more quickly over distance than the ***total magnetic field***, and so may provide a more precise measure of the location of a source. See also ***analytic signal***.

gradiometer, gradiometry: instrument and measurement of the gradient, or change in a field with location usually for ***gravity*** or ***magnetic*** surveys. Used to provide higher resolution of ***targets***, better ***interpretation*** of ***target*** geometry, independence from drift and absolute field and, for ***gravity***, accelerations of the aircraft.

gravity: Survey collecting measurements of the earth's gravitational field strength. Denser objects in the earth create stronger gravitational pull above them.

ground effect: The response from the earth. A common ***calibration*** procedure in many geophysical surveys is to fly to altitude high enough to be beyond any measurable response from the ground, and there establish ***base levels*** or ***backgrounds***.

half-space: A mathematical model used to describe the earth – as infinite in width, length, and depth below the surface. The most common halfspace models are ***homogeneous*** and ***layered earth***.

heading error: A slight change in the magnetic field measured when flying in opposite directions.

HEM: Helicopter ElectroMagnetic, This designation is most commonly used for helicopter-borne, ***frequency-domain*** electromagnetic systems. At present, the transmitter and receivers are normally mounted in a ***bird*** carried on a sling line beneath the helicopter.

herringbone pattern: A pattern created in geophysical data by an asymmetric system, where the **anomaly** may be extended to either side of the source, in the direction of flight. Appears like fish bones, or like the teeth of a comb, extending either side of centre, each tooth an alternate flight line.

homogeneous: This is a geological unit that has the same ***physical parameters*** throughout its volume. This unit will create the same response to an HEM system anywhere, and the HEM system will measure the same apparent ***resistivity*** anywhere. The response may change with system direction (see ***anisotropy***).

HFEM: Helicopter Frequency-domain ElectroMagnetic, This designation is used for helicopter-borne, **frequency-*domain*** electromagnetic systems. Formerly most often called HEM.

HTEM: Helicopter Time-domain ElectroMagnetic, This designation is used for the new generation of helicopter-borne, ***time-domain*** electromagnetic systems.

in-phase: the component of the measured ***secondary field*** that has the same phase as the transmitter and the ***primary field***. The in-phase component is stronger than the ***quadrature*** phase over relatively higher ***conductivity***.

induction: Any time-varying electromagnetic field will induce (cause) electrical currents to flow in any object with non-zero ***conductivity***. (see ***eddy currents***)

induction number: also called the "response parameter", this number combines many of the most significant parameters affecting the ***EM*** response into one parameter against which to compare responses. For a ***layered earth*** the response parameter is $\mu\omega\sigma h^2$ and for a large, flat, ***conductor*** it is $\mu\omega\sigma th$, where μ is the ***magnetic permeability***, ω is the angular ***frequency***, σ is the **conductivity**, t is the thickness (for the flat conductor) and h is the height of the system above the conductor.

inductive limit: When the frequency of an EM system is very high, or the **conductivity** of the target is very high, the response measured will be entirely **in-phase** with no **quadrature** (**phase** angle =0). The in-phase response will remain constant with further increase in conductivity or frequency. The system can no longer detect changes in conductivity of the target.

infinite: In geophysical terms, an "infinite' dimension is one much greater than the ***footprint*** of the system, so that the system does not detect changes at the edges of the object.

International Geomagnetic Reference Field: **[IGRF]** An approximation of the smooth magnetic field of the earth, in the absence of variations due to local geology. Once the IGRF is subtracted from the measured magnetic total field data, any remaining variations are assumed to be due to local geology. The IGRF also predicts the slow changes of the field up to five years in the future.

inversion, or **inverse modeling**: A process of converting geophysical data to an earth model, which compares theoretical models of the response of the earth to the data measured, and refines the model until the response closely fits the measured data (Huang and Palacky, 1991)

layered earth: A common geophysical model which assumes that the earth is horizontally layered – the ***physical parameters*** are constant to ***infinite*** distance horizontally, but change vertically.

lead-in: approach to a ***flight line*** outside of survey area to establish proper track and stabilize instrumentations. The lead-in for a helicopter survey is generally shorter than required for fixed-wing.

line source, or line current: a long narrow object that creates an ***anomaly*** on an ***EM*** survey. Generally man-made objects like fences, power lines, and pipelines (***culture***).

mag: common abbreviation for ***magnetic.***

magnetic: ("**mag**") a survey measuring the strength of the earth's magnetic field, to identify geology and targets by their effect on the field.

magnetic permeability: **[μ]** This is defined as the ratio of magnetic induction to the inducing magnetic field. The relative magnetic permeability [μ_r] is often quoted, which is the ratio of the rock permeability to the permeability of free space. In geology and geophysics, the ***magnetic susceptibility*** is more commonly used to describe rocks.

magnetic susceptibility: **[k]** A measure of the degree to which a body is magnetized. In SI units this is related to relative ***magnetic permeability*** by $k=\mu_r-1$, and is a dimensionless unit. For most geological material, susceptibility is influenced primarily by the percentage of magnetite. It is most often quoted in units of 10^{-6}. In HEM data this is most often apparent as a negative ***in-phase*** component over high susceptibility, high ***resistivity*** geology such as diabase dikes.

manoeuvre noise: variations in the magnetic field measured caused by changes in the relative positions of the magnetic sensor and magnetic objects or electrical currents in the aircraft. This type of noise is generally corrected by magnetic **compensation**.

model: Geophysical theory and applications generally have to assume that the geology of the earth has a form that can be easily defined mathematically, called the model. For example steeply dipping **conductor**s are generally modeled as being **infinite** in horizontal and depth extent, and very thin. The earth is generally modeled as horizontally layered, each layer infinite in extent and uniform in characteristic. These models make the mathematics to describe the response of the (normally very complex) earth practical. As theory advances, and computers become more powerful, the useful models can become more complex.

natural exposure rate: in radiometric surveys, a calculation of the total exposure rate due to natural-source gamma rays at the ground surface. It is used as a measurement of the concentration of all the natural **radioelements** at the surface. See also: **exposure rate**.

natural source: any geophysical technique for which the source of the energy is from nature, not from a man-made object. Most commonly applied to natural source ***electromagnetic*** surveys.

noise: That part of a geophysical measurement that the user does not want. Typically this includes electronic interference from the system, the atmosphere (***sferics***), and man-made sources. This can be a subjective judgment, as it may include the response from geology other than the target of interest. Commonly the term is used to refer to high frequency (short period) interference. See also ***drift***.

Occam's inversion: an ***inversion*** process that matches the measured ***electromagnetic*** data to a theoretical model of many, thin layers with constant thickness and varying resistivity (Constable et al, 1987).

off-time: In a ***time-domain electromagnetic*** survey, the time after the end of the ***primary field pulse***, and before the start of the next pulse.

on-time: In a ***time-domain electromagnetic*** survey, the time during the ***primary field pulse***.

overburden: In engineering and mineral exploration terms, this most often means the soil on top of the unweathered bedrock. It may be sand, glacial till, or weathered rock.

Phase, phase angle: The angular difference in time between a measured sinusoidal electromagnetic field and a reference – normally the primary field. The phase is calculated from $\tan^{-1}$(***in-phase / quadrature***).

physical parameters: These are the characteristics of a geological unit. For electromagnetic surveys, the important parameters are ***conductivity, magnetic permeability*** (or ***susceptibility***) and ***dielectric permittivity***; for magnetic surveys the parameter is magnetic susceptibility, and for gamma ray spectrometric surveys it is the concentration of the major radioactive elements: potassium, uranium, and thorium.

permittivity: see ***dielectric permittivity***.

permeability: see ***magnetic permeability***.

potential field: A field that obeys Laplace's Equation. Most commonly used to describe ***gravity*** and ***magnetic*** measurements.

primary field: the EM field emitted by a transmitter. This field induces ***eddy currents*** in (energizes) the conductors in the ground, which then create their own ***secondary*** **fields**.

pulse: In time-domain EM surveys, the short period of intense ***primary*** field transmission. Most measurements (the ***off-time***) are measured after the pulse. **On-time** measurements may be made during the pulse.

quadrature: that component of the measured ***secondary field*** that is phase-shifted 90° from the ***primary field***. The quadrature component tends to be stronger than the ***in-phase*** over relatively weaker ***conductivity***.

Q-coils: see ***calibration coil***.

radioelements: This normally refers to the common, naturally-occurring radioactive elements: potassium (K), uranium (U), and thorium (Th). It can also refer to man-made radioelements, most often cobalt (Co) and cesium (Cs)

radiometric: Commonly used to refer to ***gamma ray*** spectrometry.

radon: A radioactive daughter product of uranium and thorium, radon is a gas which can leak into the atmosphere, adding to the non-geological background of a gamma-ray spectrometric survey.

receiver: the ***signal*** detector of a geophysical system. This term is most often used in active geophysical systems – systems that transmit some kind of signal. In airborne ***electromagnetic*** surveys it is most often a ***coil***. (see also, ***transmitter***)

resistivity: **[ρ]** The strength with which the earth or a geological formation resists the flow of electricity, typically the flow induced by the ***primary field*** of the electromagnetic transmitter. Normally expressed in ohm-metres, it is the reciprocal of ***conductivity***.

resistivity-depth transforms: similar to ***conductivity depth transforms***, but the calculated ***conductivity*** has been converted to ***resistivity***.

resistivity section: an approximate vertical section of the resistivity of the layers in the earth. The resistivities can be derived from the ***apparent resistivity***, the ***differential resistivities***, ***resistivity-depth transforms***, or ***inversions***.

response parameter: another name for the **induction number**.

secondary field: The field created by conductors in the ground, as a result of electrical currents induced by the ***primary field*** from the ***electromagnetic*** transmitter. Airborne ***electromagnetic*** systems are designed to create and measure a secondary field.

Sengpiel section: a ***resistivity section*** derived using the ***apparent resistivity*** and an approximation of the depth of maximum sensitivity for each frequency.

sferic: Lightning, or the ***electromagnetic*** signal from lightning, it is an abbreviation of "atmospheric discharge". These appear to magnetic and electromagnetic sensors as sharp "spikes" in the data. Under some conditions lightning storms can be detected from hundreds of kilometres away. (see ***noise***)

signal: That component of a measurement that the user wants to see – the response from the targets, from the earth, etc. (See also ***noise***)

skin depth: A measure of the depth of penetration of an electromagnetic field into a material. It is defined as the depth at which the primary field decreases to 1/e of the field at the surface. It is calculated by approximately 503 x √(resistivity/frequency). Note that depth of penetration is greater at higher ***resistivity*** and/or lower ***frequency***.

spec: common abbreviation for *gamma-ray spectrometry*.

spectrometry: Measurement across a range of energies, where ***amplitude*** and energy are defined for each measurement. In gamma-ray spectrometry, the number of gamma rays are measured for each energy ***window***, to define the ***spectrum***.

spectrum: In ***gamma ray spectrometry***, the continuous range of energy over which gamma rays are measured. In ***time-domain electromagnetic*** surveys, the spectrum is the energy of the **pulse** distributed across an equivalent, continuous range of frequencies.

spheric: see ***sferic***.

stacking: Summing repeat measurements over time to enhance the repeating ***signal***, and minimize the random ***noise***.

stinger: A boom mounted on an aircraft to carry a geophysical sensor (usually ***magnetic***). The boom moves the sensor farther from the aircraft, which might otherwise be a source of ***noise*** in the survey data.

stripping: Estimation and correction for the gamma ray photons of higher and lower energy that are observed in a particular ***energy window***. See also ***Compton scattering***.

susceptibility: See ***magnetic susceptibility***.

tau: [τ] Often used as a name for the ***decay time constant***.

TDEM: ***time domain electromagnetic***.

thin sheet: A standard model for electromagnetic geophysical theory. It is usually defined as a thin, flat-lying conductive sheet, ***infinite*** in both horizontal directions. (see also ***vertical plate***)

tie-line: A survey line flown across most of the ***traverse lines***, generally perpendicular to them, to assist in measuring ***drift*** and ***diurnal*** variation. In the short time required to fly a tie-line it is assumed that the drift and/or diurnal will be minimal, or at least changing at a constant rate.

time constant: The time required for an ***electromagnetic*** field to decay to a value of 1/e of the original value. In ***time-domain*** electromagnetic data, the time constant is proportional to the size and ***conductance*** of a tabular conductive body. Also called the decay constant.

Time channel: In ***time-domain electromagnetic*** surveys the decaying ***secondary field*** is measured over a period of time, and the divided up into a series of consecutive discrete measurements over that time.

time-domain: ***Electromagnetic*** system which transmits a pulsed, or stepped ***electromagnetic*** field. These systems induce an electrical current (***eddy current***) in the ground that persists after the ***primary field*** is turned off, and measure the change over time of the ***secondary field*** created as the currents ***decay***. See also ***frequency-domain***.

total energy envelope: The sum of the squares of the three ***components*** of the ***time-domain electromagnetic secondary field***. Equivalent to the ***amplitude*** of the secondary field.

transient: Time-varying. Usually used to describe a very short period pulse of ***electromagnetic*** field.

transmitter: The source of the ***signa***l to be measured in a geophysical survey. In airborne ***EM*** it is most often a **coil** carrying a time-varying electrical current, transmitting the ***primary field***. (see also ***receiver***)

traverse line: A normal geophysical survey line. Normally parallel traverse lines are flown across the property in spacing of 50 m to 500 m, and generally perpendicular to the target geology. Also called a **flight line**.

turn-arounds: The time the aircraft is turning between one ***traverse*** or ***tie line*** and the next. Turn-arounds are generally outside the survey area, and the data collected during this time generally are not useable, because of aircraft ***manoeuvre noise***.

vertical plate: A standard model for electromagnetic geophysical theory. It is usually defined as thin conductive sheet, ***infinite*** in horizontal dimension and depth extent. (see also ***thin shee***t)

waveform: The shape of the ***electromagnetic pulse*** from a ***time-domain*** electromagnetic transmitter.

window: A discrete portion of a ***gamma-ray spectrum*** or ***time-domain electromagnetic decay***. The continuous energy spectrum or ***full-stream*** data are grouped into windows to reduce the number of samples, and reduce ***noise***.

zero, or zero level: The ***base level*** of an instrument, with no ***ground effect*** or ***drift***. Also, the act of measuring and setting the zero level.

Version 1.8, February, 2012
Greg Hodges,
Chief Geophysicist
Fugro Airborne Surveys, Toronto

Common Symbols and Acronyms

k	Magnetic susceptibility
ε	Dielectric permittivity
μ, μ_r	Magnetic permeability, relative permeability
ρ, ρ_a	Resistivity, apparent resistivity
σ,σ_a	Conductivity, apparent conductivity
σ**t**	Conductivity thickness
τ	Tau, or time constant
Ωm	ohm-metres, units of resistivity
AGS	Airborne gamma ray spectrometry.
CDT	Conductivity-depth transform, conductivity-depth imaging (Macnae and Lamontagne, 1987; Wolfgram and Karlik, 1995)
CPI, CPQ	Coplanar in-phase, quadrature
CPS	Counts per second
CTP	Conductivity thickness product
CXI, CXQ	Coaxial, in-phase, quadrature
FOM	Figure of Merit
fT	femtoteslas, common unit for measurement of B-Field in time-domain EM
EM	Electromagnetic
keV	kilo electron volts – a measure of gamma-ray energy
MeV	mega electron volts – a measure of gamma-ray energy 1MeV = 1000keV
NIA	dipole moment: turns x current x Area
nT	nanotesla, a measure of the strength of a magnetic field
nT/s	nanoteslas/second; standard unit of measurement of secondary field dB/dt in time domain EM.
nG/h	nanoGreys/hour – gamma ray dose rate at ground level
ppm	parts per million – a measure of secondary field or noise relative to the primary or radioelement concentration.
pT	picoteslas: standard unit of measurement of B-Field in time-domain EM
pT/s	picoteslas per second: Units of decay of secondary field, dB/dt
S	siemens – a unit of conductance
x:	the horizontal component of an EM field parallel to the direction of flight.
y:	the horizontal component of an EM field perpendicular to the direction of flight.
z:	the vertical component of an EM field.

References:

Constable, S.C., Parker, R.L., And Constable, C.G., 1987, Occam's inversion: a practical algorithm for generating smooth models from electromagnetic sounding data: Geophysics, 52, 289-300

Huang, H. and Fraser, D.C, 1996. The differential parameter method for muiltifrequency airborne resistivity mapping. Geophysics, 55, 1327-1337

Huang, H. and Palacky, G.J., 1991, Damped least-squares inversion of time-domain airborne EM data based on singular value decomposition: Geophysical Prospecting, v.39, 827-844

Macnae, J. and Lamontagne, Y., 1987, Imaging quasi-layered conductive structures by simple processing of transient electromagnetic data: Geophysics, v52, 4, 545-554.

Sengpiel, K-P. 1988, Approximate inversion of airborne EM data from a multi-layered ground. Geophysical Prospecting, 36, 446-459

Wolfgram, P. and Karlik, G., 1995, Conductivity-depth transform of GEOTEM data: Exploration Geophysics, 26, 179-185.

Yin, C. and Fraser, D.C. (2002), The effect of the electrical anisotropy on the responses of helicopter-borne frequency domain electromagnetic systems, Submitted to *Geophysical Prospecting*